

「高エネルギー原子核衝突で生成される渦と偏極」

# ***Vorticity and polarization in heavy-ion collisions***

**Takafumi Niida**



***Heavy Ion Pub #31 (online)***  
***September 28, 2020***

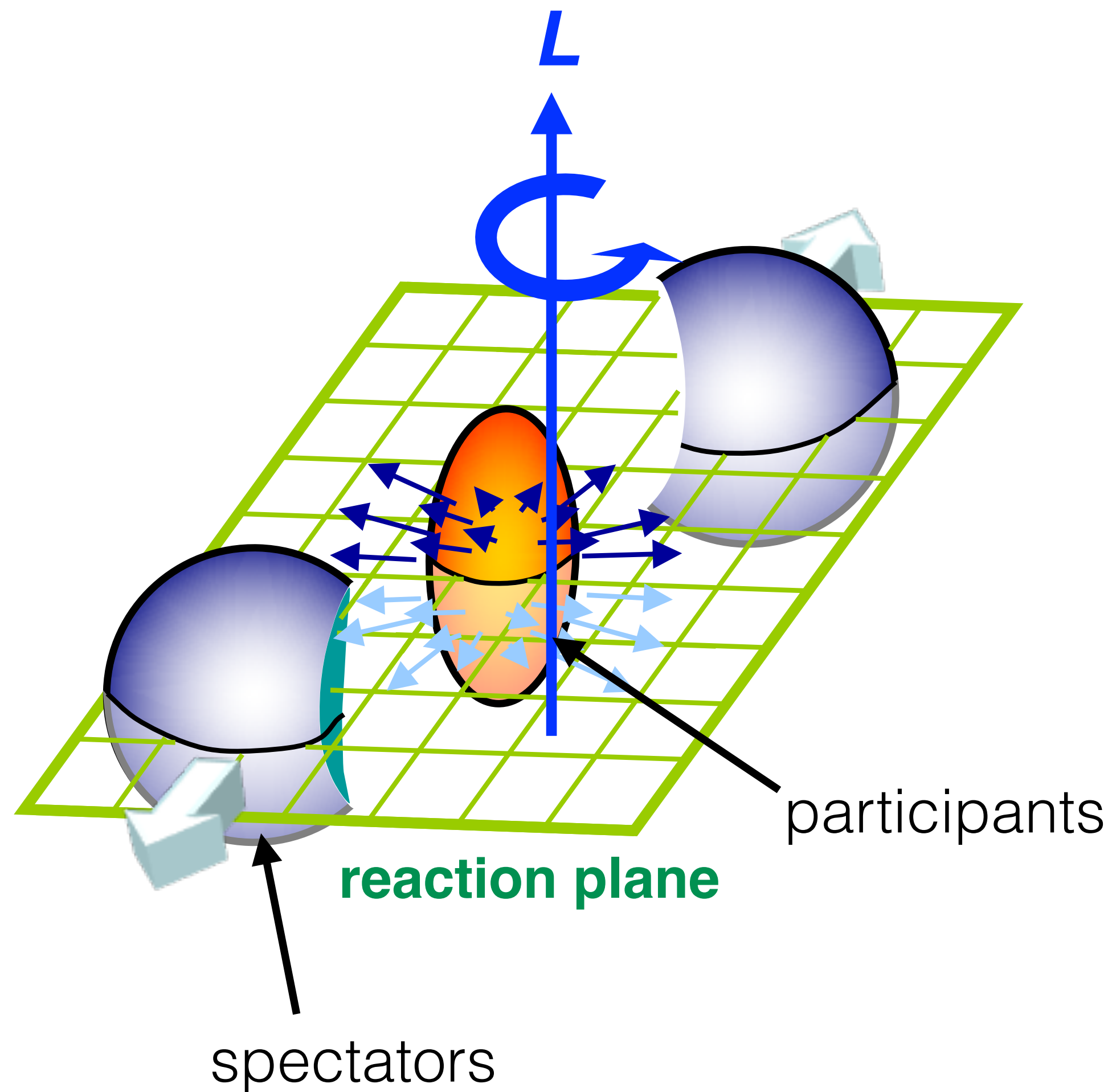
# Outline

---

- Introduction
  - Initial orbital angular momentum, magnetic field, global polarization...
- Global polarization measurements
- Experimental results and Discussion
  - Global polarization
  - Global spin alignment
  - Local polarization along the beam direction
  - and more if time permits...
- Outlook and Summary

\* Slides are prepared in English just in case...

# Important features in non-central heavy-ion collisions



Orbital angular momentum  $\mathbf{L}$

$$\mathbf{L} = \mathbf{r} \times \mathbf{p}$$
$$\sim bA\sqrt{s_{NN}}$$

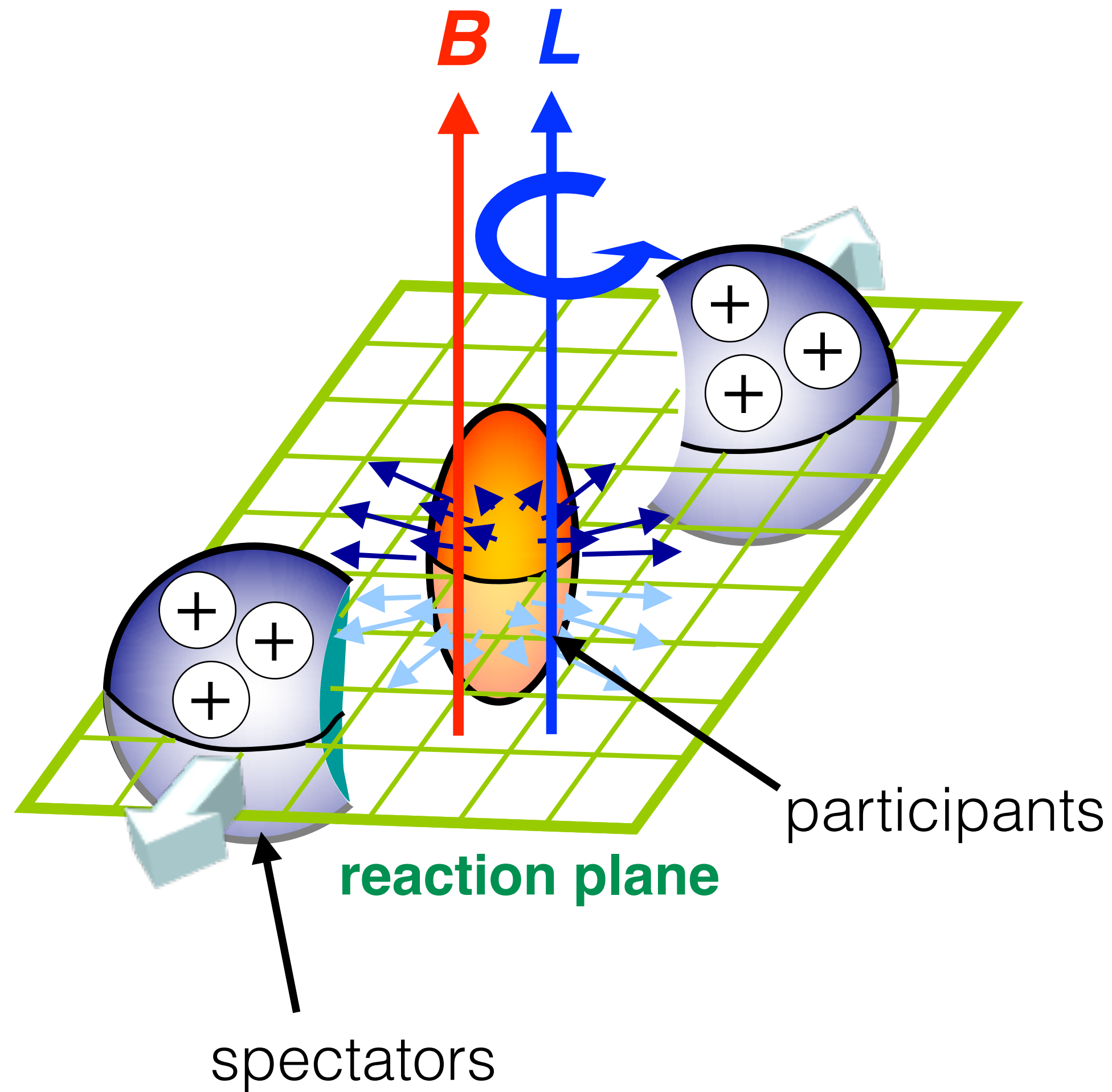
$\mathbf{b}$  : impact parameter  
(vector connecting the center of two nuclei)  
 $A$  : mass number

$$\mathbf{L} \sim bA\sqrt{s_{NN}}$$
$$\sim 10 \text{ (fm)} \times 197 \times 200 \text{ (GeV)}$$
$$= 2 \times 10^3 \times 197 \text{ (fm} \cdot \text{GeV)}$$
$$(\hbar c \sim 197 \text{ MeV} \cdot \text{fm})$$
$$\sim 10^6 \hbar$$

Z.-T. Liang and X.-N. Wang, PRL94, 102301 (2005)

# Important features in non-central heavy-ion collisions

D. Kharzeev, L. McLerran, and H. Warringa,  
Nucl.Phys.A803, 227 (2008)  
McLerran and Skokov, Nucl. Phys. A929, 184 (2014)



## Initial magnetic field $\mathbf{B}$

Approx. Biot-Savart law for a point charge

$$\mathbf{E} = \frac{q}{4\pi\epsilon_0} \frac{1 - \beta^2}{(1 - \beta^2 \sin^2 \theta)^{3/2}} \frac{\hat{\mathbf{r}}}{|\mathbf{r}|^2} \sim \frac{q}{4\pi\epsilon_0} \frac{\gamma \hat{\mathbf{r}}}{|\mathbf{r}|^2} \quad (\text{at } t \sim 0)$$

$$\mathbf{B} = \frac{1}{c^2} \mathbf{v} \times \mathbf{E}$$

$$B \sim \frac{q\mu_0}{4\pi} \frac{\gamma \mathbf{v} \times \hat{\mathbf{r}}}{|\mathbf{r}|^2} \sim (Z\alpha\hbar/e)(\gamma\beta/r^2)$$

$$eB \sim \hbar Z\alpha\gamma\beta/r^2 \quad [1/\text{fm}^2] \quad (\text{assume } r \sim 10 \text{ fm}, \gamma \sim 106.58)$$

$$\sim \hbar Z\alpha$$

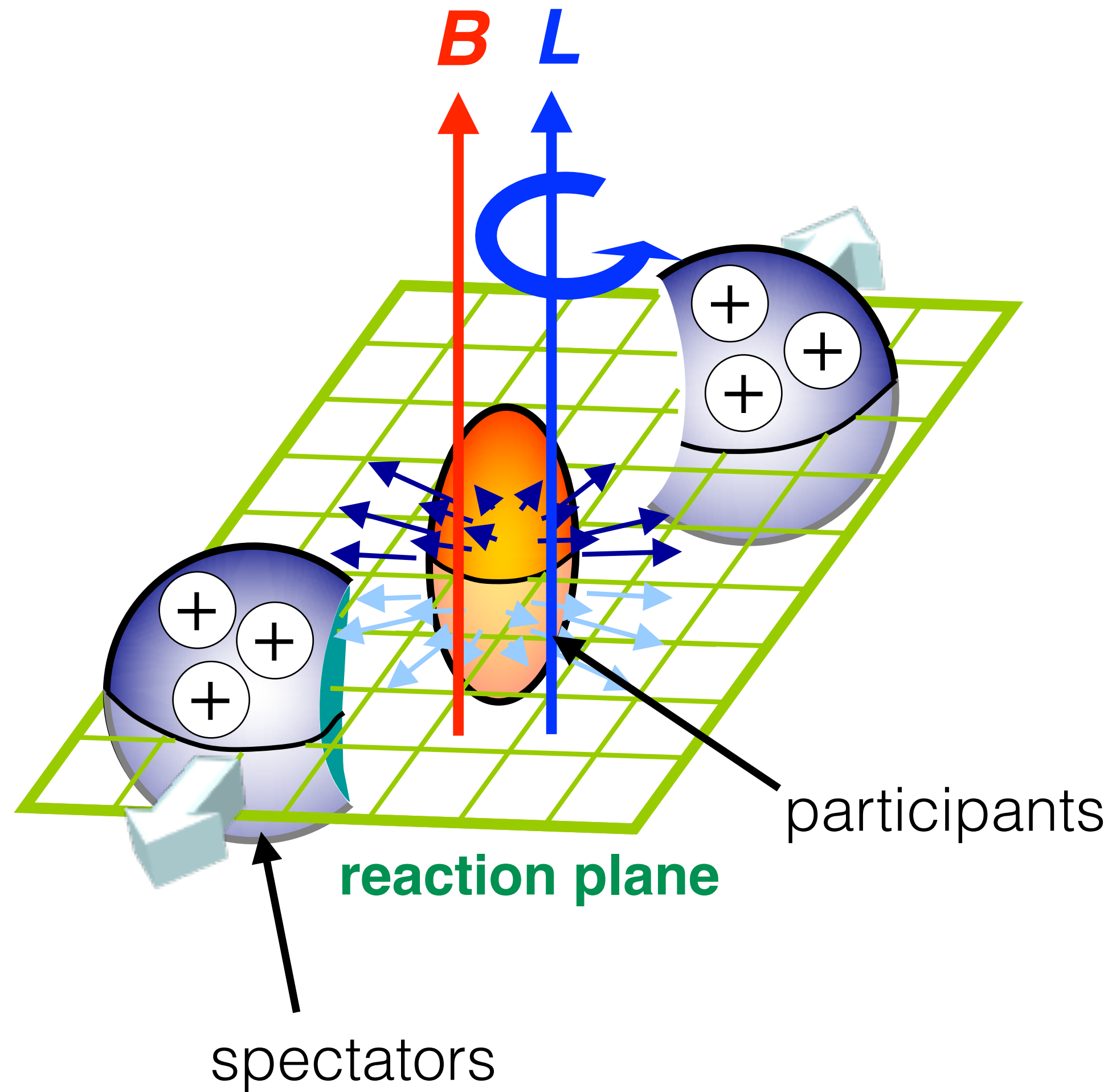
$$\sim m_\pi^2$$

$$B \sim 10^{13} \text{ T}$$

# Important features in non-central heavy-ion collisions

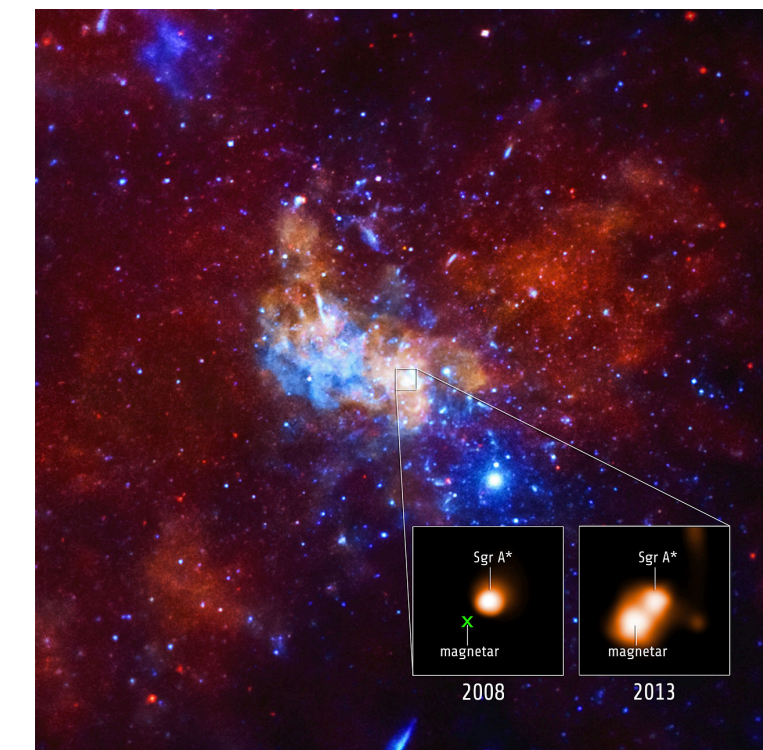
D. Kharzeev, L. McLerran, and H. Warringa,  
 Nucl.Phys.A803, 227 (2008)  
 McLerran and Skokov, Nucl. Phys. A929, 184 (2014)

## Initial magnetic field **B**



typical magnet

magnetar, wikipedia



surface on magnetar

HI (200 GeV)

$$B \sim 0.1 - 0.5 \text{ T}$$

$$B \sim 10^{11} \text{ T}$$

$$B \sim 10^{13} \text{ T}$$

- \* Lifetime of B-field is likely short ( $< 0.5 \text{ fm}/c$ ), depending on conductivity
- \* Rotating charged fluid also produces the field

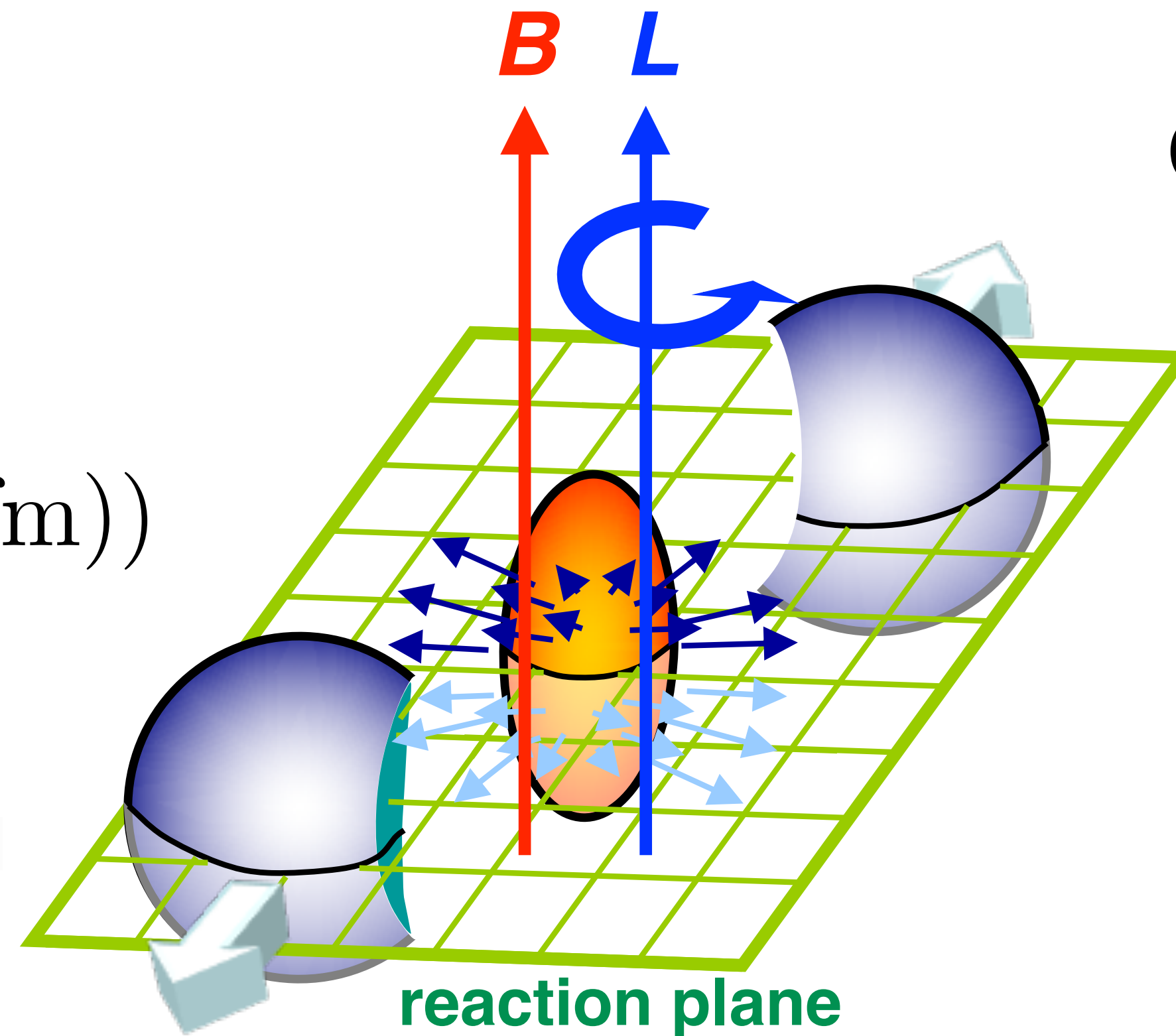
# Important features in non-central heavy-ion collisions

Strong magnetic field

$$B \sim 10^{13} \text{ T}$$

$$(eB \sim m_{\pi}^2 (\tau \sim 0.2 \text{ fm}))$$

D. Kharzeev, L. McLerran, and H. Warringa,  
Nucl.Phys.A803, 227 (2008)  
McLerran and Skokov, Nucl. Phys. A929, 184 (2014)



Orbital angular momentum

$$\mathbf{L} = \mathbf{r} \times \mathbf{p}$$

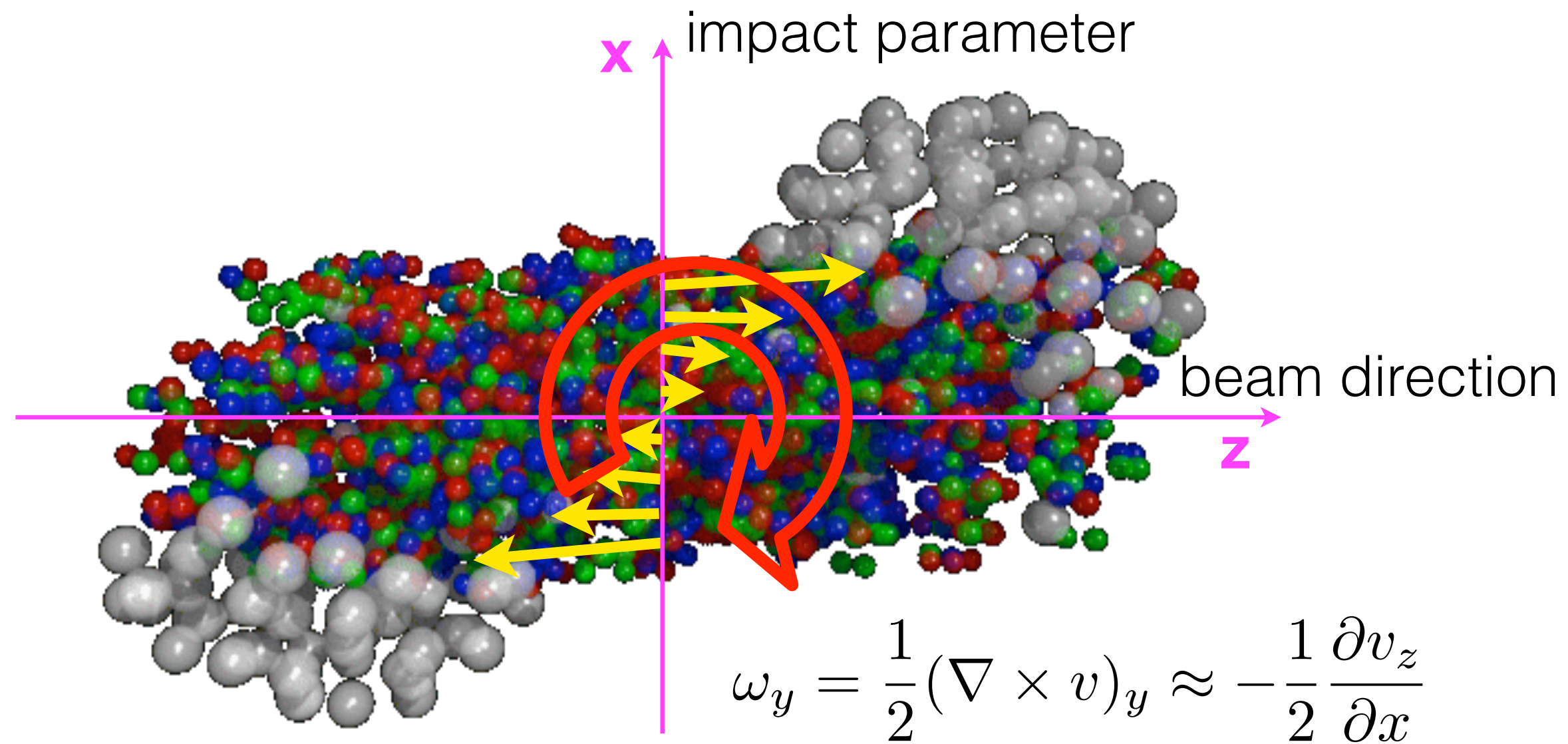
$$\sim bA\sqrt{s_{NN}} \sim 10^6 \hbar$$

Z.-T. Liang and X.-N. Wang, PRL94, 102301 (2005)

→ Chiral magnetic effect  
Chiral magnetic wave  
**Particle polarization**

→ Chiral vortical effect  
→ **Particle polarization**

# Global polarization



Z.-T. Liang and X.-N. Wang, PRL94, 102301 (2005)

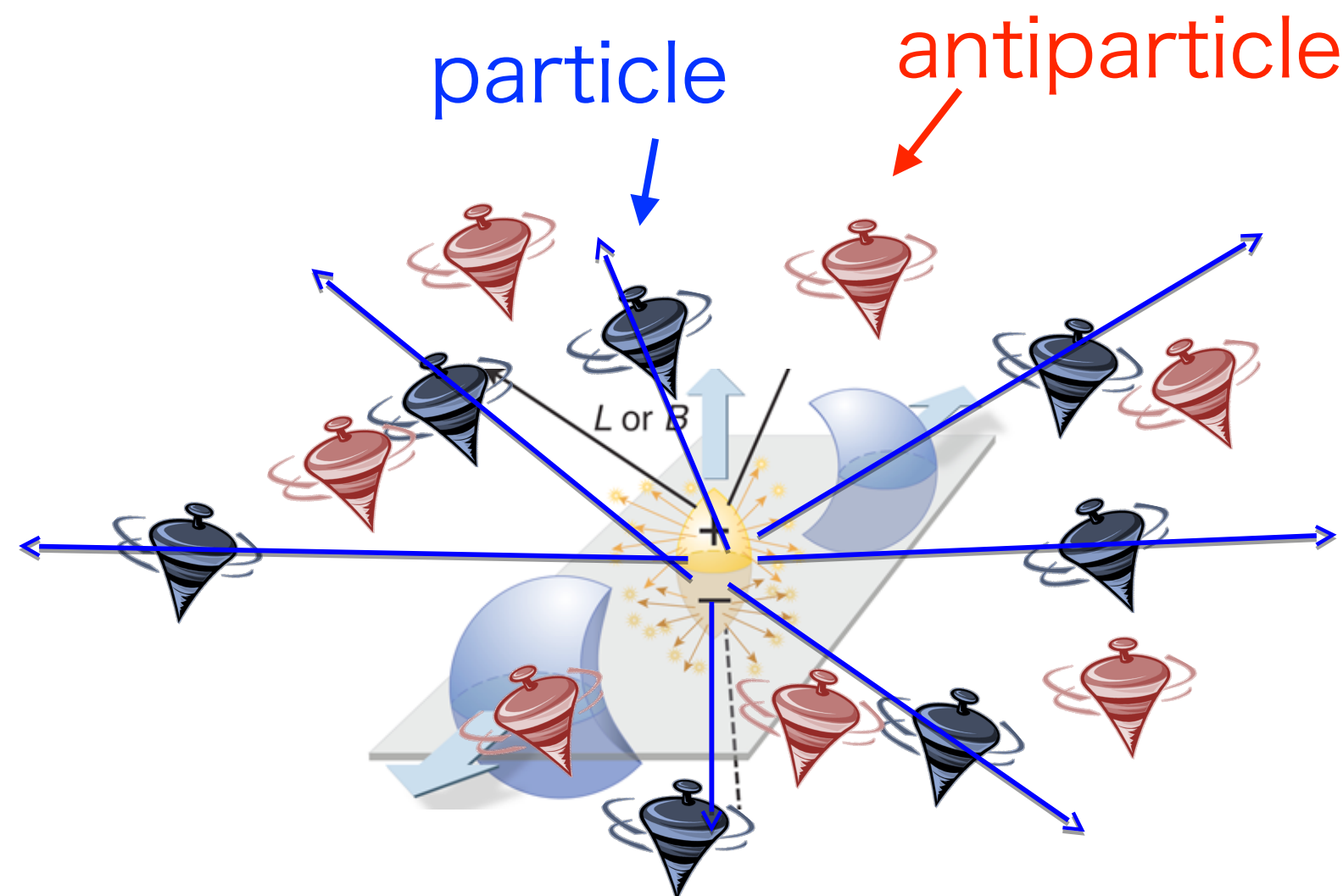
S. Voloshin, nucl-th/0410089 (2004)

□ Orbital angular momentum is transferred to particle spin

○ Particles' and anti-particles' spins are aligned along angular momentum,  $\mathbf{L}$

□ Magnetic field align particle's spin

○ Particles' and antiparticles' spins are aligned in opposite direction along  $\mathbf{B}$  due to the opposite sign of magnetic moment



Produced particles will be “globally” polarized along  $\mathbf{L}$  and  $\mathbf{B}$ .  $\mathbf{B}$  might be studied by particle-antiparticle difference.

# Rotation vs. Polarization

Barnett effect:  
rotation → polarization

Magnetization of an uncharged body  
when spun on its axis S. Barnett, Phys. Rev. 6, 239 (1915)

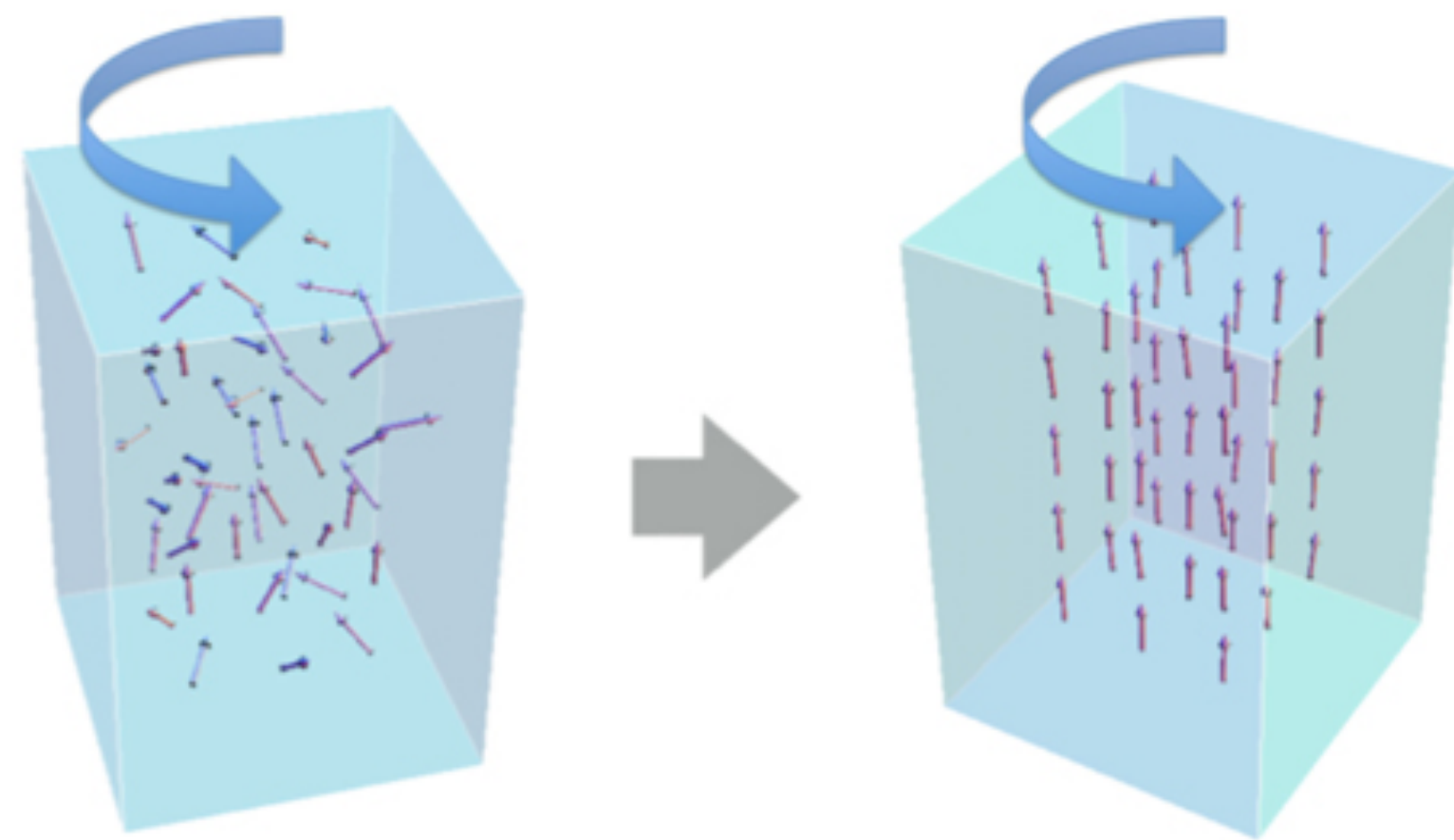


figure: M. Matsuo et al., Front. Phys., 30 (2015)

$$M = \frac{\chi\omega}{\gamma}$$

$\chi$ : magnetic susceptibility  
 $\gamma$ : gyromagnetic ratio

Einstein-de-Haas effect:  
polarization → rotation



Rotation of a ferromagnet under  
change in the direction/strength  
of magnetic-field to conserve the  
total angular momentum.

$$\vec{J} = \vec{L} + \vec{S}$$

A.Einstein, W. J. de Haas,  
B.Koninklijke Akademie van Wetenschappen te Amsterdam,  
C.Proceedings, 18 I, 696-711 (1915)

“the only experiment by Einstein”



# How to measure the polarization?

## Parity-violating weak decay of hyperons (“self-analyzing”)

Daughter baryon is preferentially emitted in the direction of hyperon’s spin (opposite for anti-particle)

$$\frac{dN}{d \cos \theta^*} \propto 1 + \alpha_H P_H \cos \theta^*$$

$P_H$ :  $\Lambda$  polarization

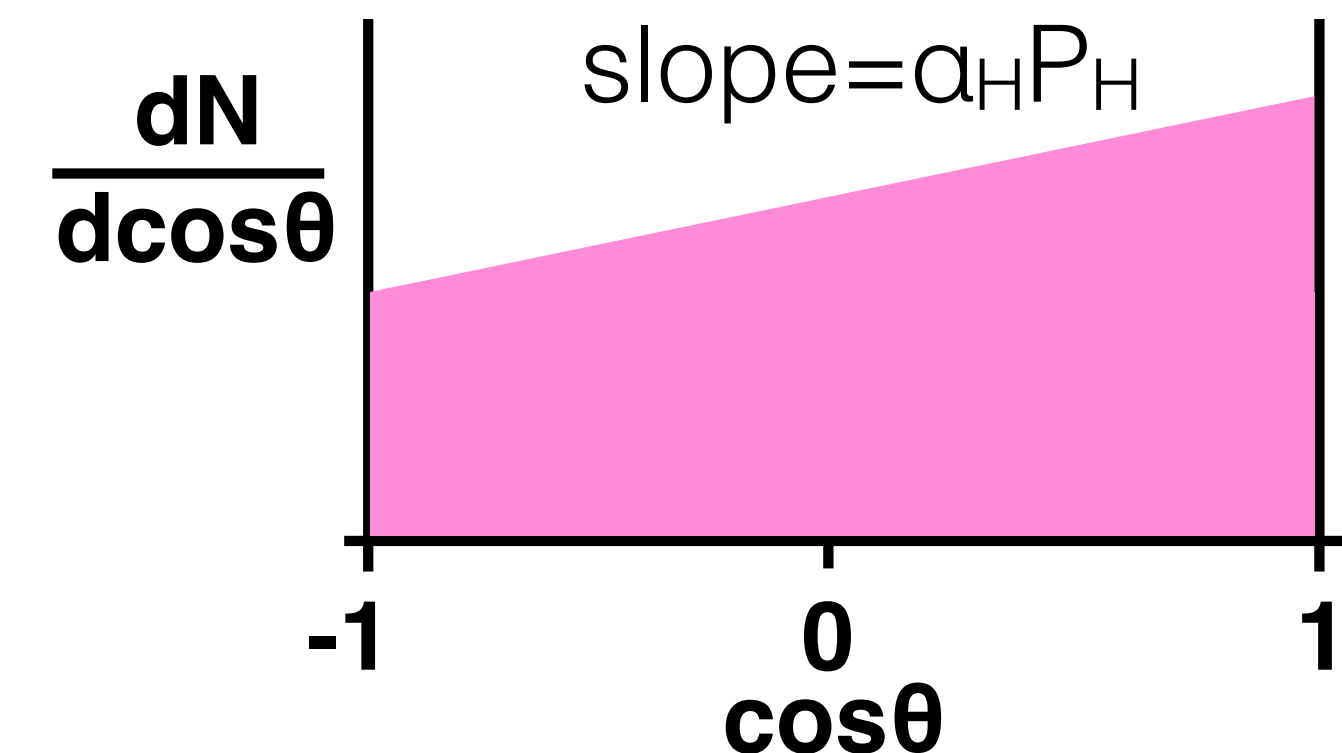
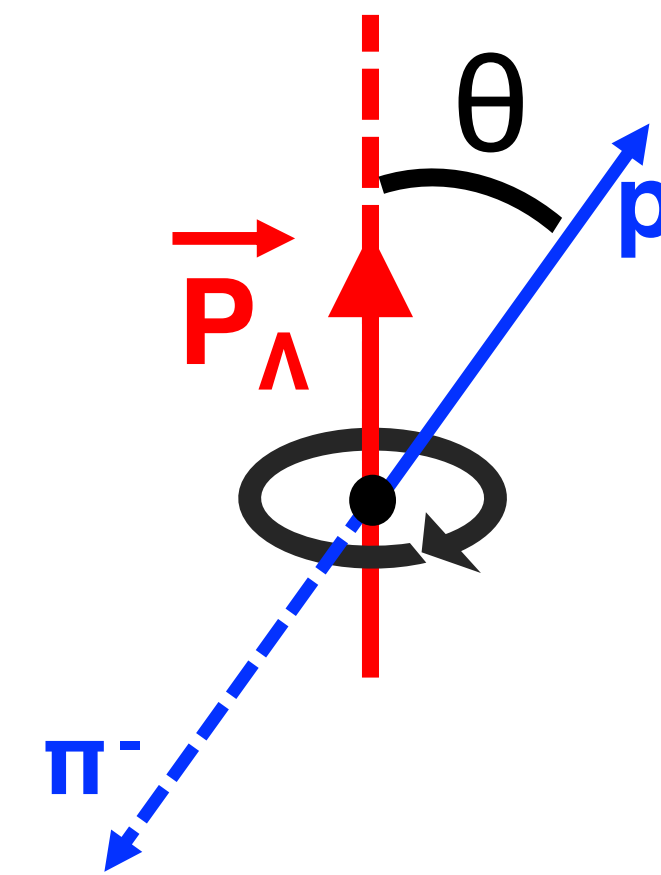
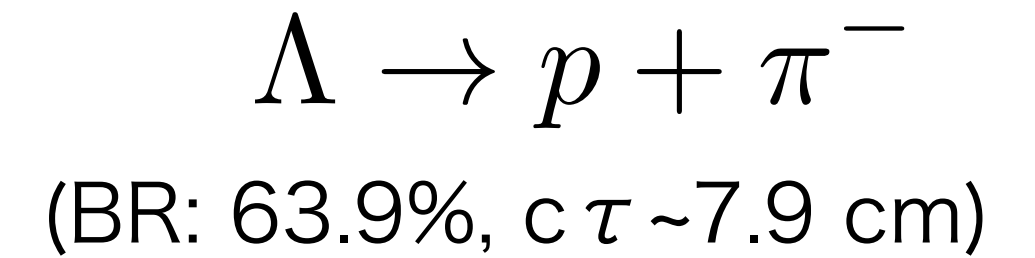
$\theta^*$ : polar angle of proton relative to the polarization direction in  $\Lambda$  rest frame

$\alpha_H$ :  $\Lambda$  decay parameter

Note:  $\alpha_H$  recently updated by BESIII Collaboration

$\alpha_\Lambda = 0.732 \pm 0.014$ ,  $\alpha_{\bar{\Lambda}} = -0.758 \pm 0.012$

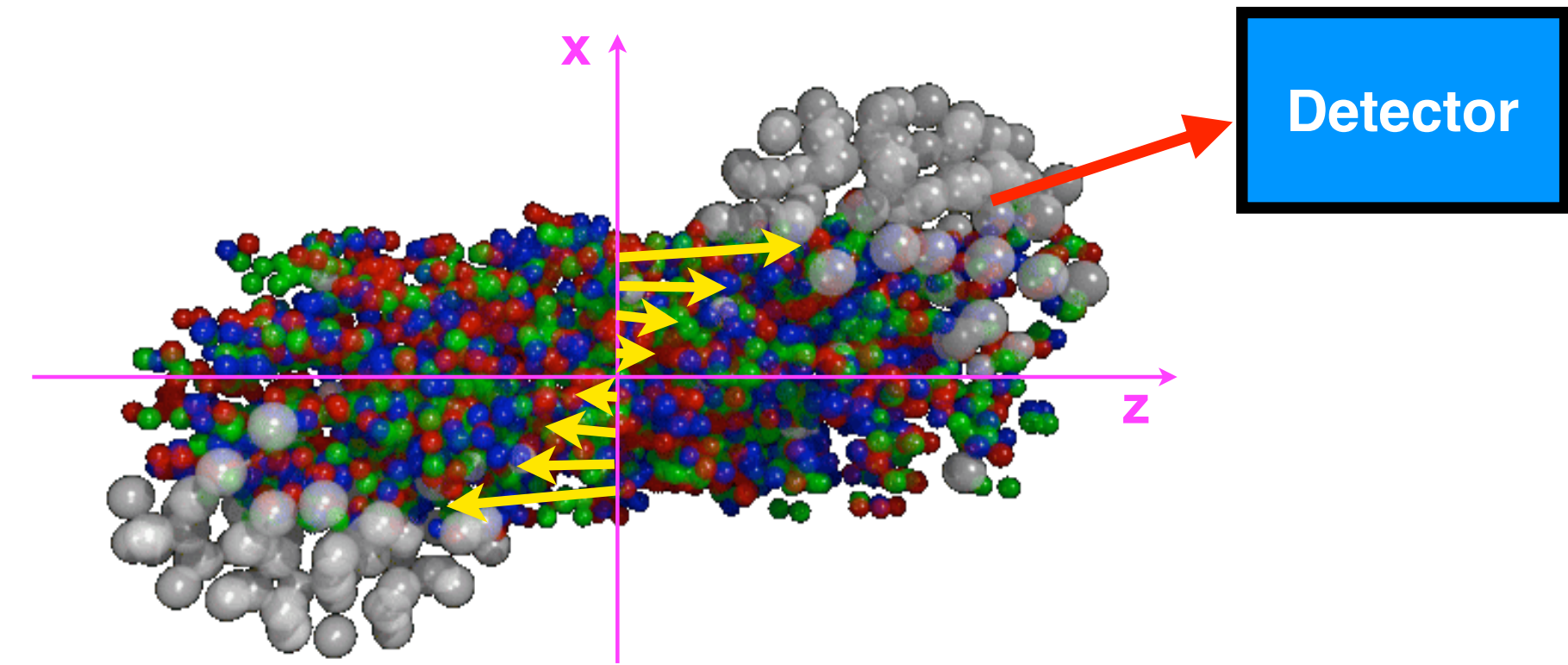
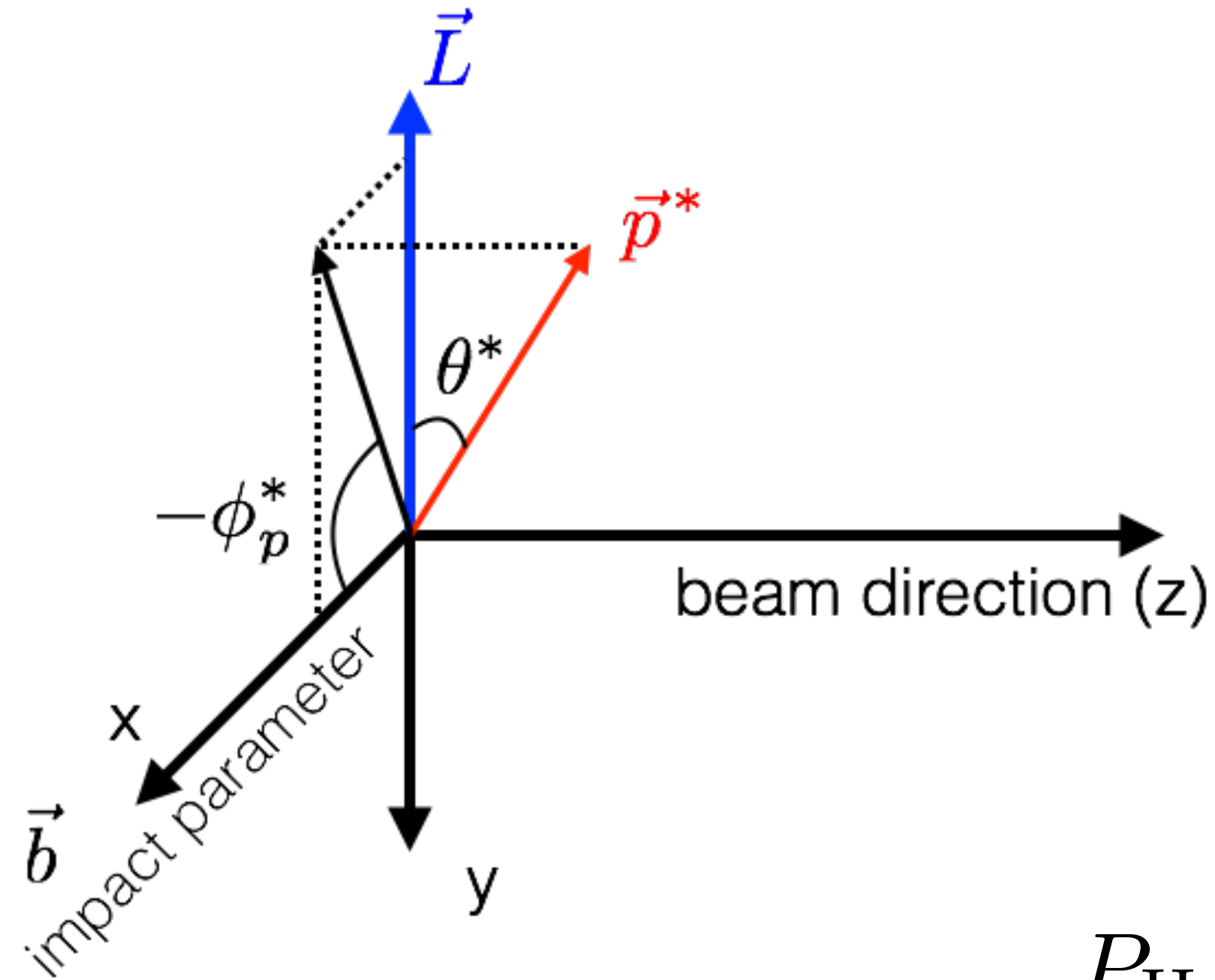
P.A. Zyla et al. (PDG), Prog.Theor.Exp.Phys.2020.083C01



# How to measure the “global” polarization?

“global” polarization : spin alignment along the initial angular momentum

Projection onto the transverse plane



Angular momentum direction can be determined by spectator deflection (spectators deflect outwards)

S. Voloshin and TN, PRC94.021901(R)(2016)

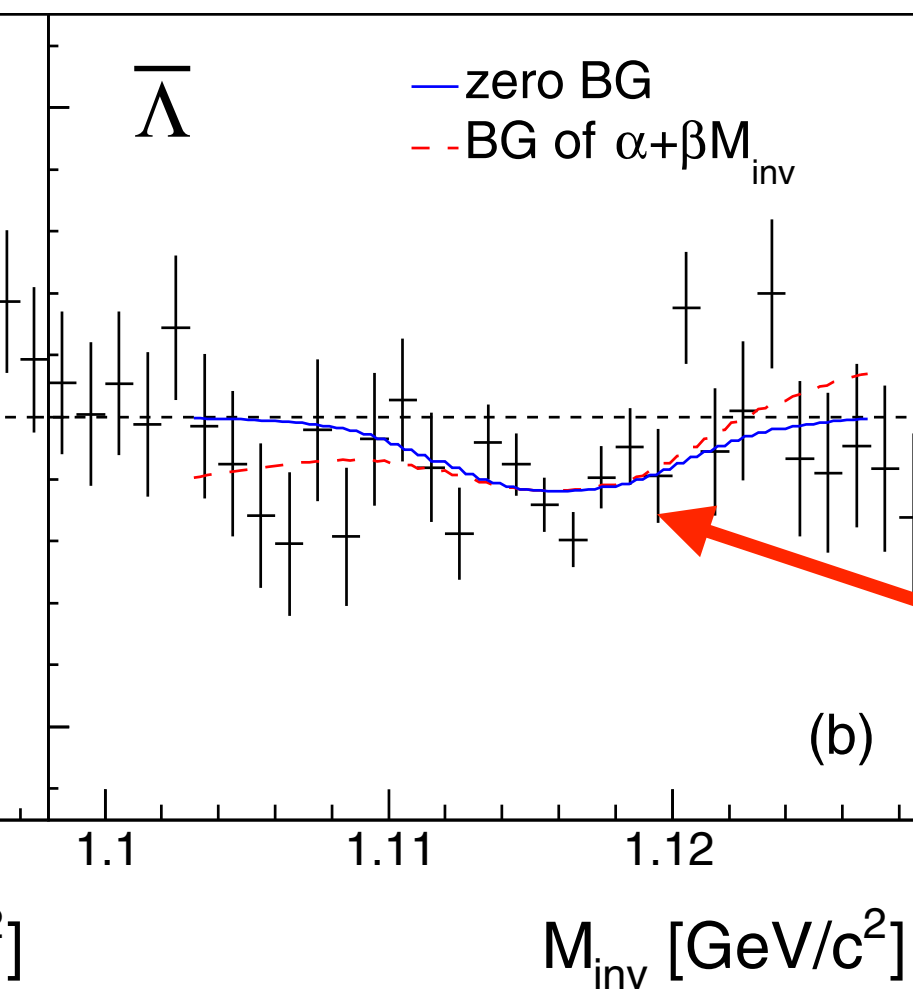
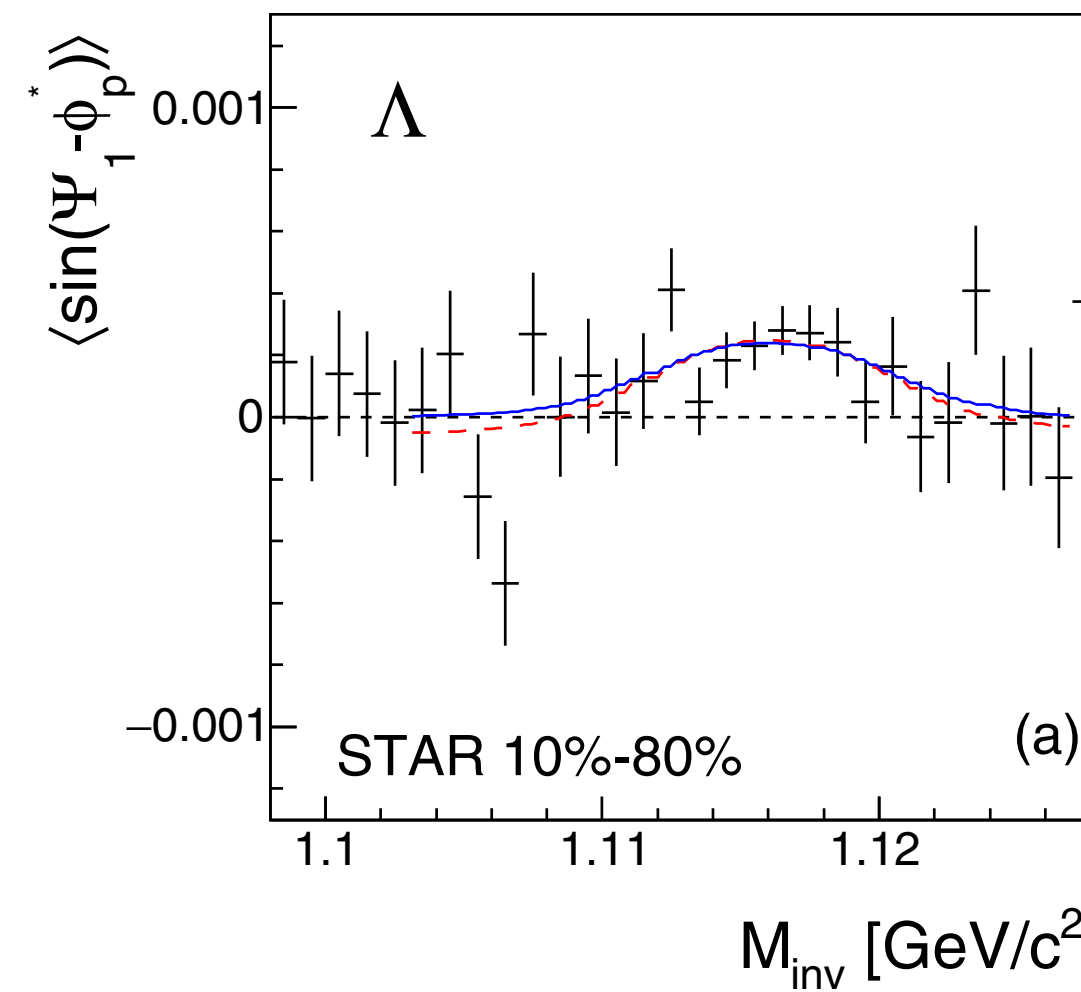
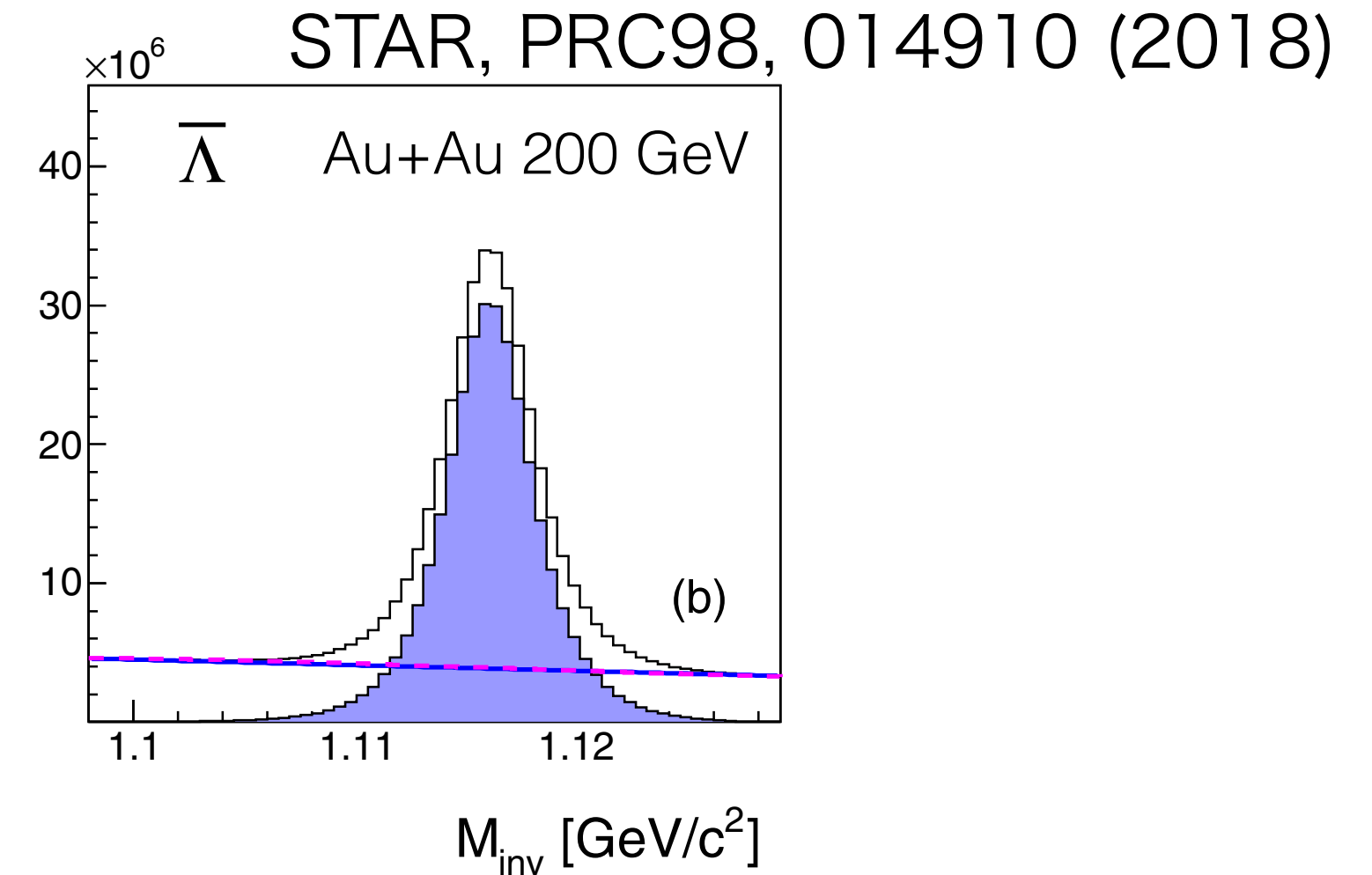
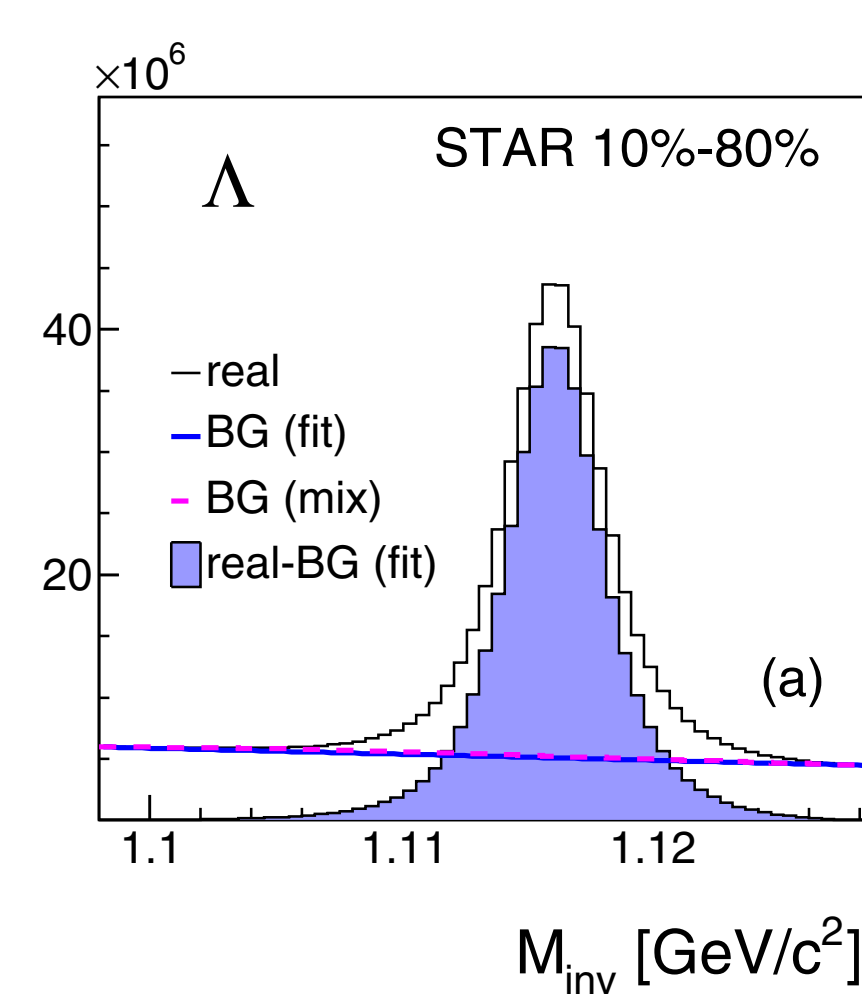
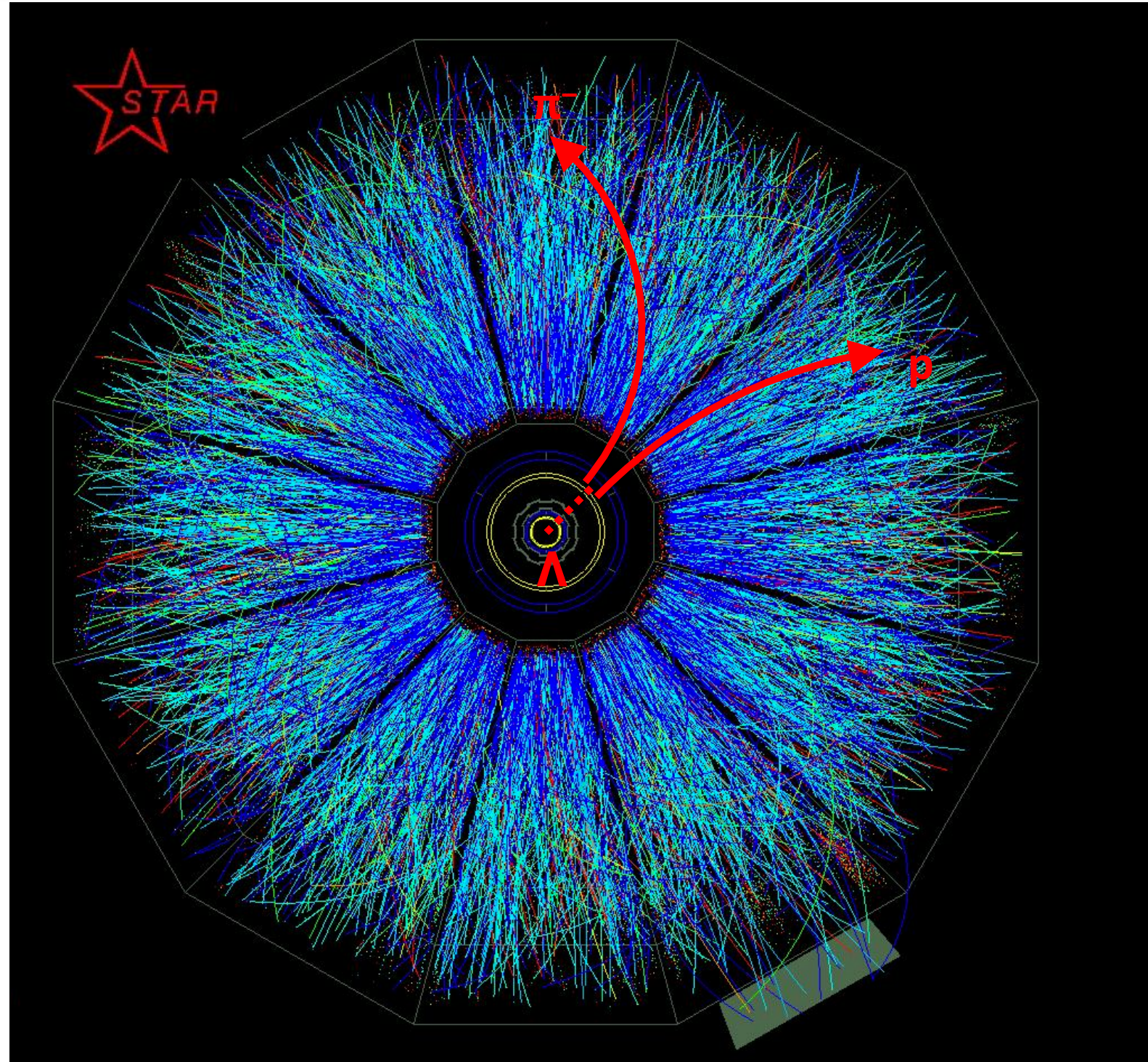
$$P_H = \frac{8}{\pi\alpha_H} \frac{\langle \sin(\Psi_1 - \phi_p^*) \rangle}{\text{Res}(\Psi_1)}$$

$\Psi_1$ : azimuthal angle of b

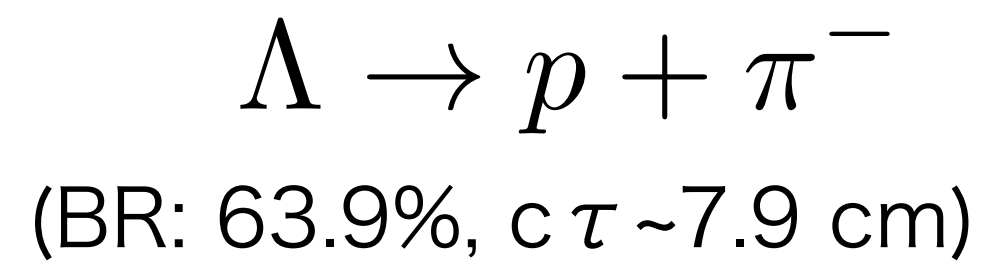
$\phi_p^*$ :  $\phi$  of daughter proton in  $\Lambda$  rest frame

STAR, PRC76, 024915 (2007)

# Signal extraction with $\Lambda$ hyperons

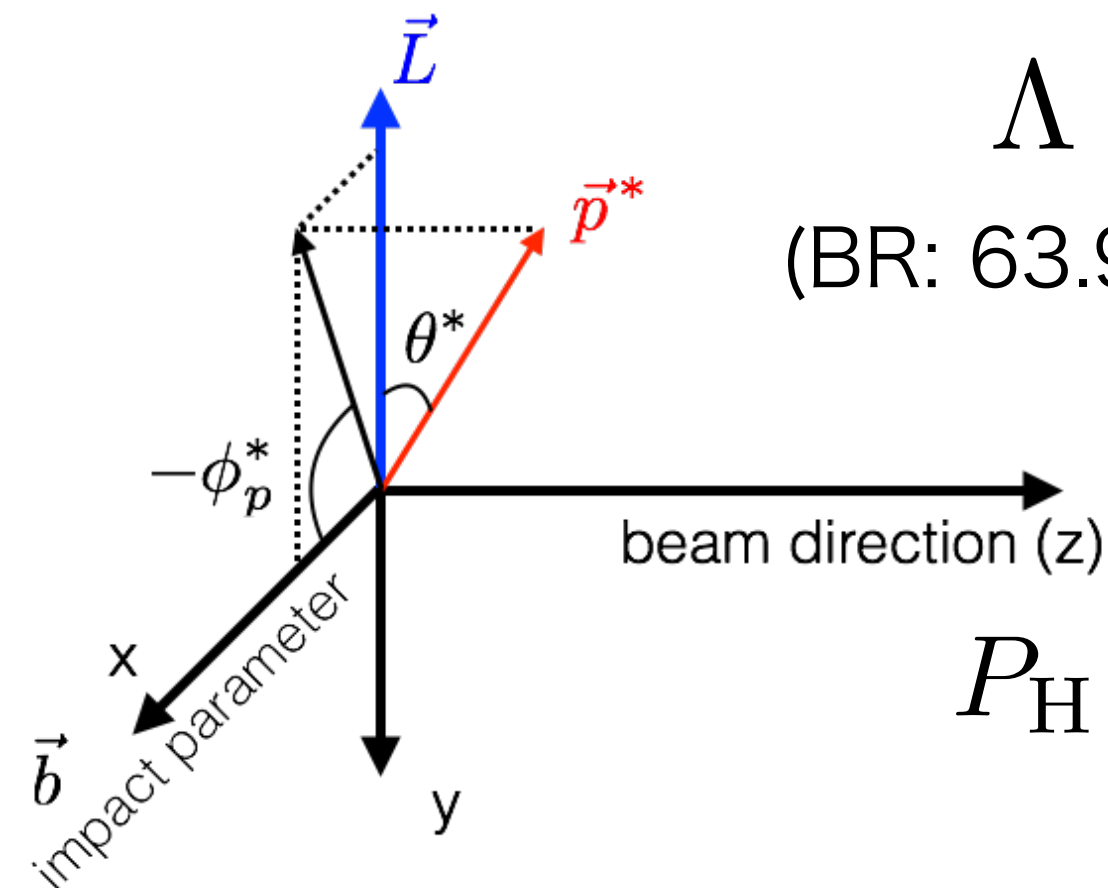


negative for anti- $\Lambda$   
 $\alpha_H = -\alpha_{\bar{H}}$



$$P_H = \frac{8}{\pi\alpha_H} \frac{\langle \sin(\Psi_1 - \phi_p^*) \rangle}{\text{Res}(\Psi_1)}$$

$$\begin{aligned} \langle \sin(\Psi_1 - \phi_p^*) \rangle^{\text{obs}} &= (1 - f^{\text{Bg}}(M_{\text{inv}})) \langle \sin(\Psi_1 - \phi_p^*) \rangle^{\text{Sg}} \\ &+ f^{\text{Bg}}(M_{\text{inv}}) \langle \sin(\Psi_1 - \phi_p^*) \rangle^{\text{Bg}}, \end{aligned}$$



# Feed-down effect

- ~60% of measured  $\Lambda$  are feed-down from  $\Sigma^* \rightarrow \Lambda \pi$ ,  $\Sigma^0 \rightarrow \Lambda \gamma$ ,  $\Xi \rightarrow \Lambda \pi$
- Polarization of parent particle R is transferred to its daughter  $\Lambda$   
(Polarization transfer could be negative!)

$C_{\Lambda R}$  : coefficient of spin transfer from parent R to  $\Lambda$   
 $S_R$  : parent particle's spin  
 $f_{\Lambda R}$  : fraction of  $\Lambda$  originating from parent R  
 $\mu_R$  : magnetic moment of particle R

$$\mathbf{S}_{\Lambda}^* = C \mathbf{S}_R^* \quad \langle S_y \rangle \propto \frac{S(S+1)}{3} (\omega + \frac{\mu}{S} B)$$

$$\begin{pmatrix} \varpi_c \\ B_c/T \end{pmatrix} = \begin{bmatrix} \frac{2}{3} \sum_R (f_{\Lambda R} C_{\Lambda R} - \frac{1}{3} f_{\Sigma^0 R} C_{\Sigma^0 R}) S_R(S_R+1) & \frac{2}{3} \sum_R (f_{\Lambda R} C_{\Lambda R} - \frac{1}{3} f_{\Sigma^0 R} C_{\Sigma^0 R}) (S_R+1) \mu_R \\ \frac{2}{3} \sum_{\bar{R}} (f_{\Lambda \bar{R}} C_{\Lambda \bar{R}} - \frac{1}{3} f_{\Sigma^0 \bar{R}} C_{\Sigma^0 \bar{R}}) S_{\bar{R}}(S_{\bar{R}}+1) & \frac{2}{3} \sum_{\bar{R}} (f_{\Lambda \bar{R}} C_{\Lambda \bar{R}} - \frac{1}{3} f_{\Sigma^0 \bar{R}} C_{\Sigma^0 \bar{R}}) (S_{\bar{R}}+1) \mu_{\bar{R}} \end{bmatrix}^{-1} \begin{pmatrix} P_{\Lambda}^{\text{meas}} \\ P_{\Lambda}^{\text{meas}} \end{pmatrix}$$

Becattini, Karpenko, Lisa, Upsal, and Voloshin, PRC95.054902 (2017)

Decay	C
Parity conserving: $1/2^+ \rightarrow 1/2^+ 0^-$	-1/3
Parity conserving: $1/2^- \rightarrow 1/2^+ 0^-$	1
Parity conserving: $3/2^+ \rightarrow 1/2^+ 0^-$	1/3
Parity-conserving: $3/2^- \rightarrow 1/2^+ 0^-$	-1/5
$\Xi^0 \rightarrow \Lambda + \pi^0$	+0.900
$\Xi^- \rightarrow \Lambda + \pi^-$	+0.927
$\Sigma^0 \rightarrow \Lambda + \gamma$	-1/3

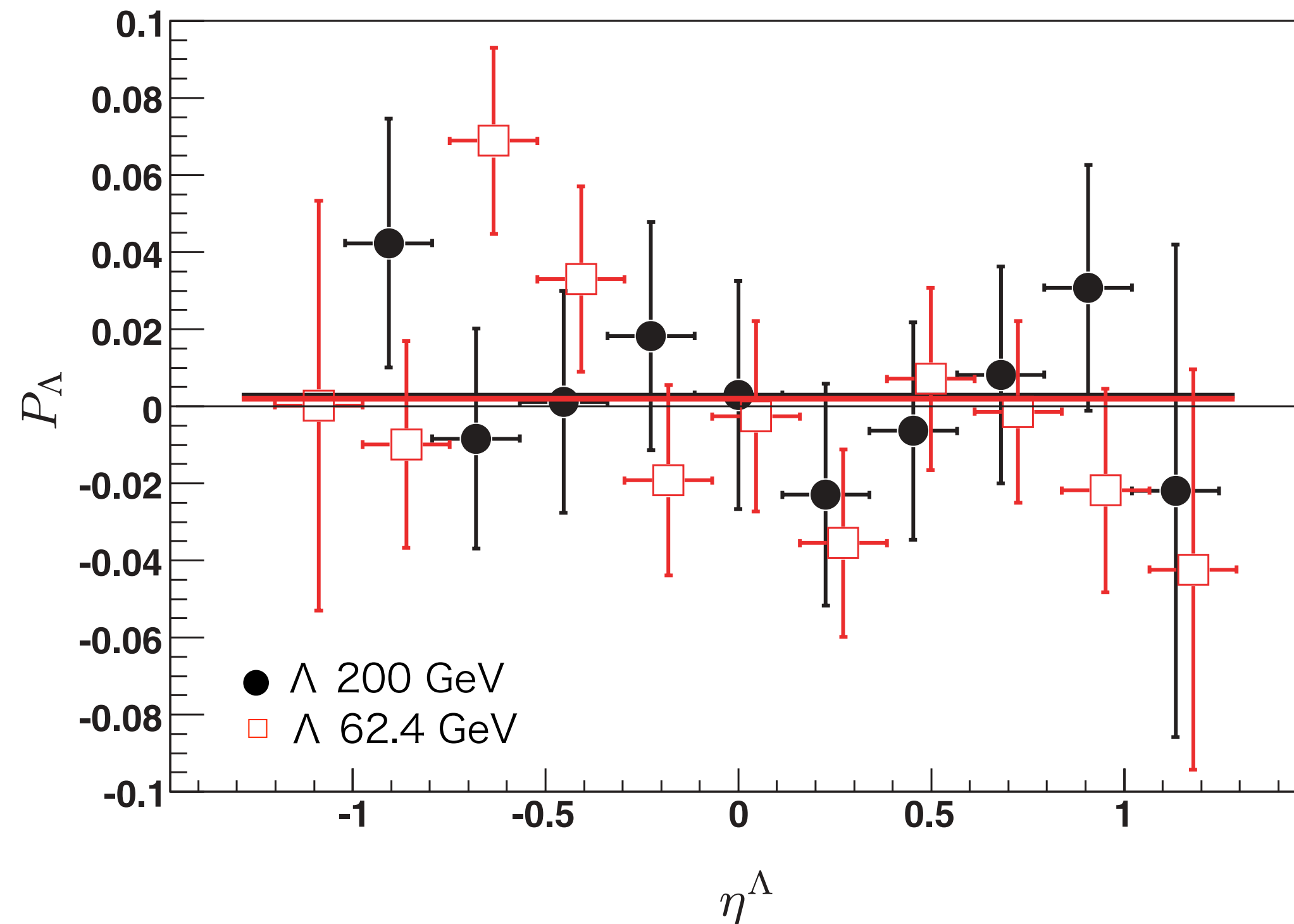
Primary  $\Lambda$  polarization will be diluted by 15%-20%  
(model-dependent)

This also suggests that the polarization of daughter particles can be used to measure the polarization of its parent! e.g.  $\Xi$ ,  $\Omega$

# First paper from STAR in 2007

PHYSICAL REVIEW C 76, 024915 (2007)

## Global polarization measurement in Au+Au collisions



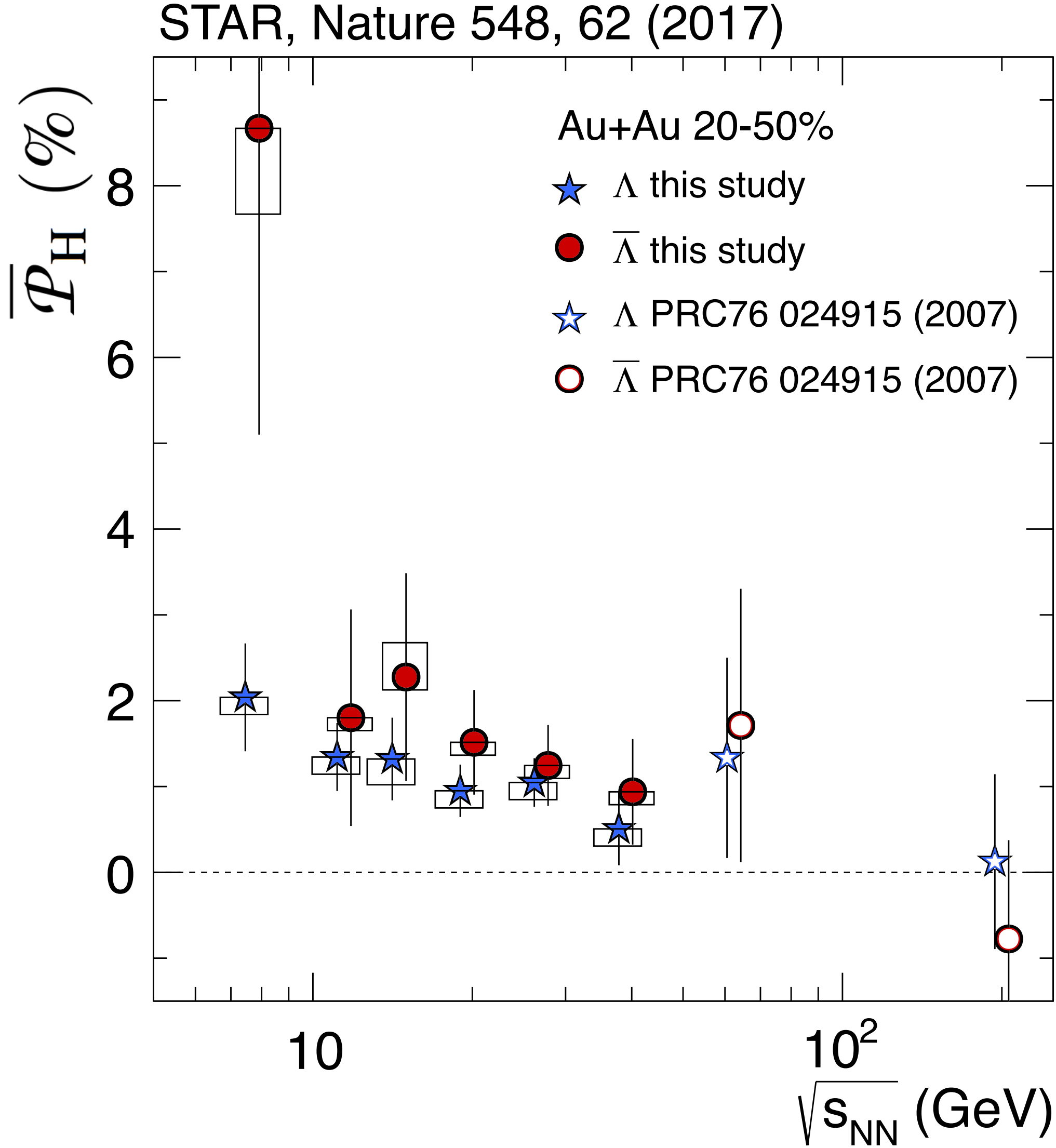
Au+Au collisions at  $\sqrt{s_{NN}} = 62.4$  and 200 GeV in 2004 with very limited statistics ( $\sim 9$ M events)

### III. CONCLUSION

The  $\Lambda$  and  $\bar{\Lambda}$  hyperon global polarization has been measured in Au+Au collisions at center-of-mass energies  $\sqrt{s_{NN}} = 62.4$  and 200 GeV with the STAR detector at RHIC. An upper limit of  $|P_{\Lambda, \bar{\Lambda}}| \leq 0.02$  for the global polarization of  $\Lambda$  and  $\bar{\Lambda}$  hyperons within the STAR detector acceptance is

Results were consistent with zero..., giving an upper limit of  $P_H < 2\%$

# First observation in BES-I



Positive polarization signal at lower energies!

-  $P_H$  looks to increase in lower energies

Becattini, Karpenko, Lisa, Upsal, and Voloshin, PRC95.054902 (2017)

$$P_{\Lambda} \simeq \frac{1}{2} \frac{\omega}{T} + \frac{\mu_{\Lambda} B}{T}$$

$$P_{\bar{\Lambda}} \simeq \frac{1}{2} \frac{\omega}{T} - \frac{\mu_{\Lambda} B}{T}$$

$$\omega = (P_{\Lambda} + P_{\bar{\Lambda}}) k_B T / \hbar$$

$$\sim 0.02-0.09 \text{ fm}^{-1}$$

$$\sim 0.6-2.7 \times 10^{22} \text{ s}^{-1}$$

$\mu_{\Lambda}$ :  $\Lambda$  magnetic moment  
 T: temperature at thermal equilibrium  
 (T=160 MeV)

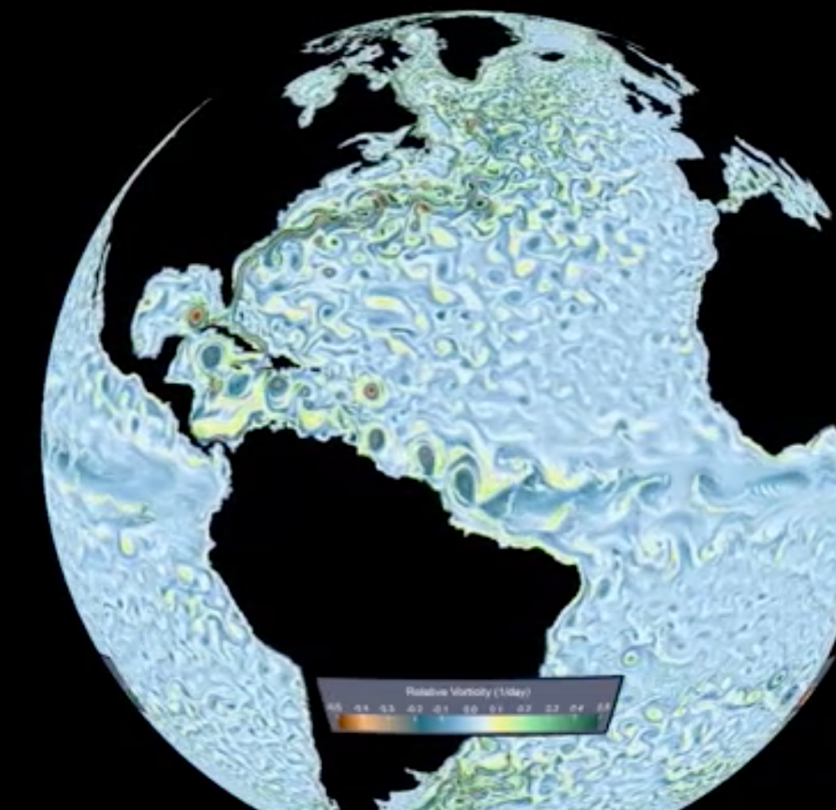
- The most vortical fluid!

Hint of the difference between  $\Lambda$  and anti- $\Lambda$   $P_H$   
 - Effect of the initial magnetic field? (discuss later)

# Fastest vorticity

- Ocean surface vorticity  $\sim 10^{-5} \text{ s}^{-1}$
- Jupiter's great red spot  $\sim 10^{-4} \text{ s}^{-1}$
- Core of supercell tornado  $\sim 10^{-1} \text{ s}^{-1}$
- Rotating, heated soap bubbles  $\sim 10^2 \text{ s}^{-1}$
- Superfluid helium nano droplet  $\sim 10^6 \text{ s}^{-1}$
- Matter in heavy ion collisions  $\sim 10^{22} \text{ s}^{-1}$**

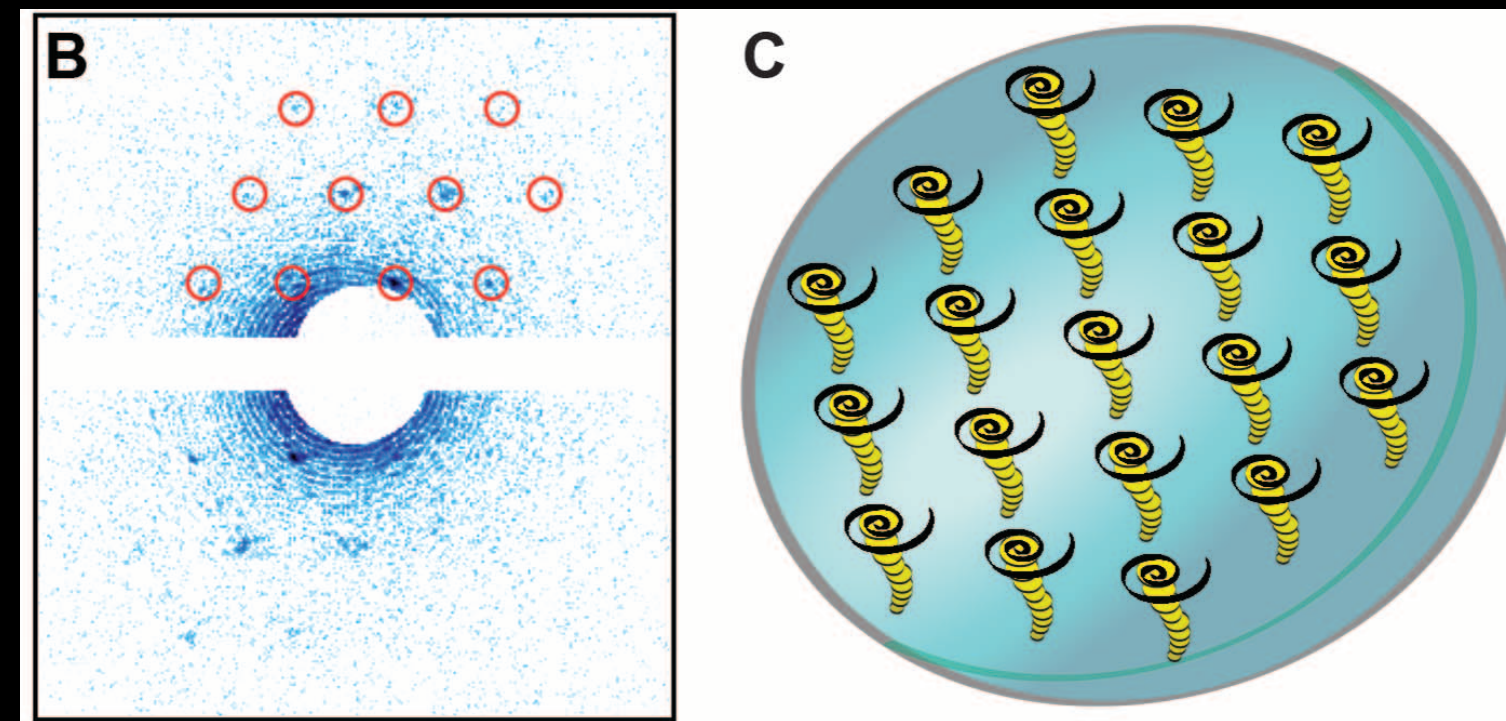
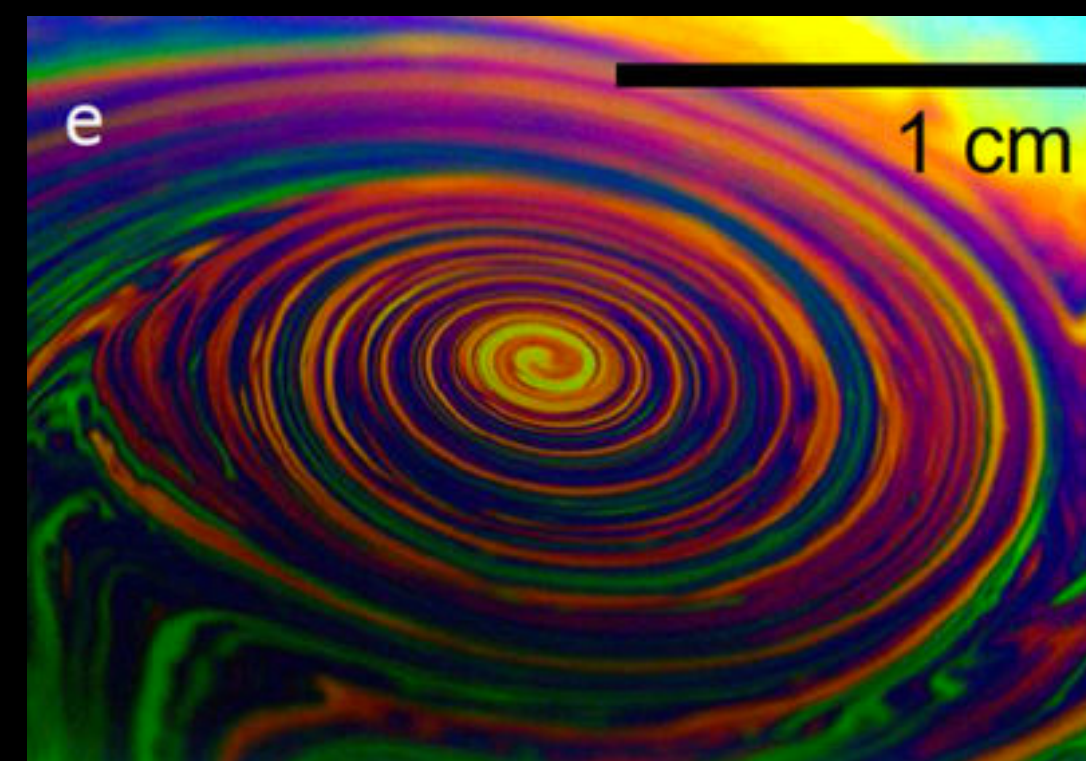
Great red spot of Jupiter (picture: NASA)  
6/27, 2019 by Hubble Space Telescope



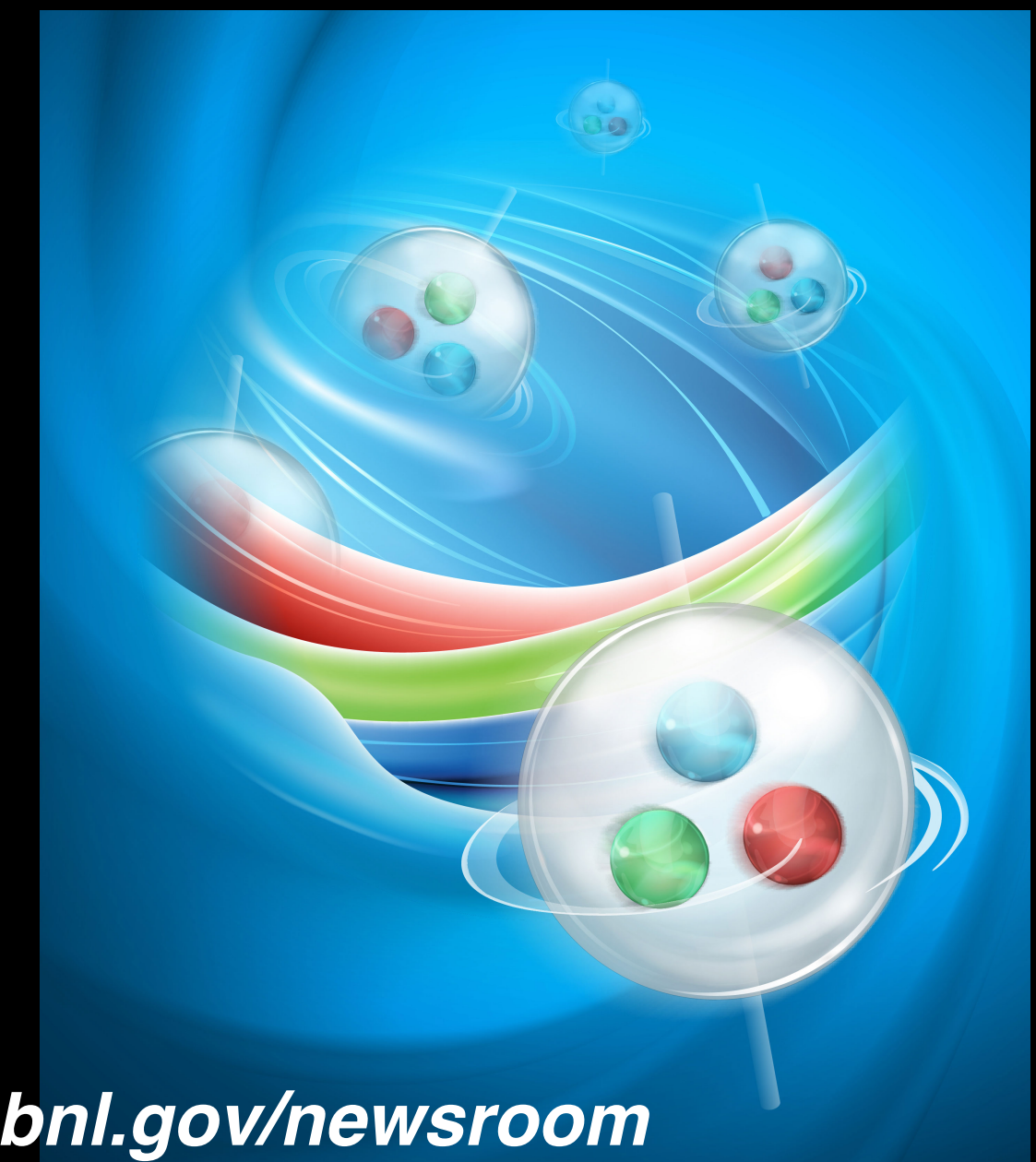
Ocean surface vorticity  
<https://sos.noaa.gov/datasets/ocean-surface-vorticity/>



vortex of soap bubble  
T. Muel et al., Scientific Report 3, 3455 (2013)



vortex aligned to x-ray beam in He droplets  
T. Muel et al., Scientific Report 3, 3455 (2013)

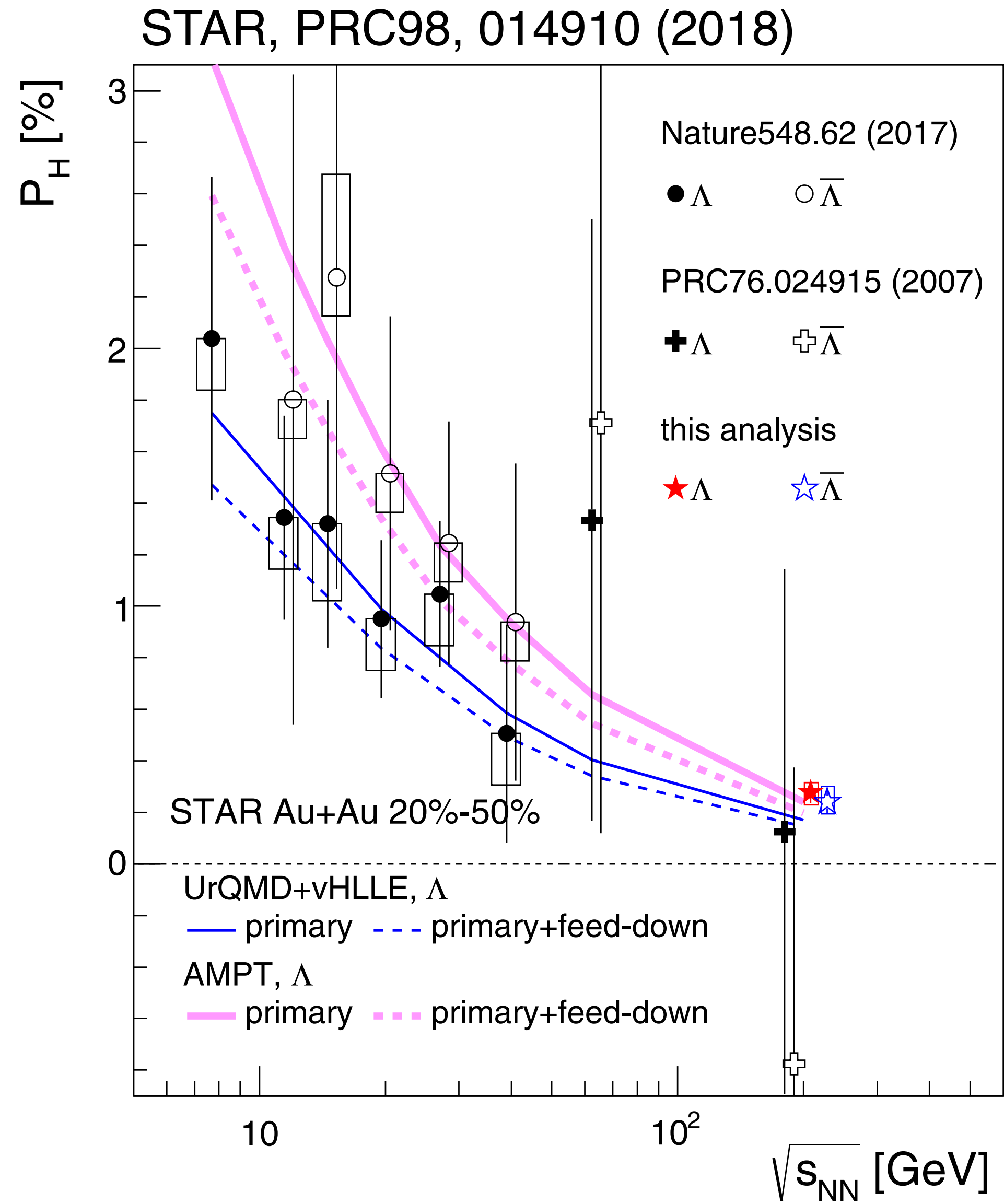


[bnl.gov/newsroom](http://bnl.gov/newsroom)

**Perfect liquid is the most vortical fluid**

Supercell in Oklahoma (2016)  
<http://www.silverliningtours.com/tag/tornado/page/3/>

# Precise measurements at $\sqrt{s_{NN}} = 200$ GeV



Confirmed energy dependence with new results at 200 GeV

- $>5\sigma$  significance utilizing 1.5B events
- partly due to stronger shear flow structure in lower  $\sqrt{s_{NN}}$  because of baryon stopping

$$P_H(\Lambda) [\%] = 0.277 \pm 0.040(\text{stat}) \pm_{0.049}^{0.039}(\text{sys})$$

$$P_H(\bar{\Lambda}) [\%] = 0.240 \pm 0.045(\text{stat}) \pm_{0.045}^{0.061}(\text{sys})$$

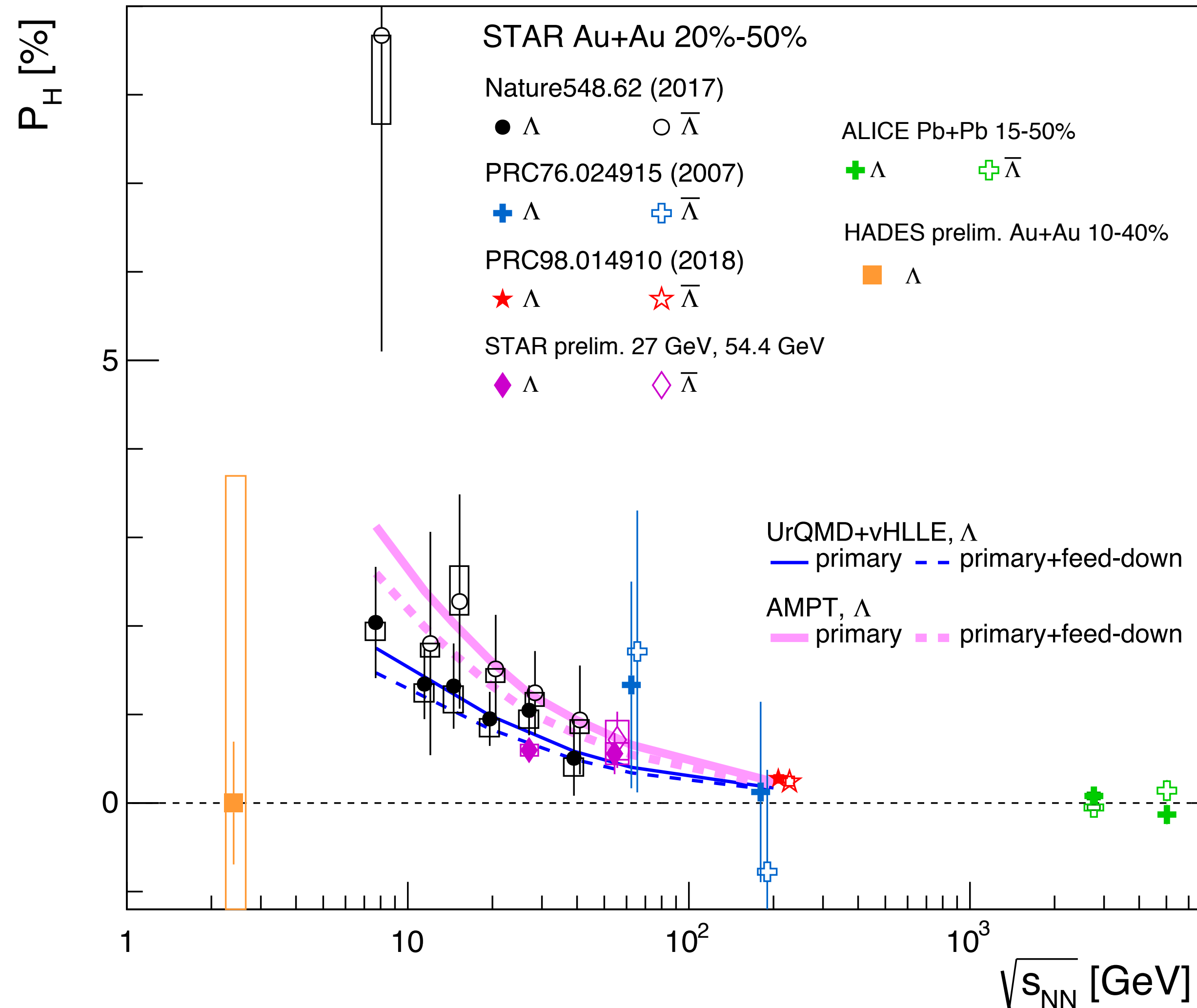
Theoretical models can describe the data well

- I. Karpenko and F. Becattini, EPJC(2017)77:213, UrQMD+vHLLLE
- H. Li et al., PRC96, 054908 (2017), AMPT
- Y. Sun and C.-M. Ko, PRC96, 024906 (2017), CKE
- Y. Xie et al., PRC95, 031901(R) (2017), PICR
- D.-X. Wei et al., PRC99, 014905 (2019), AMPT



# Collection of recent results

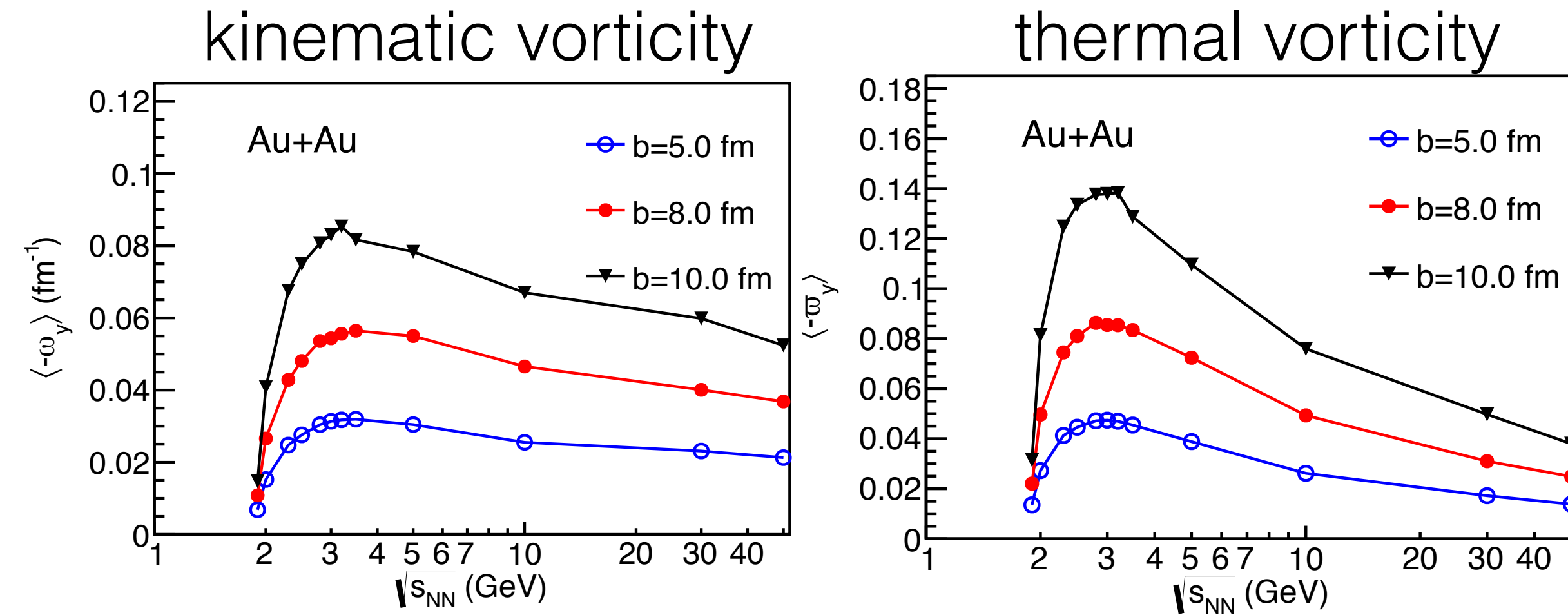
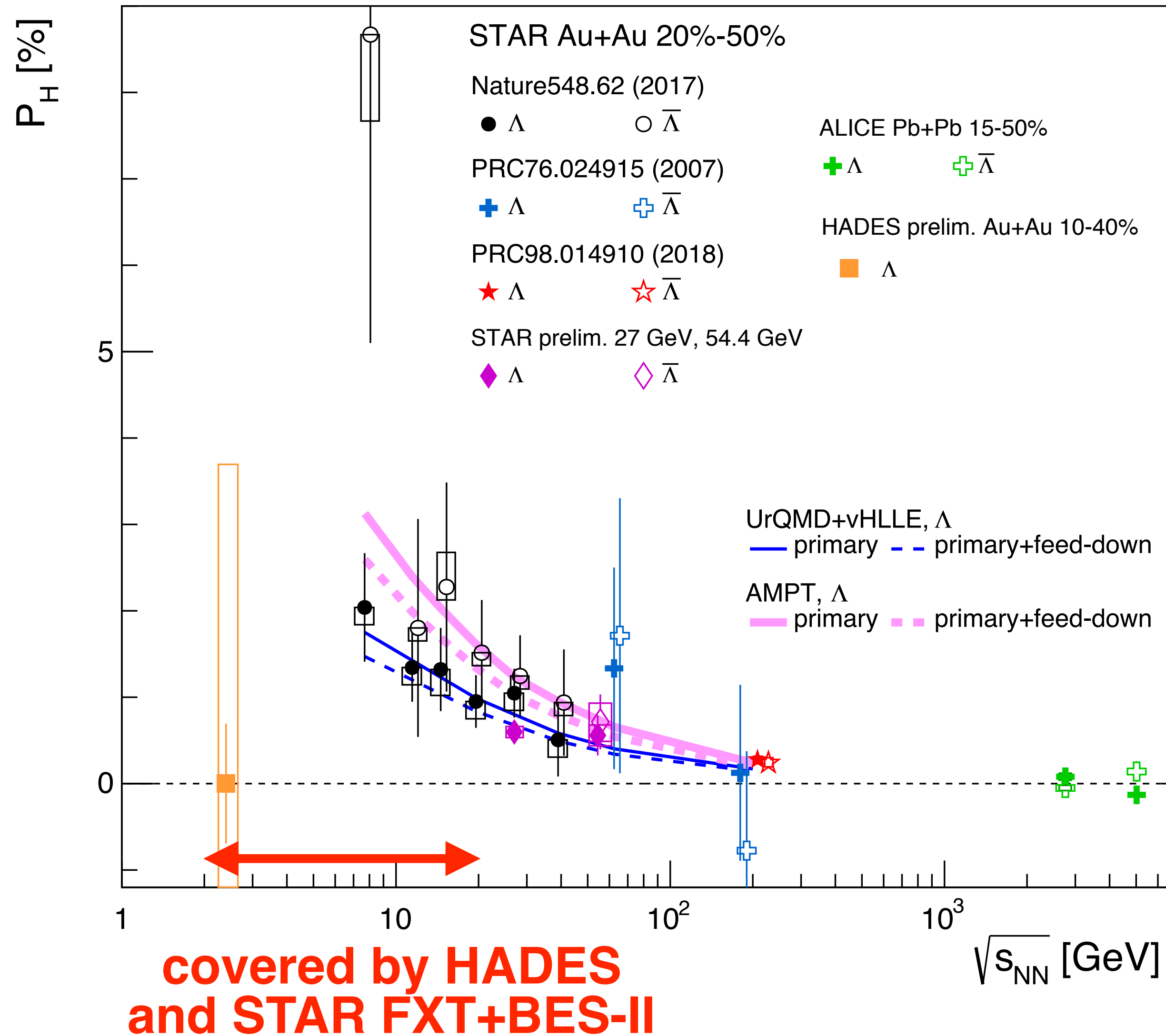
ALICE, PRC101.044611 (2020)  
F. Kornas (HADES), SQM2019  
J. Adams, K. Okubo (STAR), QM2019



- ALICE at 2.76 and 5.02 TeV
- Expected signal is of the order of current statistical uncertainty
- HADES at 2.4 GeV
- still preliminary
- hopefully reduce systematic uncertainty
- Preliminary of STAR at 27 and 54.4 GeV

# Collection of recent results

ALICE, PRC101.044611 (2020)  
 F. Kornas (HADES), SQM2019  
 J. Adams, K. Okubo (STAR), QM2019



Energy dependence of kinematic and thermal vorticity with UrQMD  
 X.-G. Deng et al., PRC101.064908 (2020)

HADES: 2.0-2.4 GeV  
 STAR FXT: 3-7.7 GeV  
 STAR BES II: 7.7-19 GeV

# A possible probe of B-field

Becattini, Karpenko, Lisa, Upsal, and Voloshin, PRC95.054902 (2017)

$$P_{\Lambda} \simeq \frac{1}{2} \frac{\omega}{T} + \frac{\mu_{\Lambda} B}{T}$$

$$P_{\bar{\Lambda}} \simeq \frac{1}{2} \frac{\omega}{T} - \frac{\mu_{\Lambda} B}{T}$$

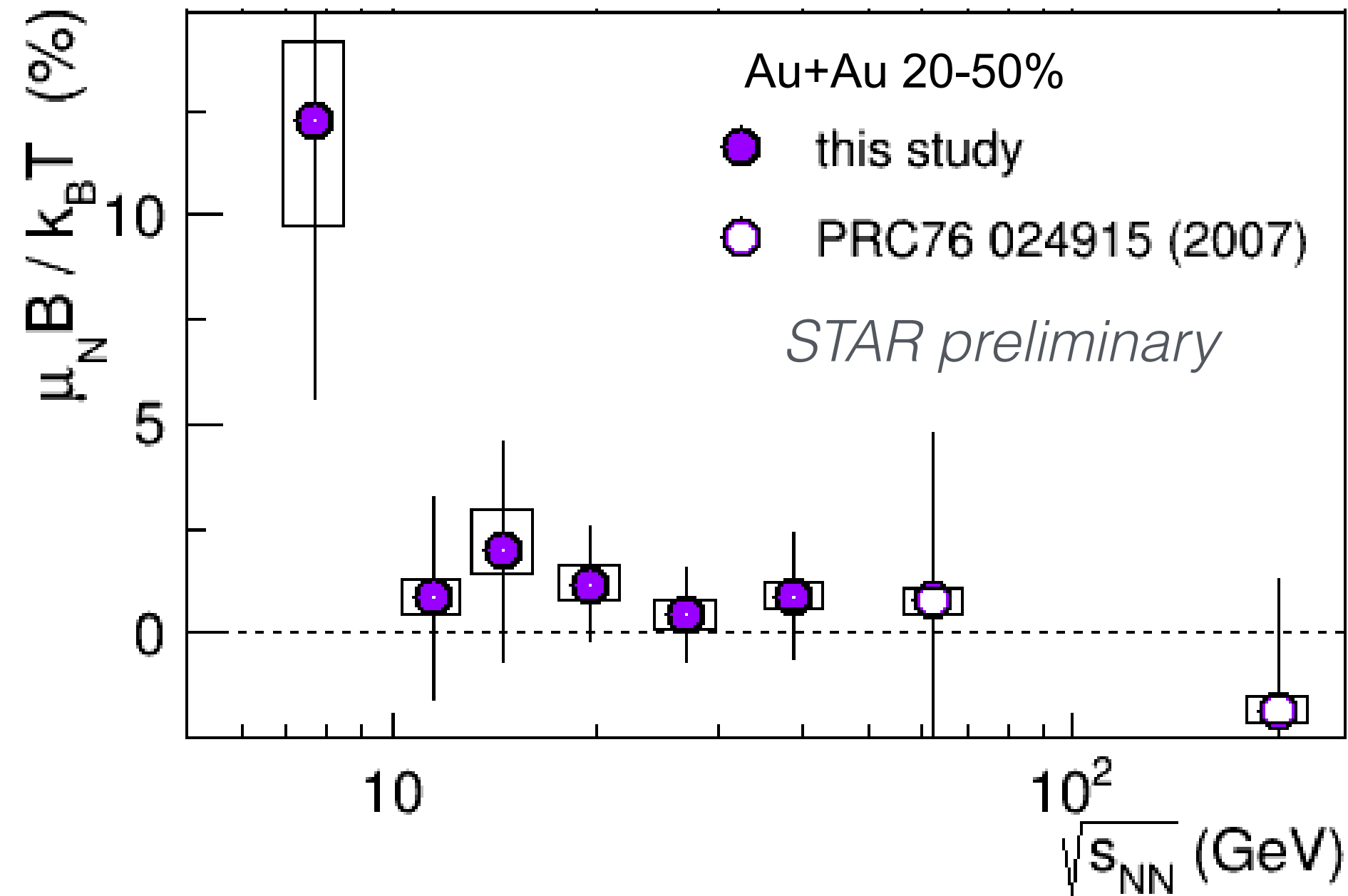
$\mu_{\Lambda}$ :  $\Lambda$  magnetic moment

$$B = (P_{\Lambda} - P_{\bar{\Lambda}}) k_B T / \mu_N$$

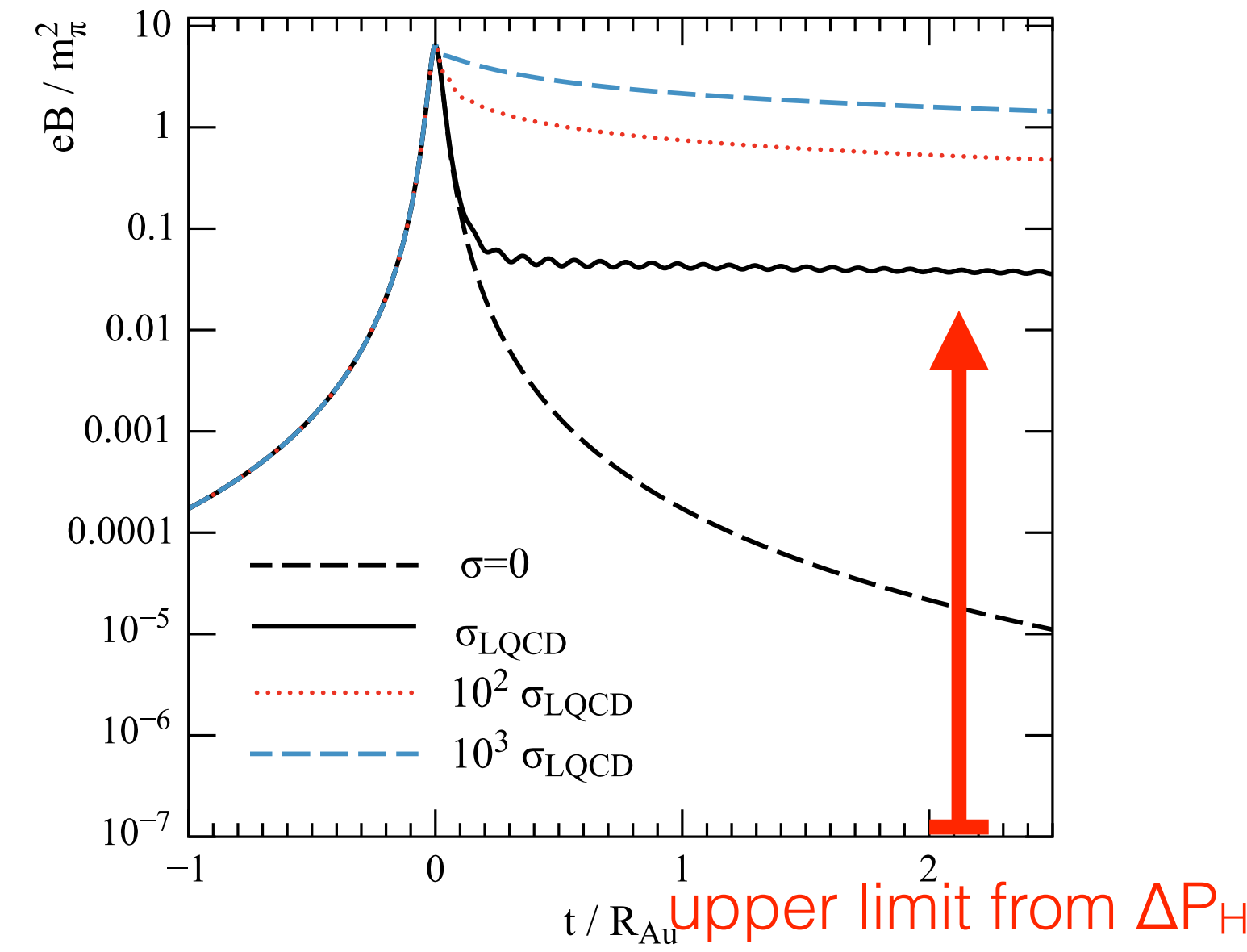
$$\sim 5.0 \times 10^{13} \text{ [Tesla]}$$

nuclear magneton  $\mu_N = -0.613 \mu_{\Lambda}$

QM17, I. Upsal (STAR)



McLerran and Skokov, Nucl. Phys. A929, 184 (2014)



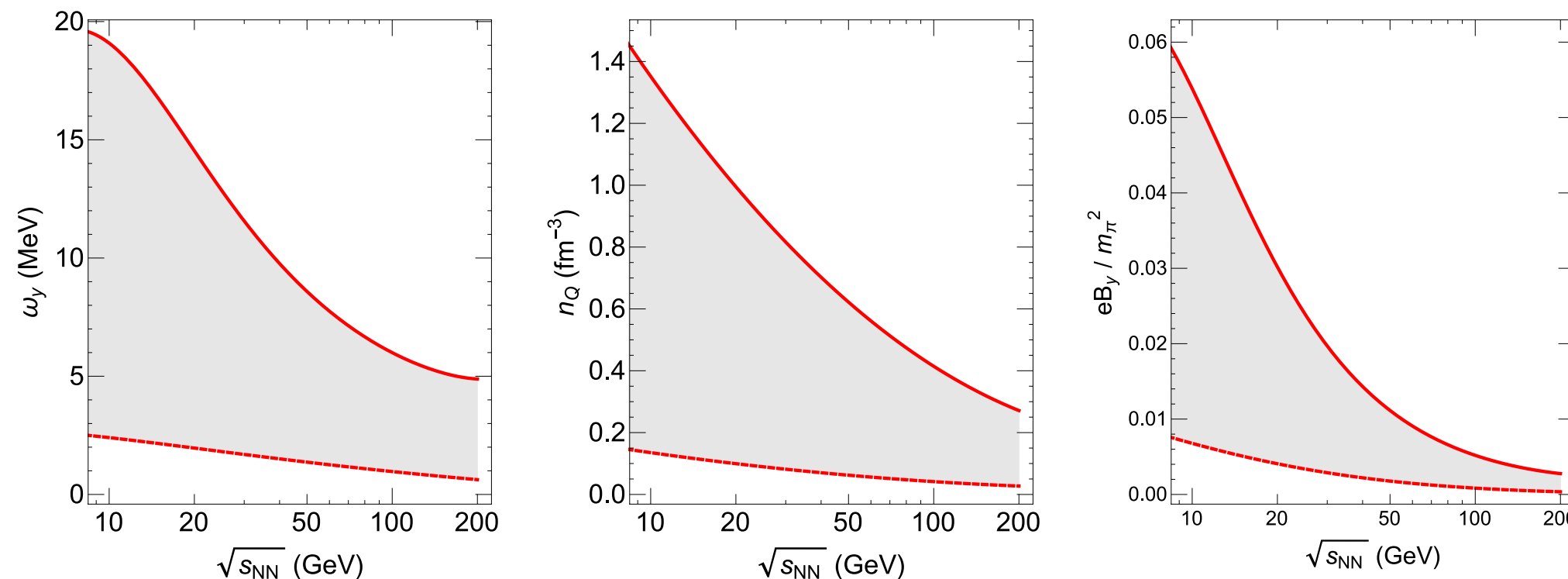
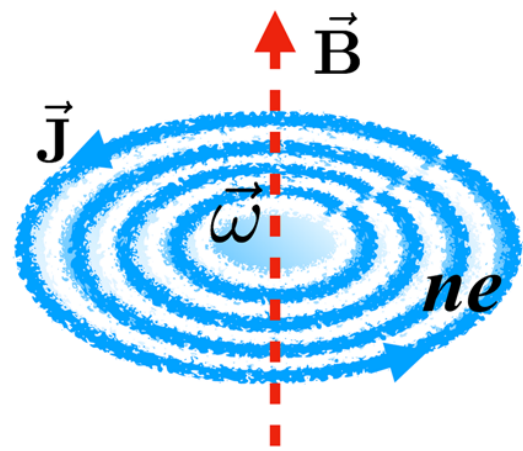
Conductivity increases lifetime.

- B-field at freeze-out could be probed by  $\Lambda$ -anti $\Lambda$  splitting
  - Current results are consistent with zero (except 7.7 GeV)
  - The small splitting could be also due to other effects

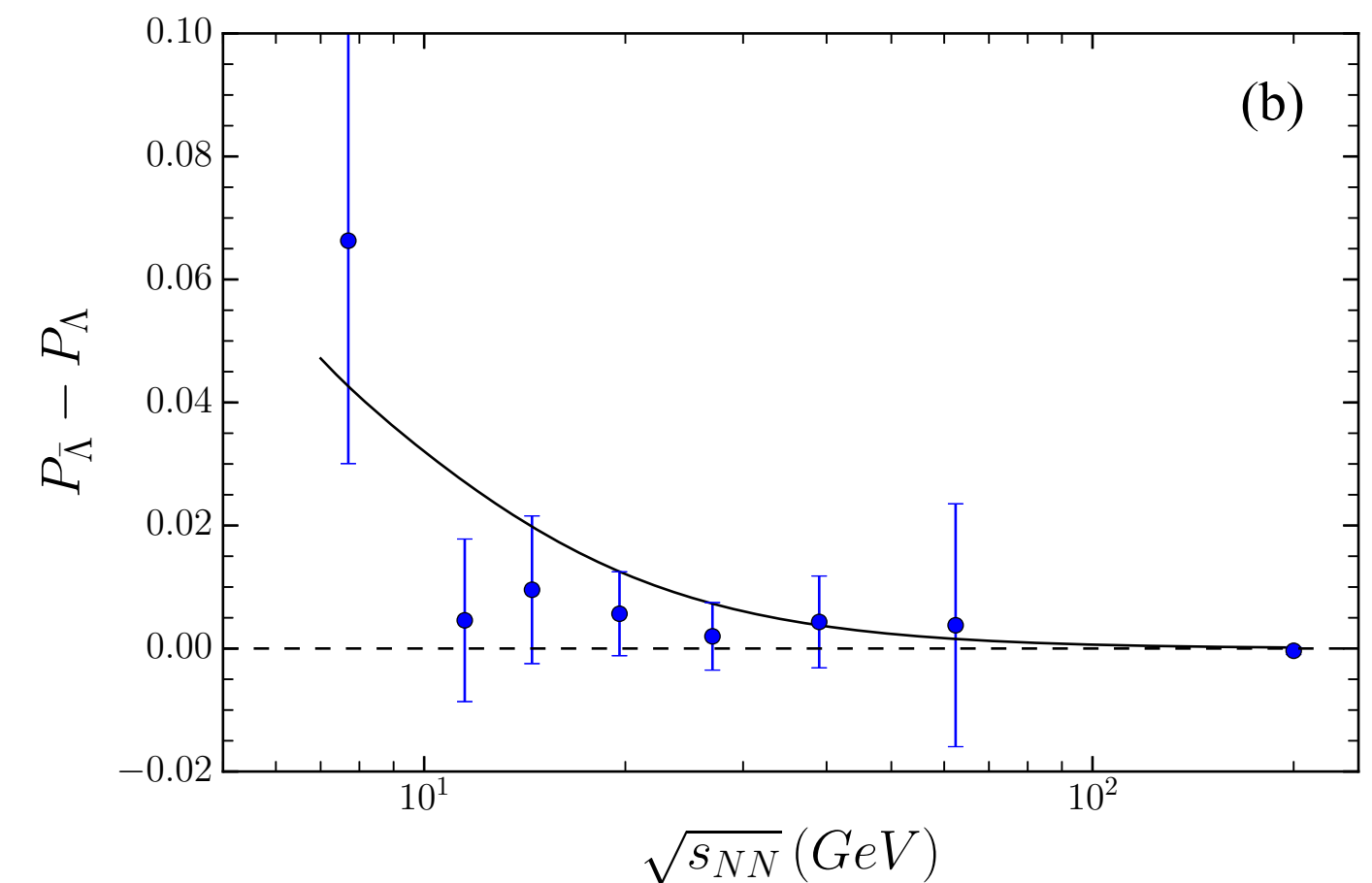
# But need caution for the interpretation

$\Lambda$ -anti $\Lambda$   $P_H$  splitting could be also due to other effects:

- Effect of chemical potential, expected to be small  
R. Fang et al., PRC94, 024904 (2016)
- Rotating charged fluid produces B-field with longer lifetime  
X. Guo, J. Liao, and E. Wang, PRC99.021901(R) (2019)
- Spin interaction with the meson field generated by the baryon current  
L. Csernai, J. Kapusta, and T. Welle, PRC99.021901(R) (2019)
- Different space time distributions and freeze-out of  $\Lambda$  and anti $\Lambda$   
O. Vitiuk, L.Bravina, E. Zabrodin, PLB803(2020)135298

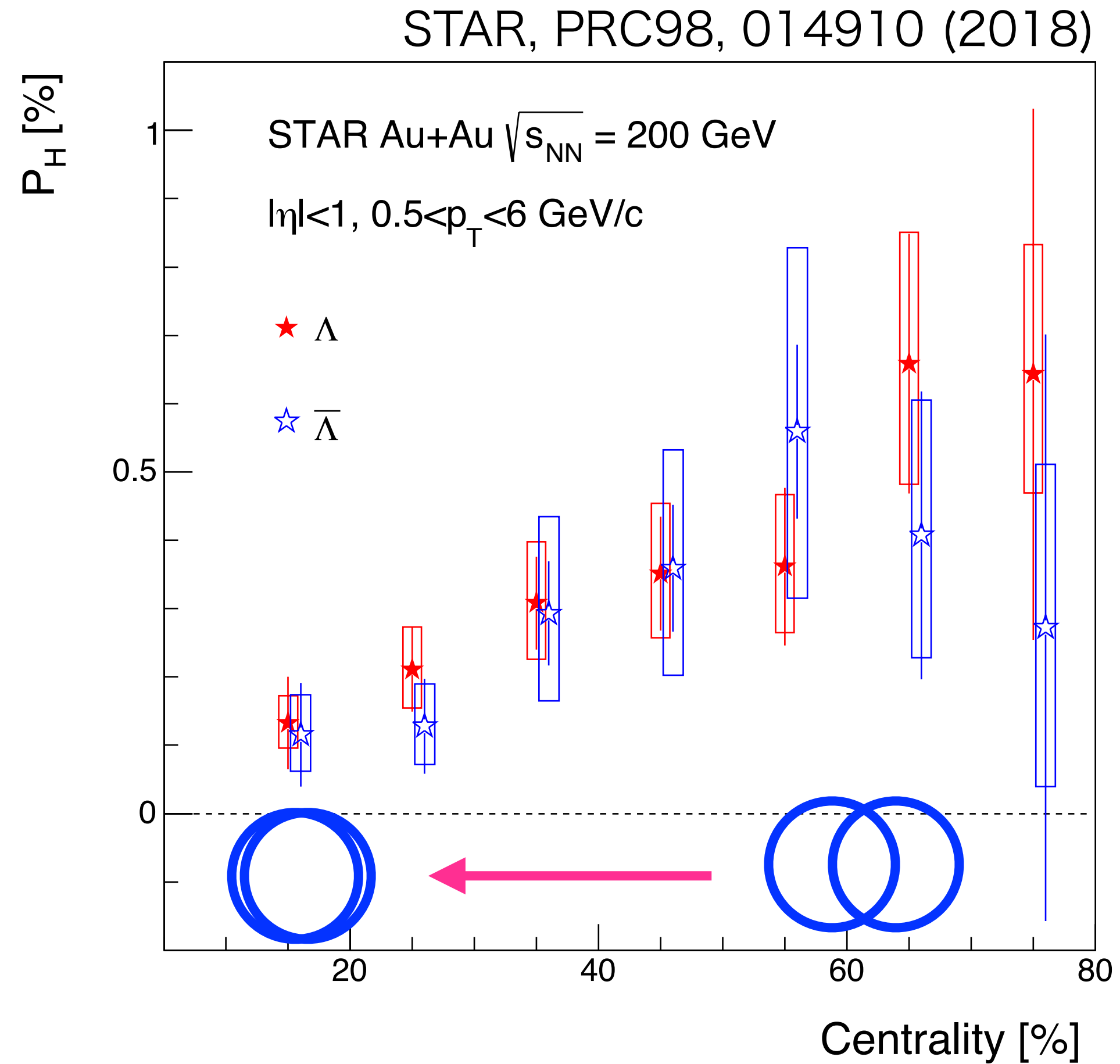


X. Guo, J. Liao, and E. Wang, PRC99.021901(R) (2019)

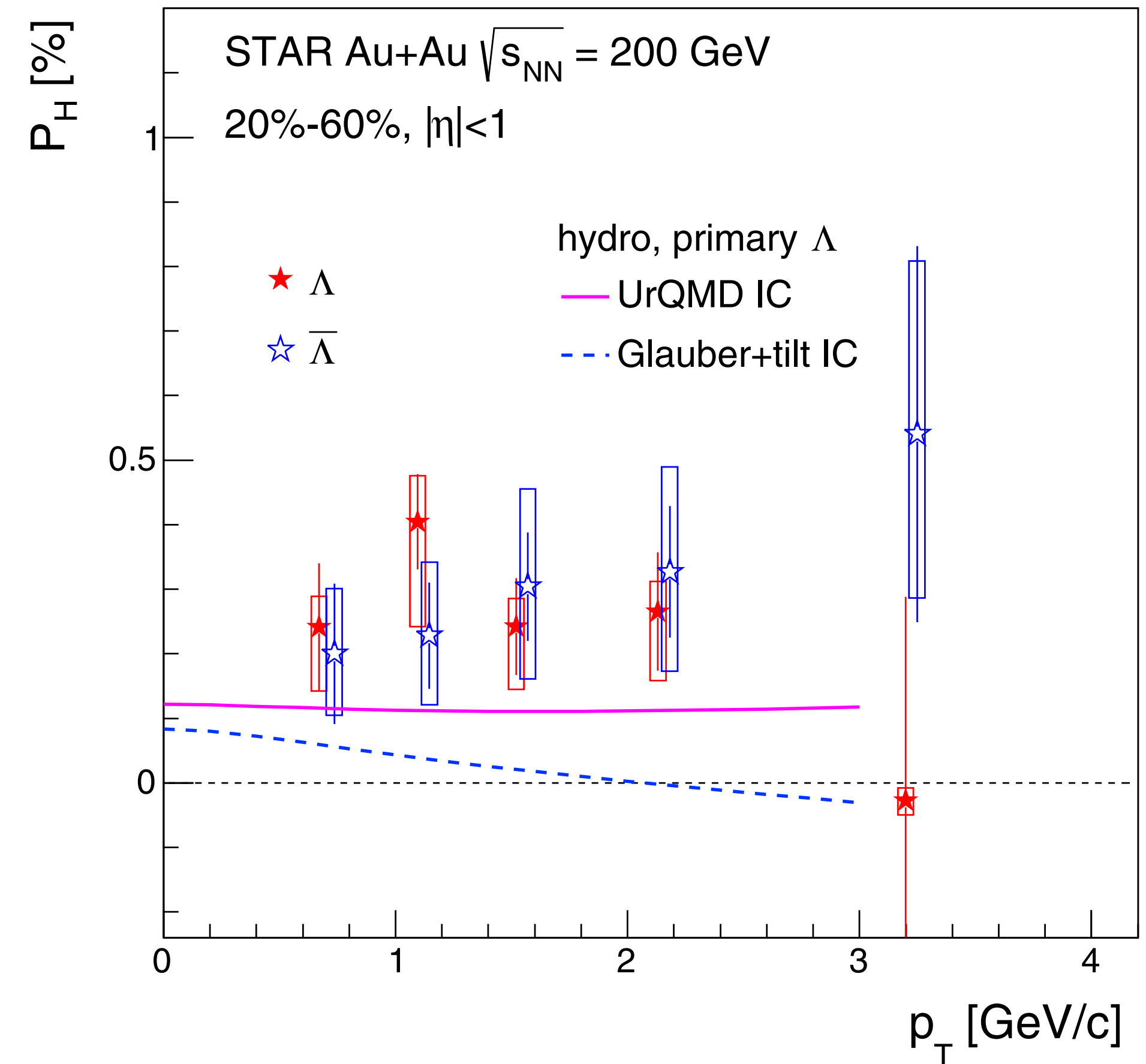


L. Csernai, J. Kapusta, and T. Welle, PRC99.021901(R) (2019)

# Differential measurements: centrality and $p_T$

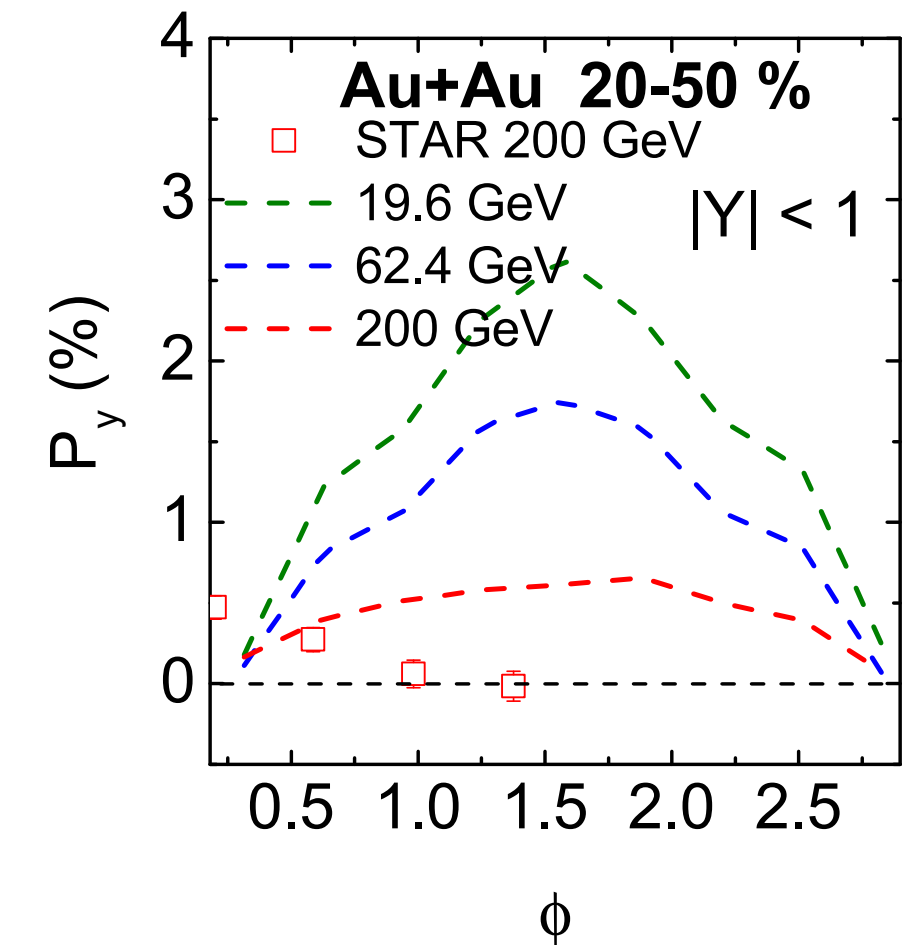
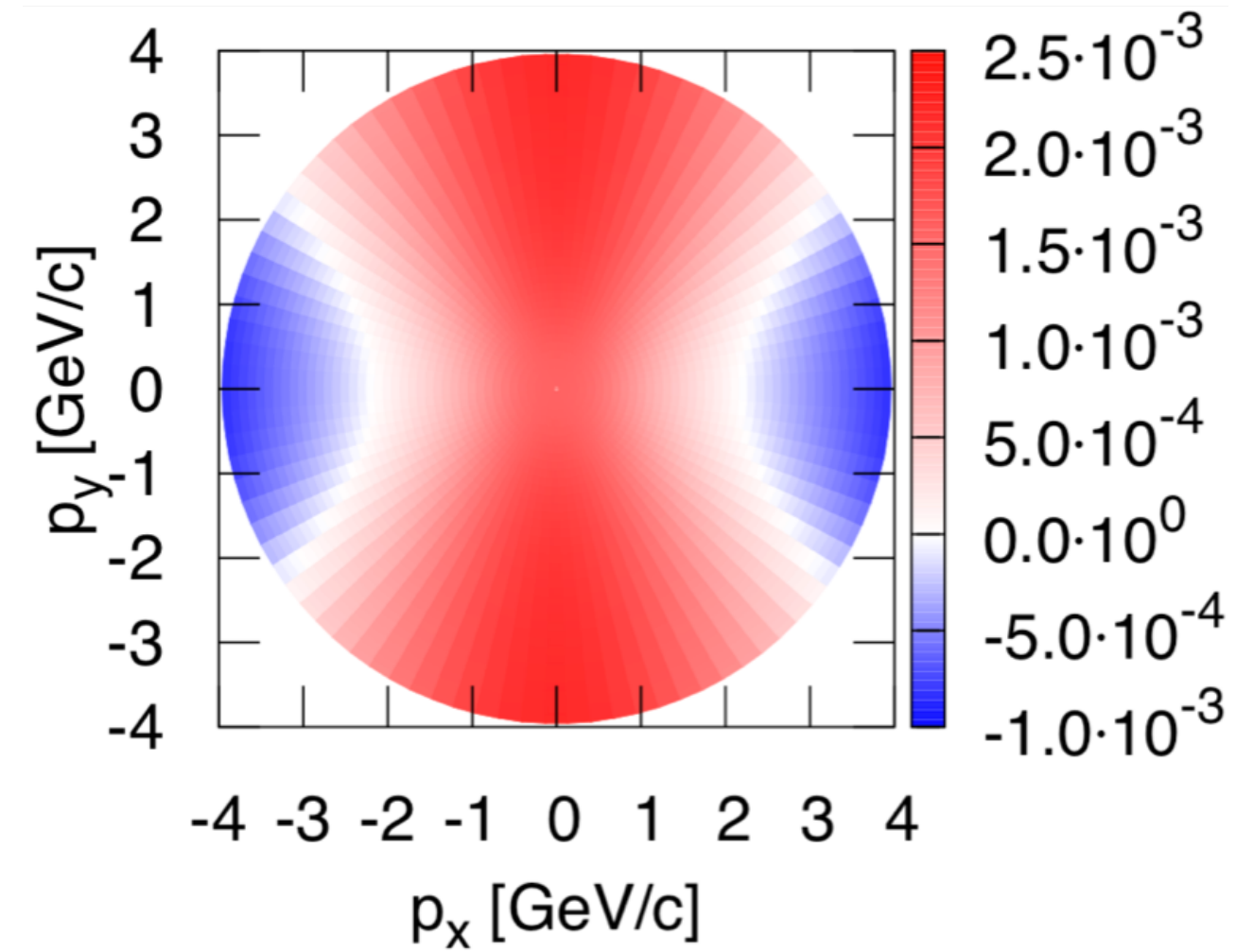
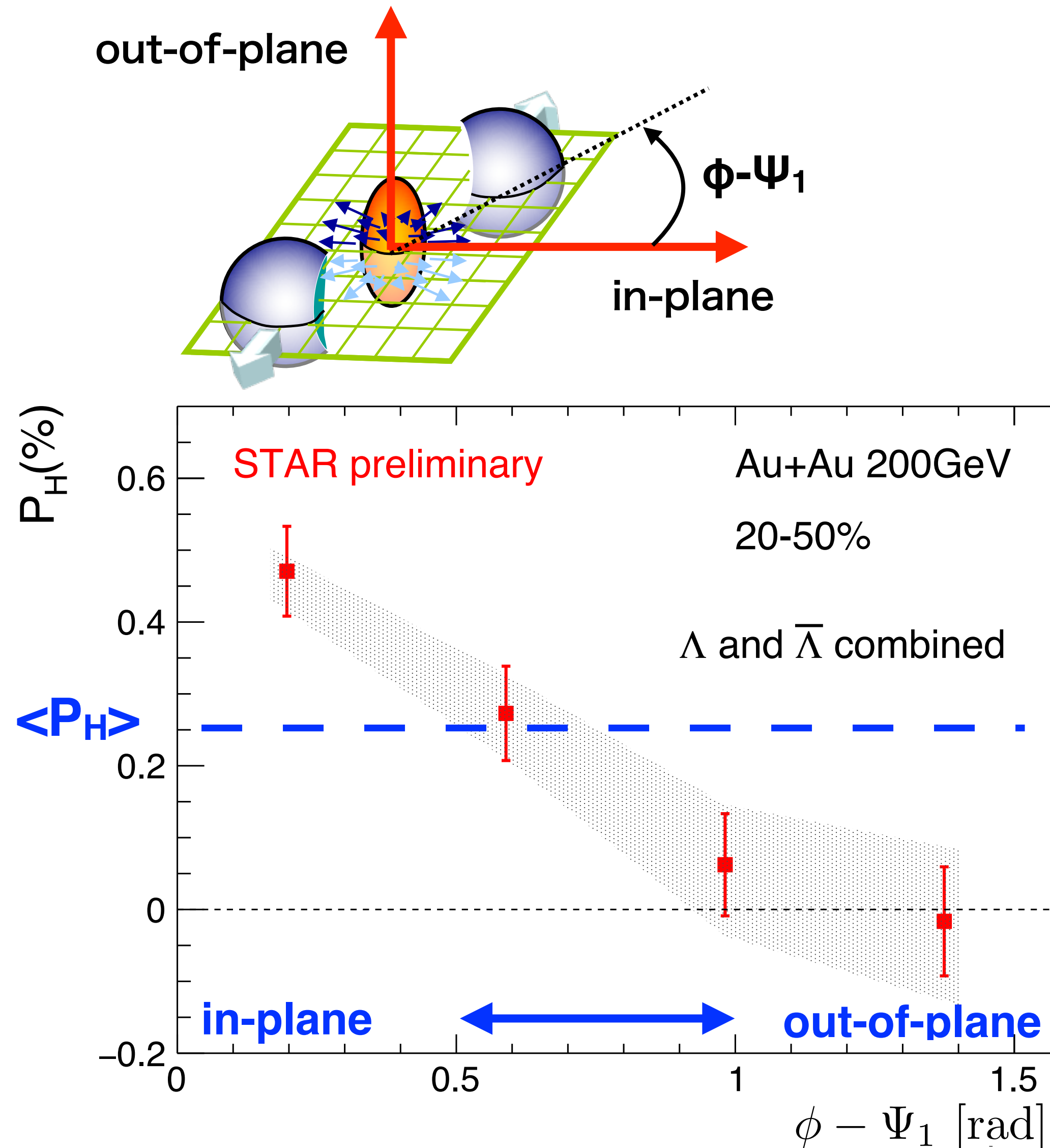


In most central collision  $\rightarrow$  no initial angular momentum  
 The polarization decreases in more central collisions.



- Naive expectation of smaller  $P_H$  due to scattering at low  $p_T$ , fragmented at high  $p_T$
- No clear  $p_T$  dependence with current precision

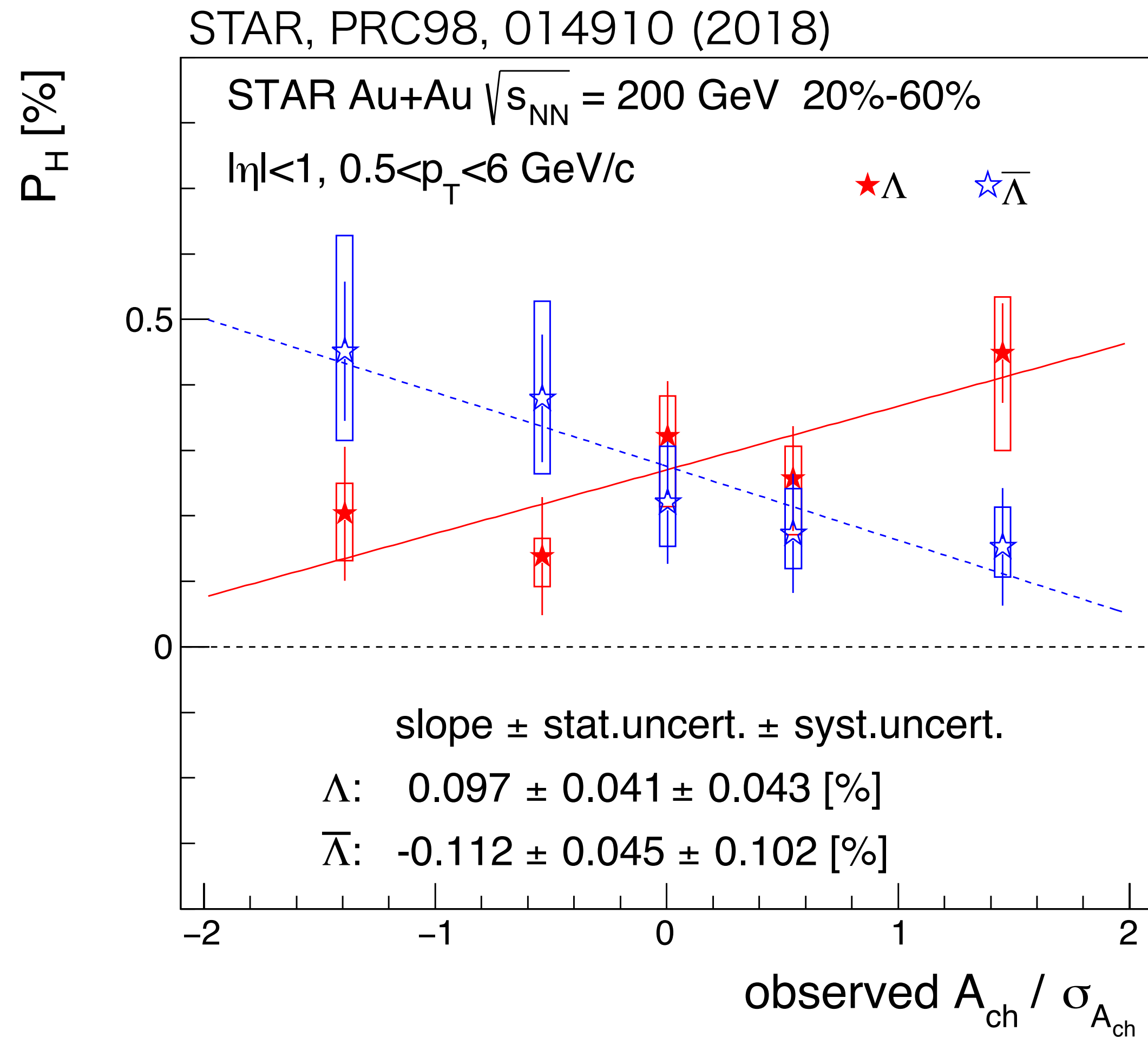
# Differential measurements: azimuthal angle



I. Karpenko and F. Becattini, EPJC(2017)77.213  
 D. Wei, W. Deng, and X. Huang,  
 PRC99.014905 (2019)  
 H. Wu et al., PR.Research1.033058 (2019)

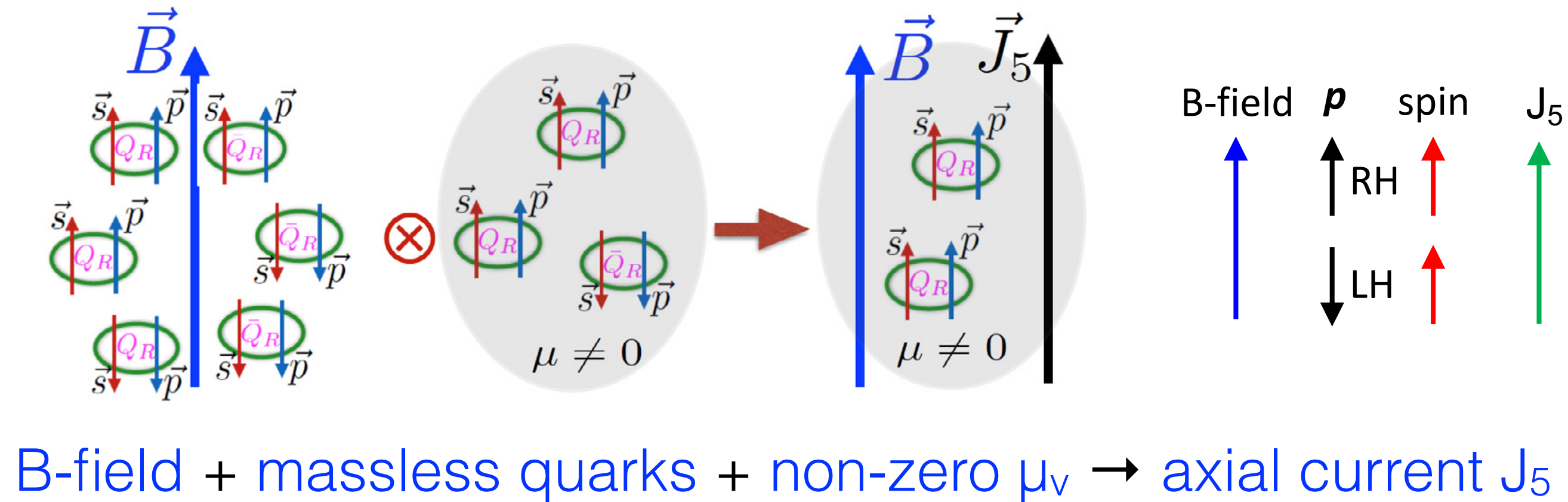
- The data shows larger polarization in in-plane, while many models predict the opposite, i.e. larger in out-of-plane
- Not fully understood yet

# Differential measurements: charge asymmetry



$$\mu_v / T \propto \frac{\langle N_+ - N_- \rangle}{\langle N_+ + N_- \rangle} = A_{ch}$$

Chiral Separation Effect  $\mathbf{J}_5 \propto e\mu_v \mathbf{B}$



- $A_{ch}$  dependence observed
  - Slopes of  $\Lambda$  and anti- $\Lambda$  seem to be opposite ( $\sim 2\sigma$  level)
- Possible contribution from axial charge or
- Quark vector chemical potential may explain the data

Sun and Ko, INT20-1-c

# Spin alignment of vector mesons

Angular distribution of the decay products can be written with spin density matrix  $\rho_{nn}$ .

$$\frac{dN}{d \cos \theta^*} \propto \rho_{0,0}|Y_{1,0}|^2 + \rho_{1,1}|Y_{1,-1}|^2 + \rho_{-1,-1}|Y_{1,1}|^2 \propto \rho_{0,0} \cos^2 \theta^* + \frac{1}{2}(\rho_{1,1} + \rho_{-1,-1}) \sin^2 \theta^*$$

$$\propto (1 - \rho_{0,0}) + (3\rho_{0,0} - 1) \cos^2 \theta^*$$

$$\rho_{00} = \frac{1}{3} - \frac{8}{3} \langle \cos[2(\phi_p^* - \Psi_{RP})] \rangle$$

Deviation from 1/3 in  $\rho_{00}$  indicates spin alignment.

\* sign of the polarization cannot be determined.  
Therefore it's called "spin alignment measurement" rather than "polarization measurement"

Z.-T. Liang and X.-N. Wang, PRL94.102301(2005)  
Y. Yang et al., PRC97.034917(2018)

Species	$K^{*0}$	$\phi$
Quark content	$\bar{d}s$	$s\bar{s}$
Mass (MeV/c <sup>2</sup> )	896	1020
Lifetime (fm/c)	4	45
Spin (J <sup>P</sup> )	1 <sup>-</sup>	1 <sup>-</sup>
Decays	K $\pi$	KK
Branching ratio	<b>~100%</b>	66%

Theoretical expectation for  $\rho_{00}$

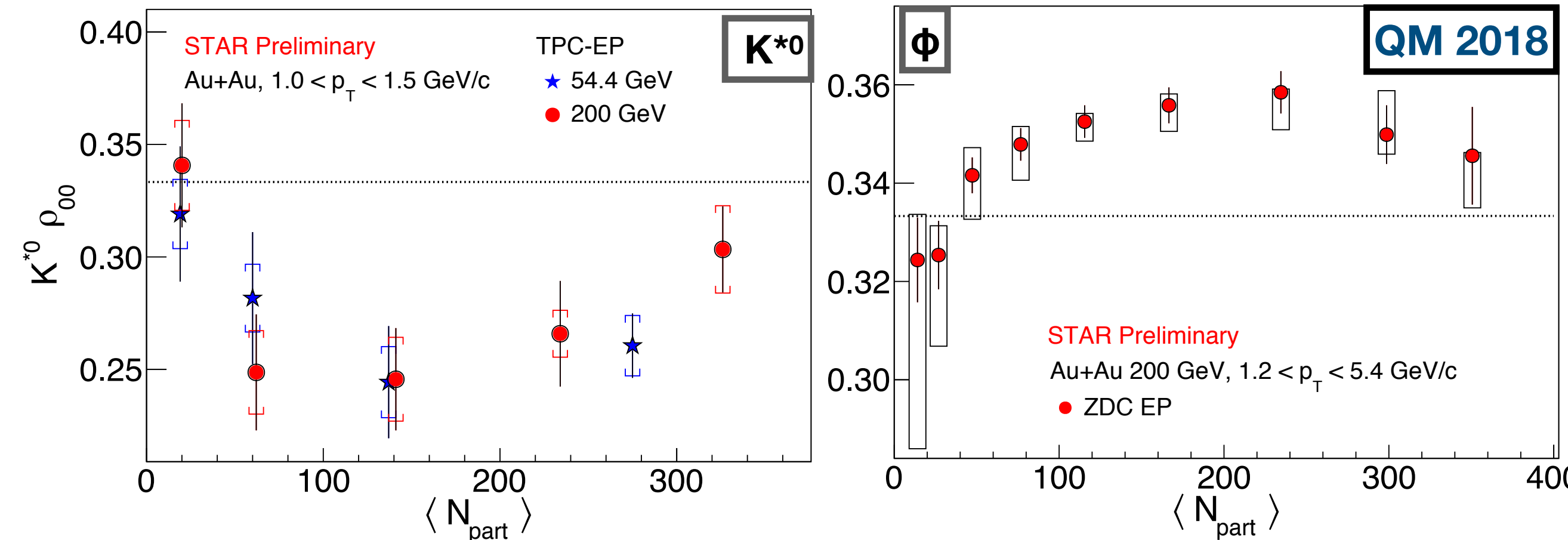
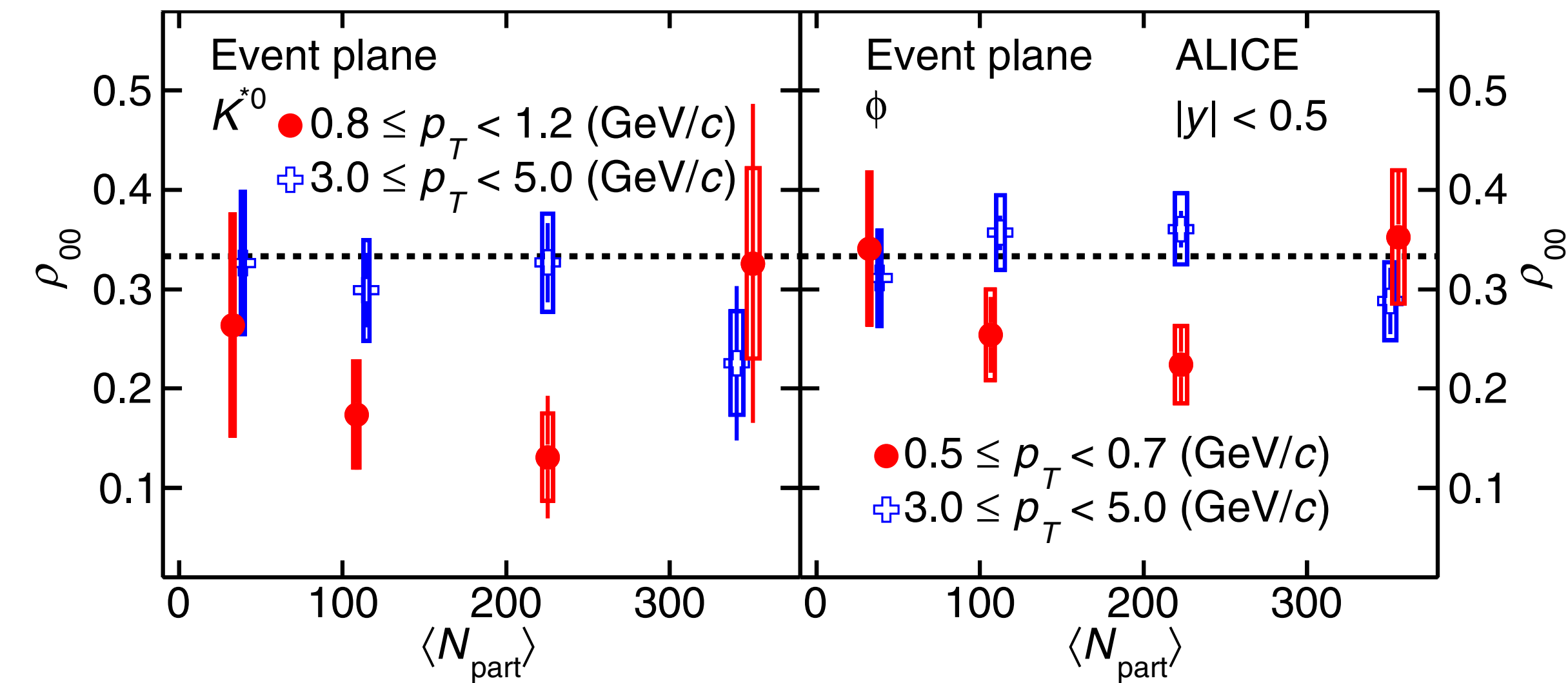
Vorticity recombination	$\rho_{00} < 1/3$
fragmentation	$\rho_{00} > 1/3$
Magnetic field	$\rho_{00} > 1/3$ (for neutral vector mesons)



# Results from LHC and RHIC

ALICE, PRL125.012301 (2020)

STAR, QM18, QM19



- Large deviation from  $1/3$ , which cannot be explained by vorticity picture

$$\rho_{00} = 1/[3 + (\omega/T)^2].$$

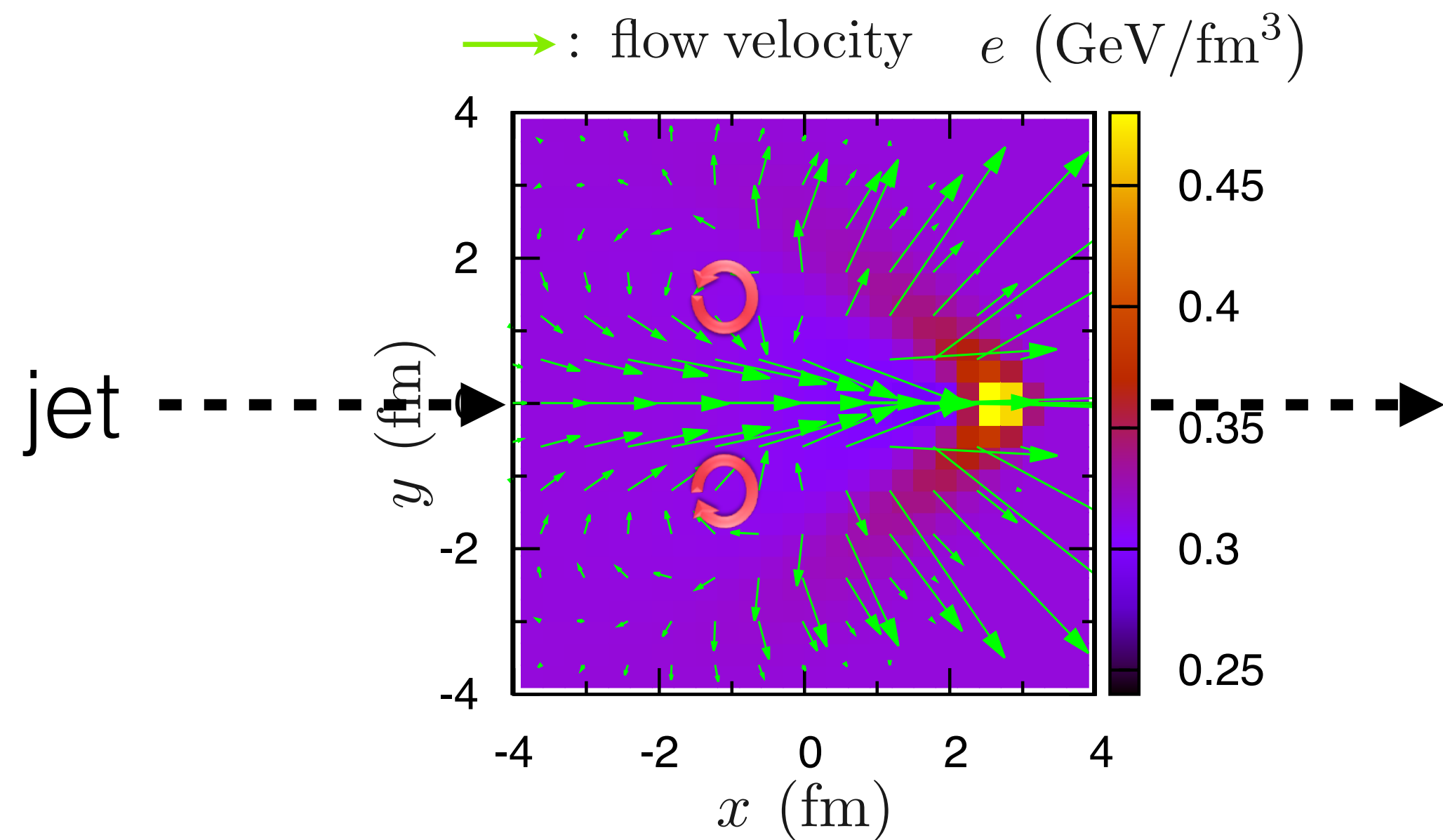
- The deviation in opposite way between:
  - $K^*$  and  $\phi$  at RHIC
  - LHC and RHIC for  $\phi$

Mean field of  $\phi$  meson may play a role?  
Does it change from RHIC to LHC only for  $\phi$ ?

X. Sheng, L. Oliva, and Q. Wang, PRD101.096005(2020)  
X. Sheng, Q.Wang, and X. Wang, PRD102.056013 (2020)

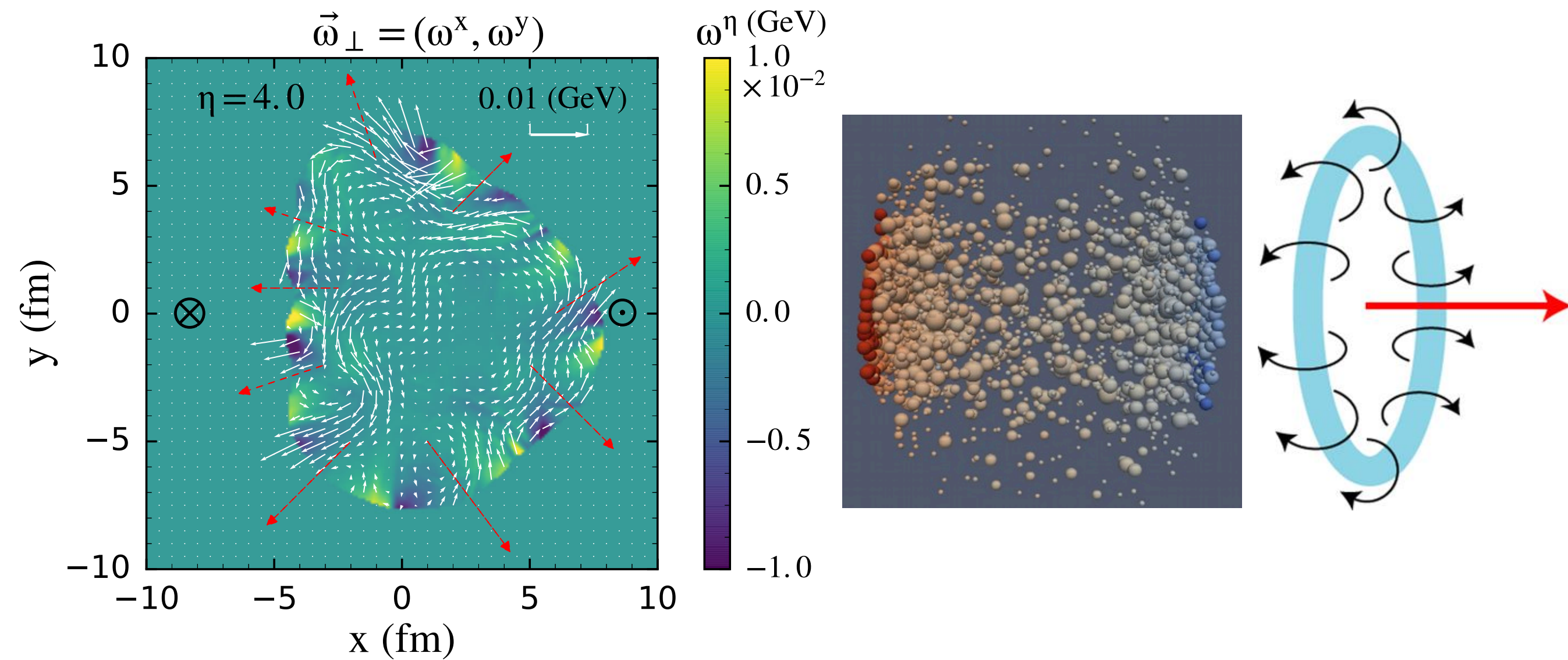
# Local vorticity

Vortex induced by jet



Y. Tachibana and T. Hirano, NPA904-905 (2013) 1023  
 B. Betz, M. Gyulassy, and G. Torrieri, PRC76.044901 (2007)

Local vorticity induced by collective flow

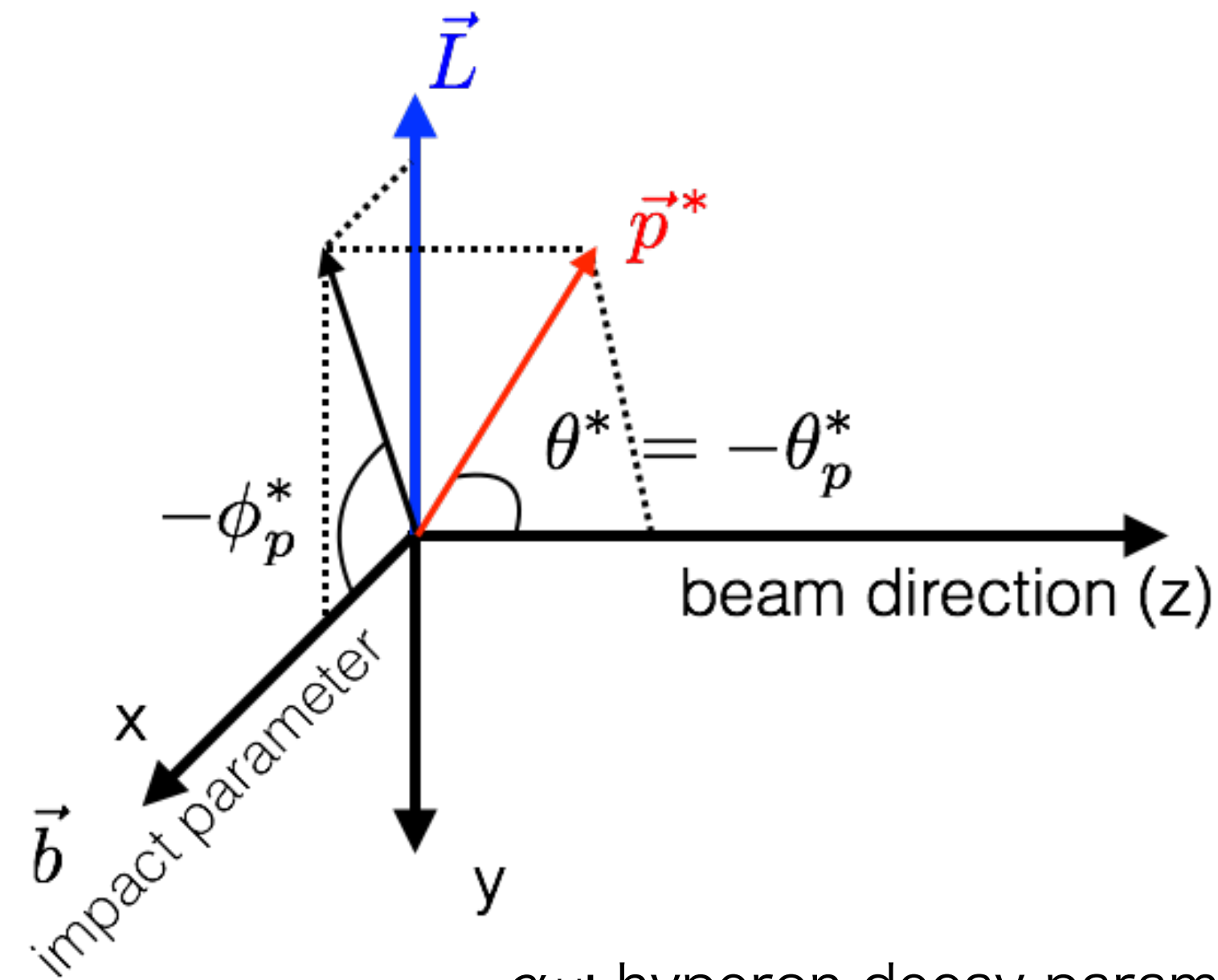
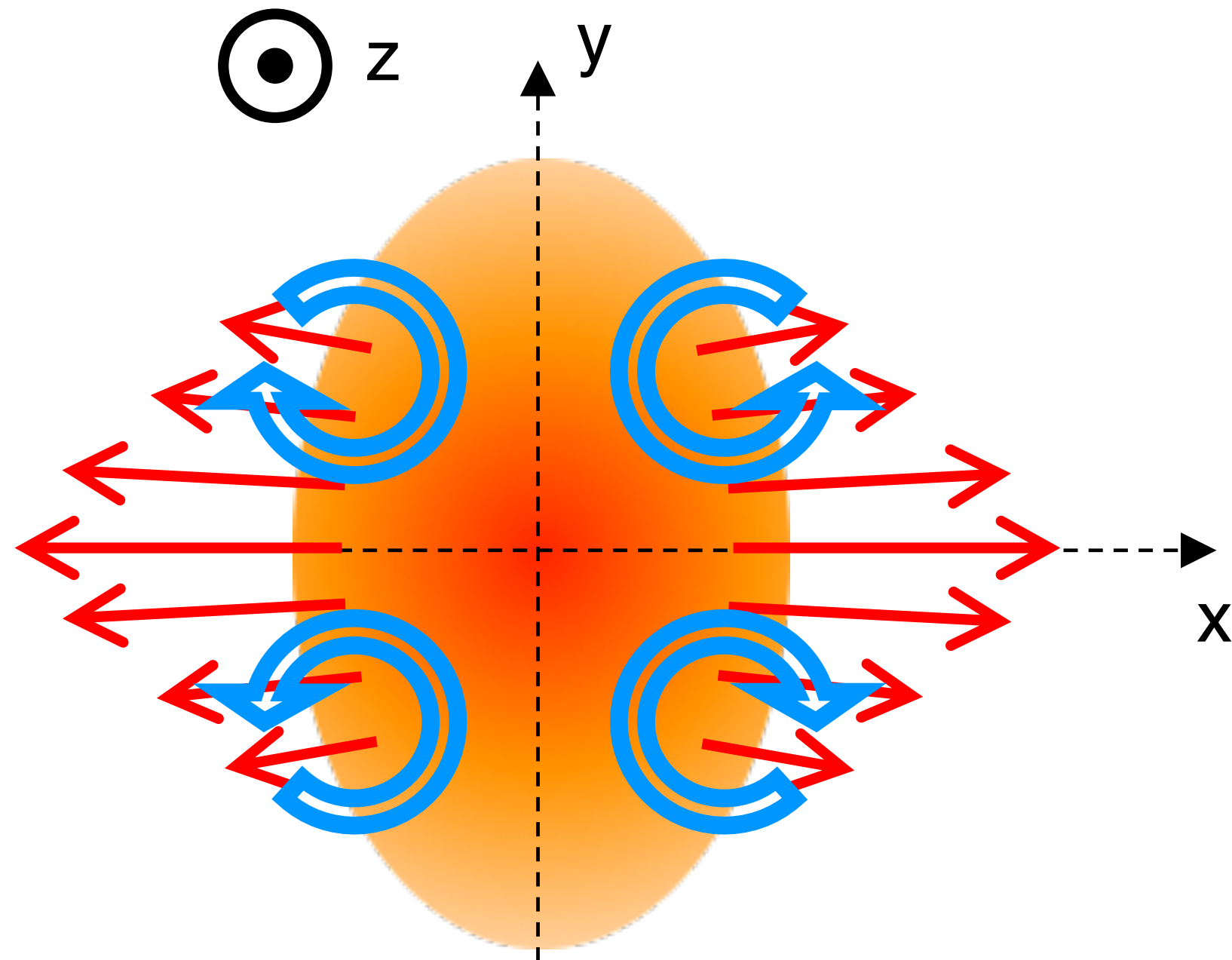


L.-G. Pang, H. Peterson, Q. Wang, and X.-N. Wang, PRL117, 192301 (2016)  
 F. Becattini and I. Karpenko, PRL120.012302 (2018)  
 S. Voloshin, EPJ Web Conf.171, 07002 (2018)  
 X.-L. Xia et al., PRC98.024905 (2018)

# Polarization along the beam direction

S. Voloshin, SQM2017

F. Becattini and I. Karpenko, PRL120.012302 (2018)



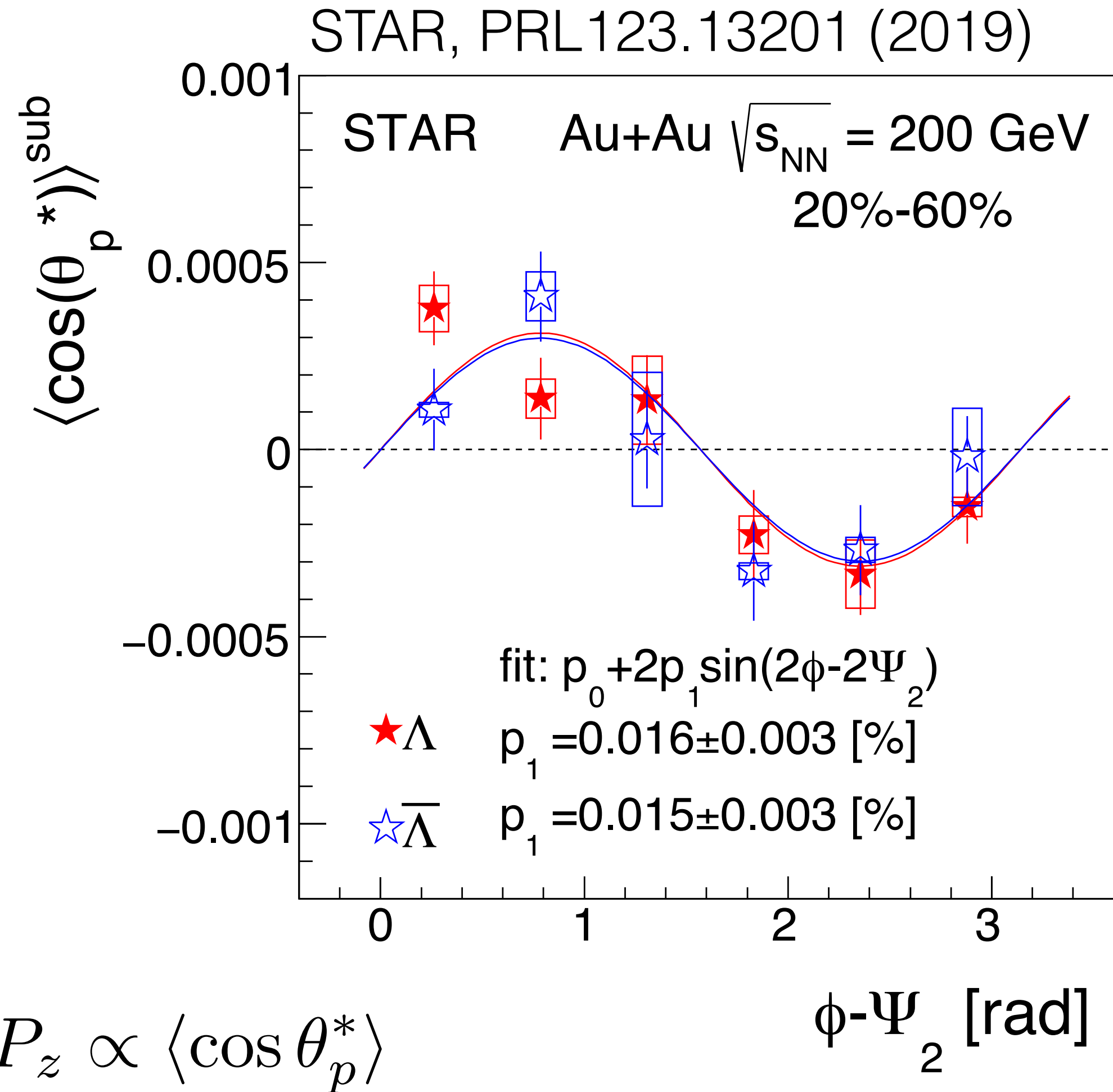
$\alpha_H$ : hyperon decay parameter

$\theta_p^*$ :  $\theta$  of daughter proton in  $\Lambda$  rest frame

$$\begin{aligned} \frac{dN}{d\Omega^*} &= \frac{1}{4\pi} (1 + \alpha_H \mathbf{P}_H \cdot \mathbf{p}_p^*) \\ \langle \cos \theta_p^* \rangle &= \int \frac{dN}{d\Omega^*} \cos \theta_p^* d\Omega^* \\ &= \alpha_H P_z \langle (\cos \theta_p^*)^2 \rangle \\ \therefore P_z &= \frac{\langle \cos \theta_p^* \rangle}{\alpha_H \langle (\cos \theta_p^*)^2 \rangle} \\ &= \frac{3 \langle \cos \theta_p^* \rangle}{\alpha_H} \quad (\text{if perfect detector}) \end{aligned}$$

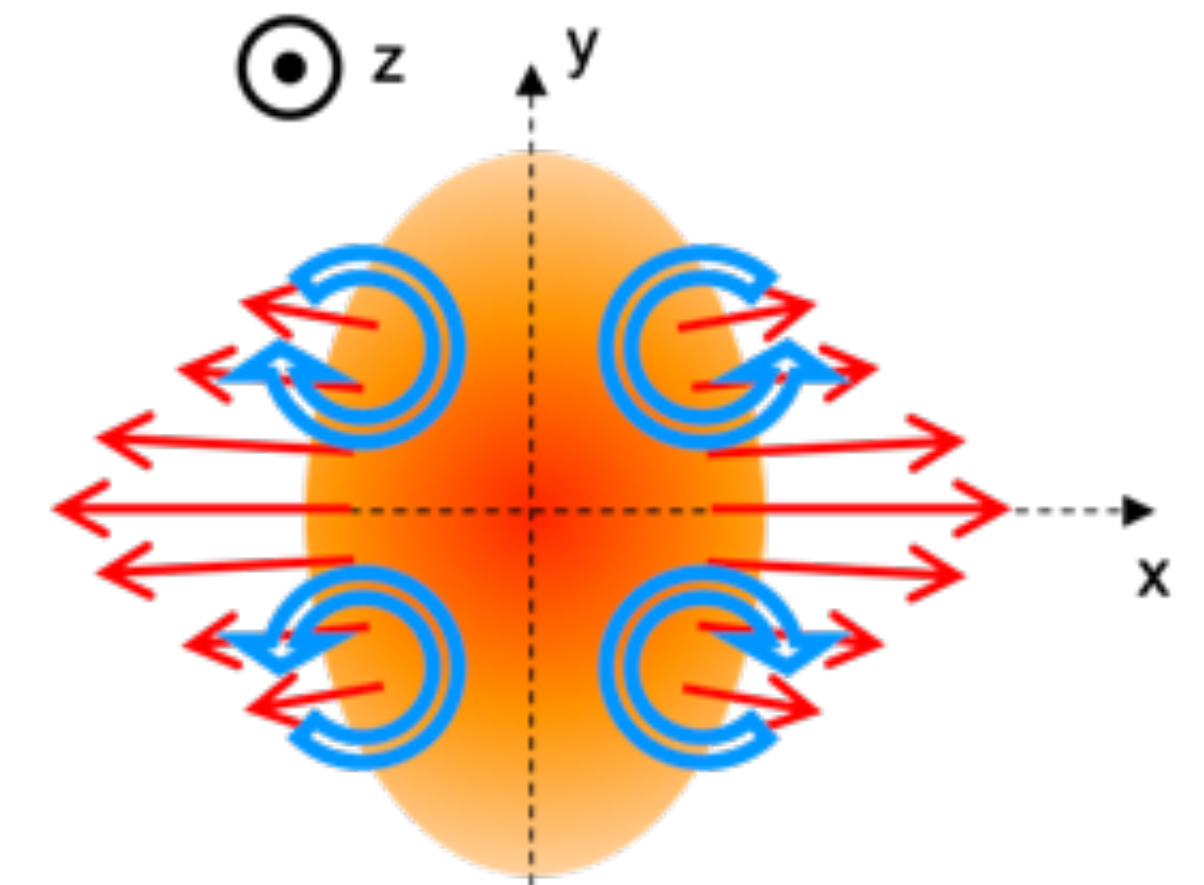
Stronger flow in in-plane than in out-of-plane  
could make local vorticity along beam axis, thus polarization

# Polarization along the beam direction



- Sine structure as expected from the elliptic flow
- Some models cannot describe the sign but some can do. Note that they reasonably describe “global”  $P_H$ .

- F. Becattini and I. Karpenko, PRL.120.012302 (2018)
- X. Xia et al., PRC98.024905 (2018)
- Y. Sun and C.-M. Ko, PRC99, 011903(R) (2019)
- Y. Xie, D. Wang, and L. P. Csernai, Eur. Phys. J. C (2020) 80:39
- W. Florkowski et al., Phys. Rev. C 100, 054907 (2019)
- H.-Z. Wu et al., Phys. Rev. Research 1, 033058 (2019)



# Disagreement in $P_z$ sign

## Opposite sign

- UrQMD IC + hydrodynamic model  
F. Becattini and I. Karpenko, PRL.120.012302 (2018)
- AMPT  
X. Xia, H. Li, Z. Tang, Q. Wang, PRC98.024905 (2018)

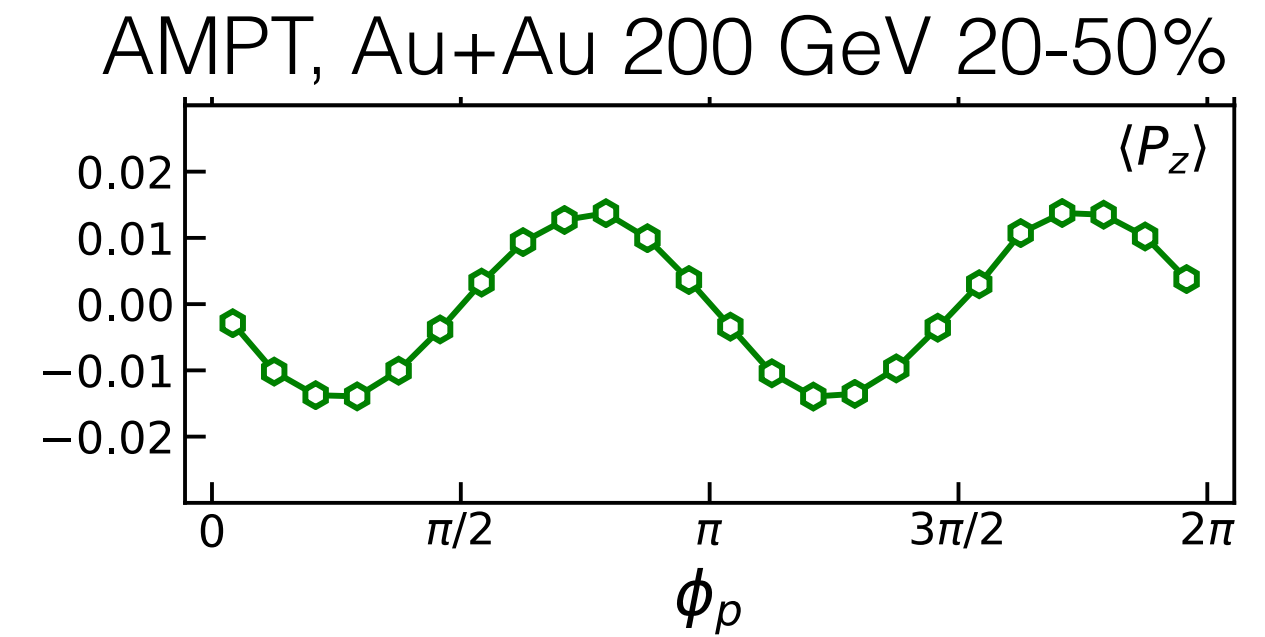
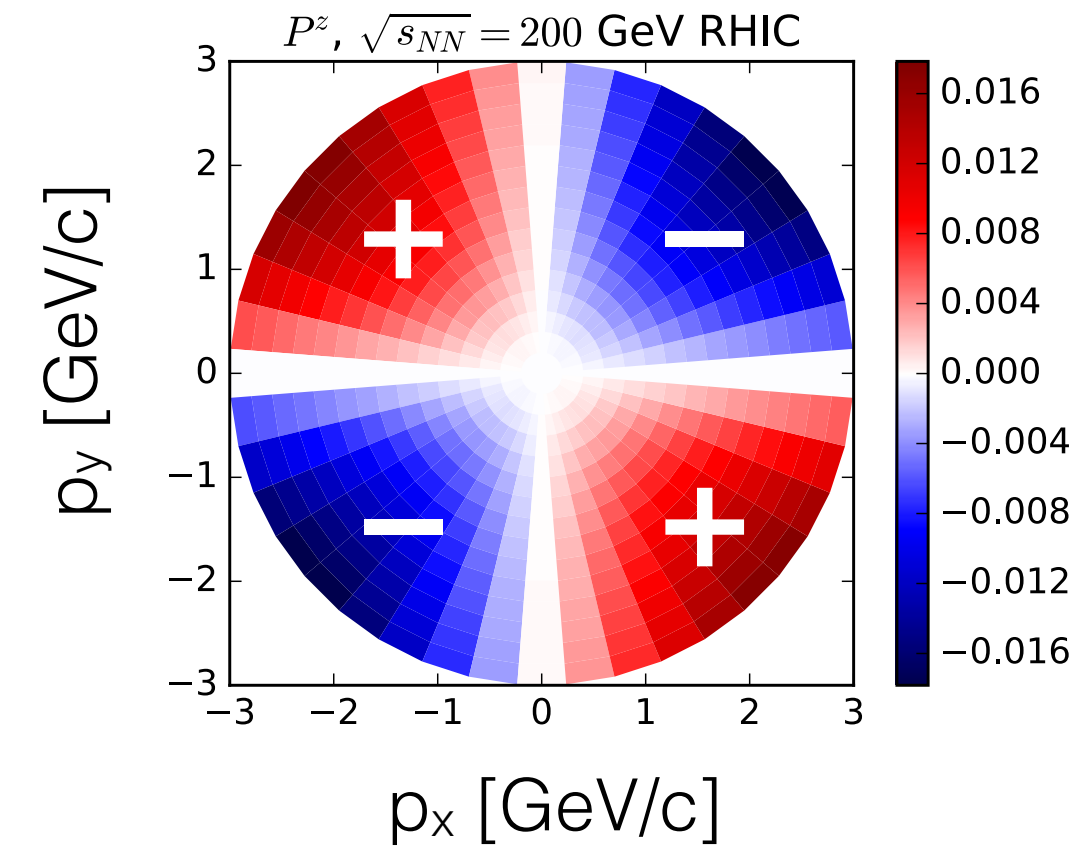
## Same sign

- Chiral kinetic approach  
Y. Sun and C.-M. Ko, PRC99, 011903(R) (2019)
- High resolution (3+1)D PICR hydrodynamic model  
Y. Xie, D. Wang, and L. P. Csernai, EPJC80.39 (2020)
- Blast-wave model  
S. Voloshin, EPJ Web Conf.171, 07002 (2018), STAR, PRL123.13201

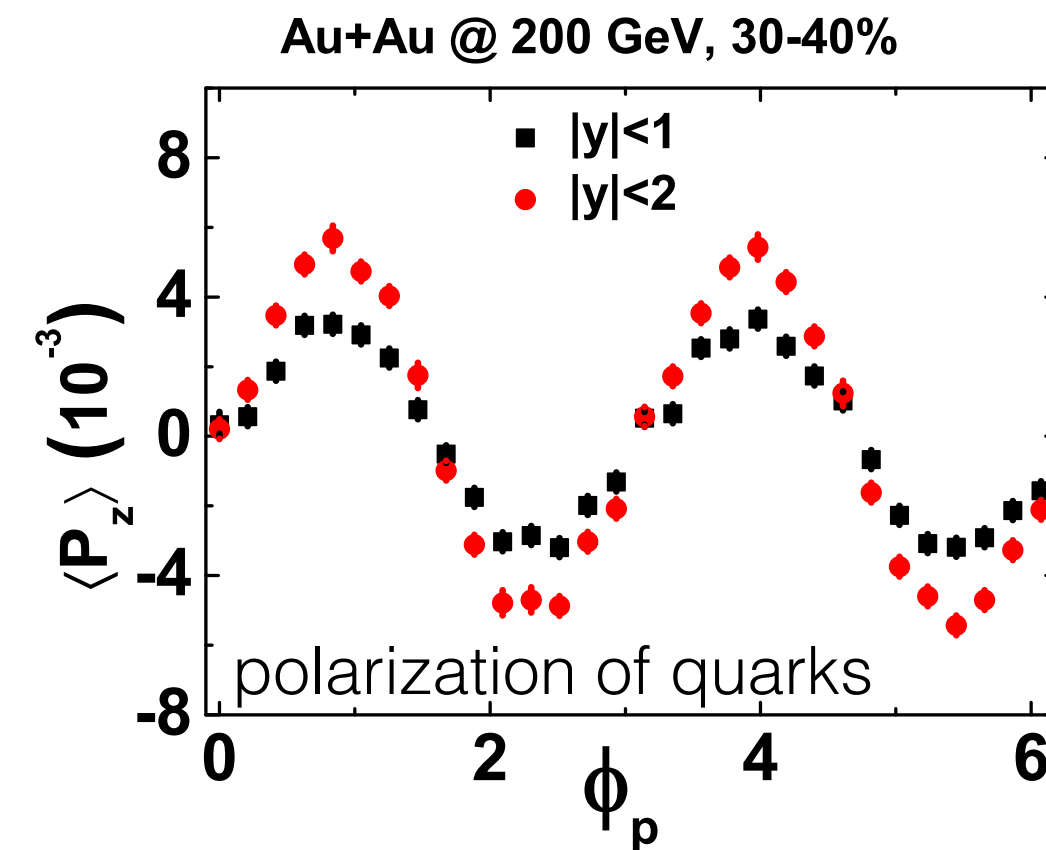
## Partly (one of component showing the same sign)

- Glauber/AMPT IC + (3+1)D viscous hydrodynamics  
H.-Z. Wu et al., Phys. Rev. Research 1, 033058 (2019)
- Thermal model  
W. Florkowski et al., Phys. Rev. C 100, 054907 (2019)

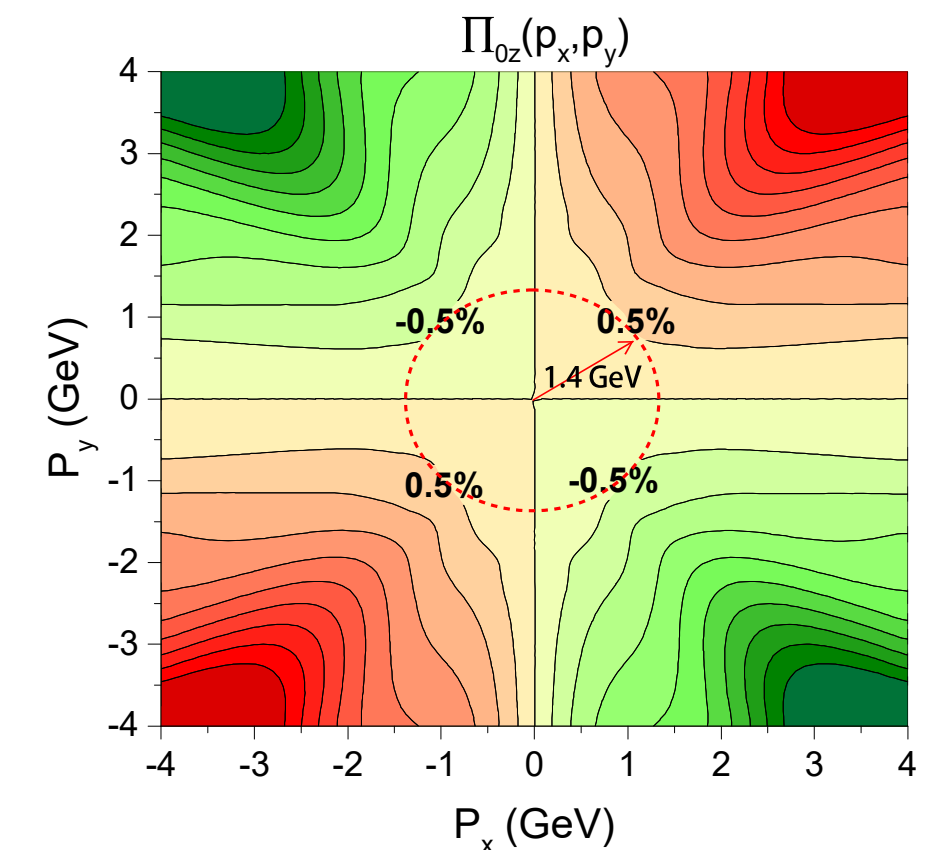
Hydrodynamic model



Chiral kinetic approach



PICR model

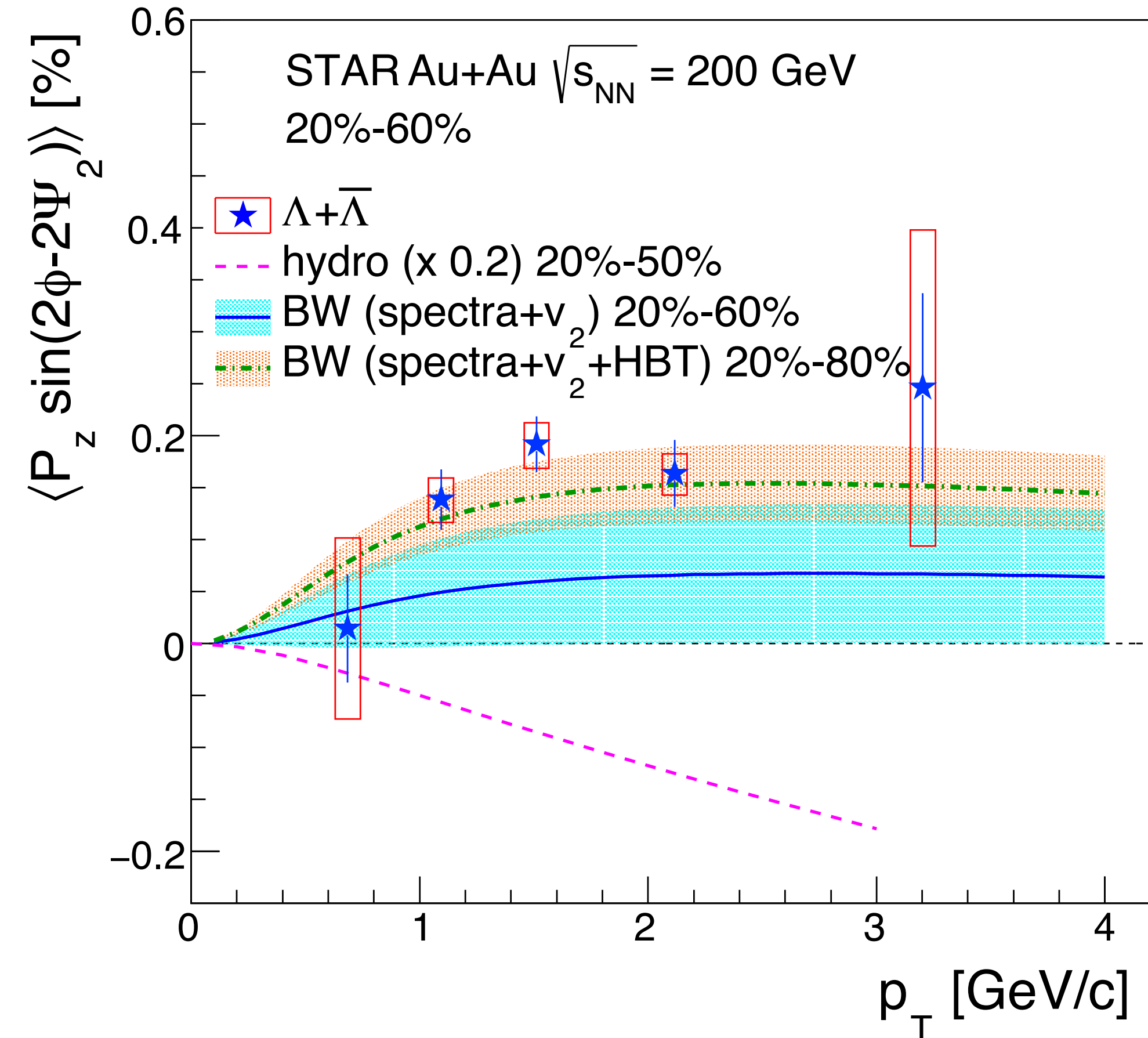
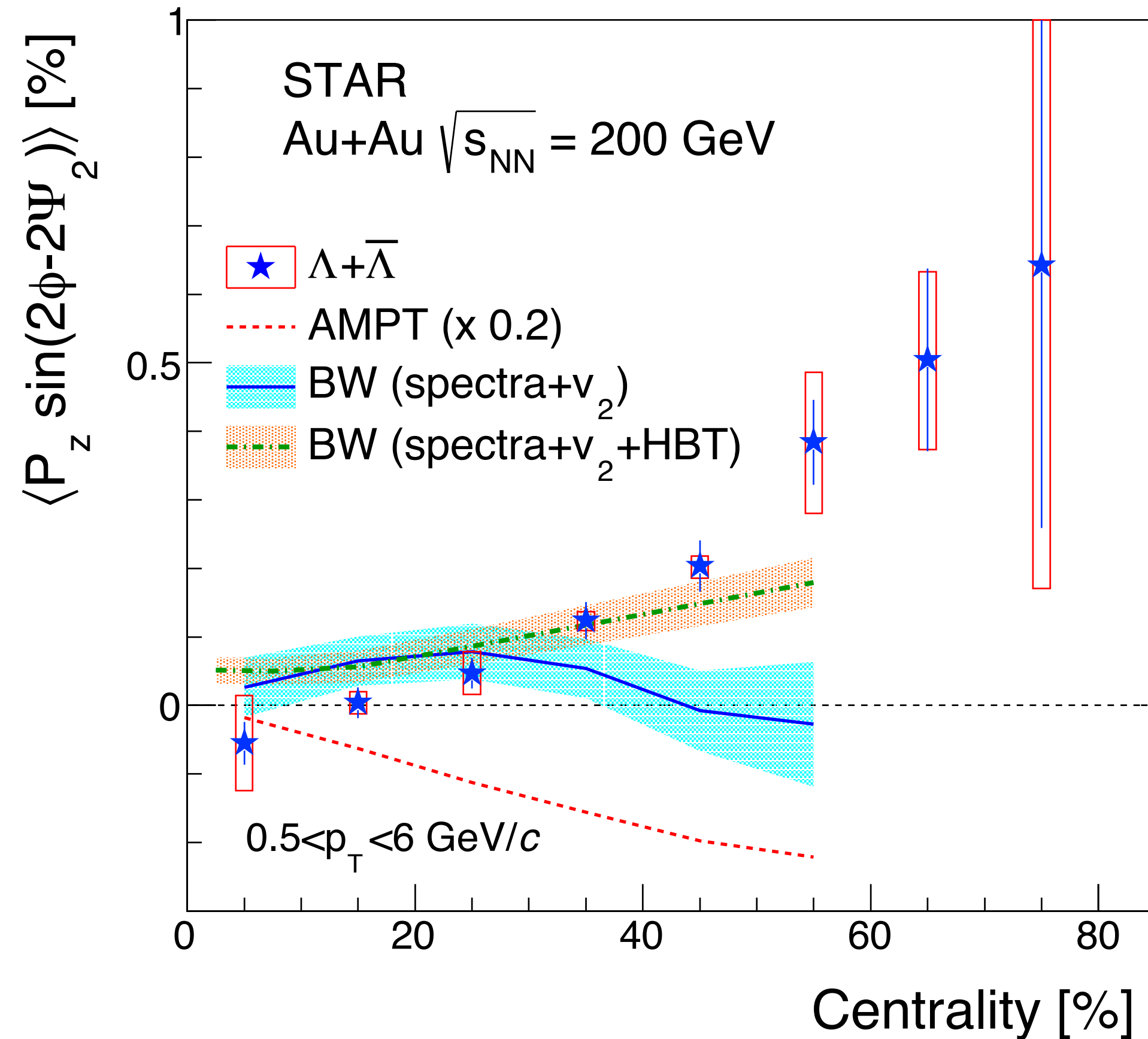


*Incomplete thermal equilibrium of spin degree of freedom?*

# Centrality and $p_T$ dependence of $P_z$ modulation

STAR, PRL123.13201 (2019)

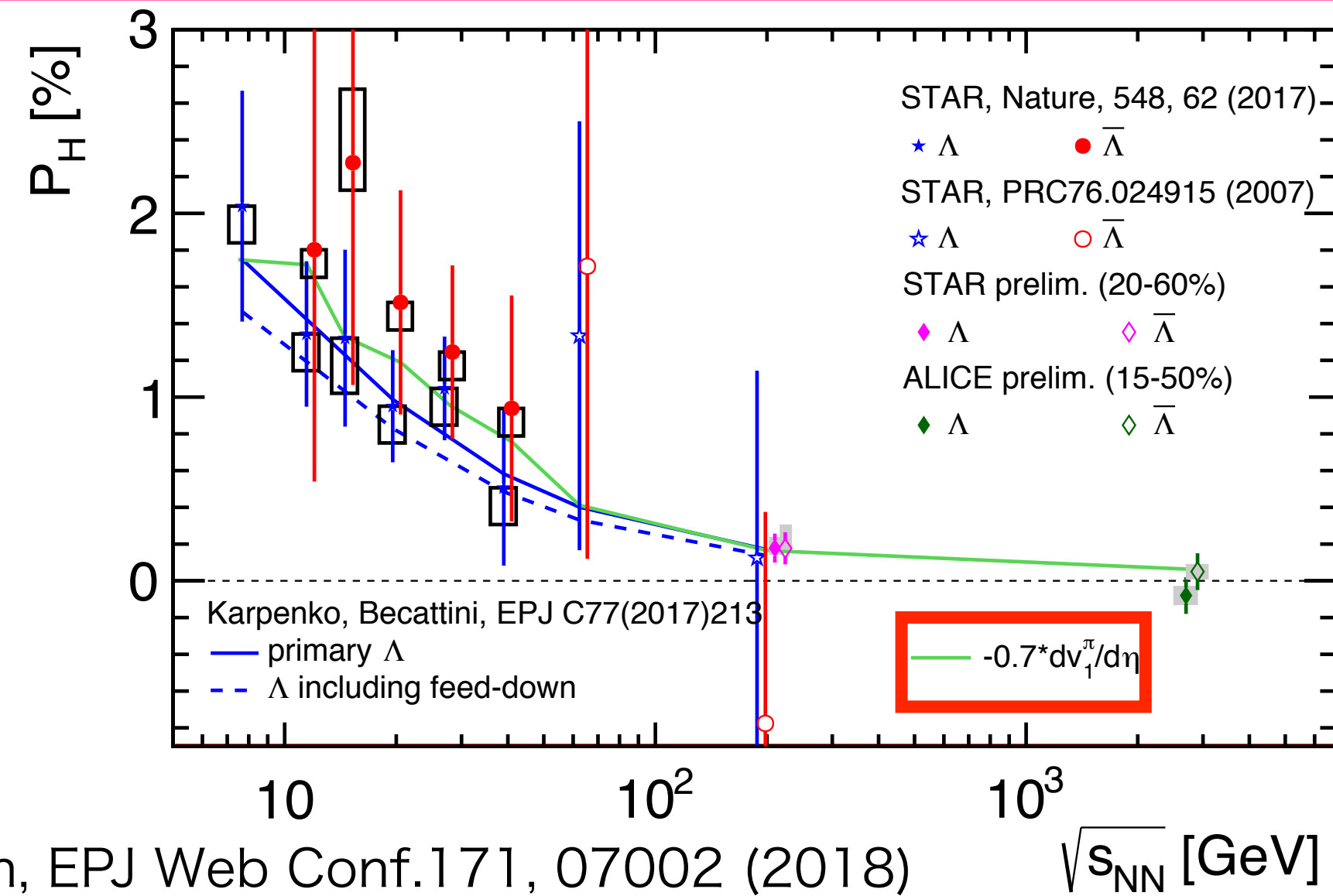
BW parameters obtained with HBT: STAR, PRC71.044906 (2005)



- Strong centrality dependence as in  $v_2$
- No strong  $p_T$  dependence but a hint of drop-off at  $p_T < 1$  GeV/c
- Blast-Wave model as a simple estimate for kinematic vorticity can describe the data

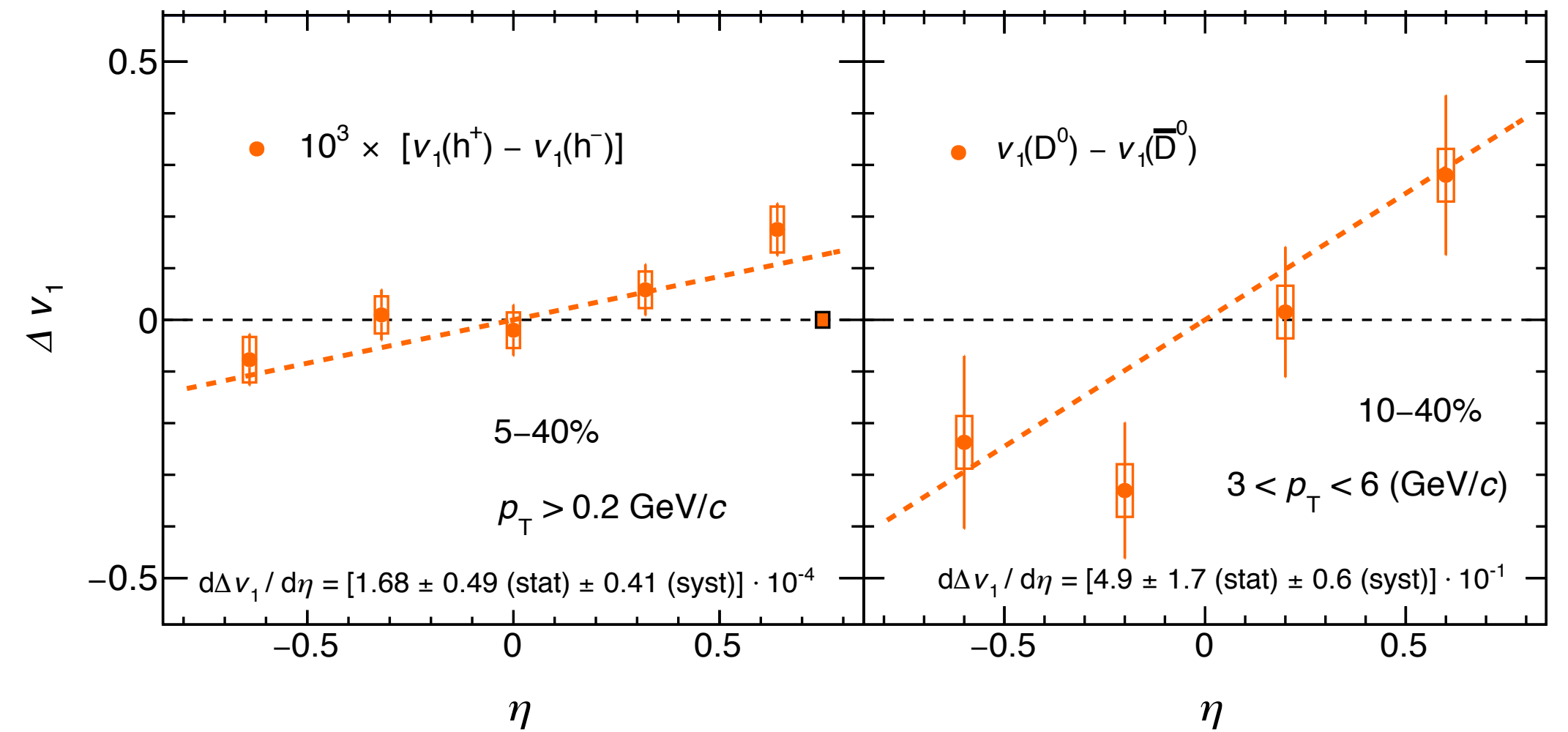
# $v_1$ and vorticity/EM-field

$v_1$ : sensitive to the initial tilt and EM-field



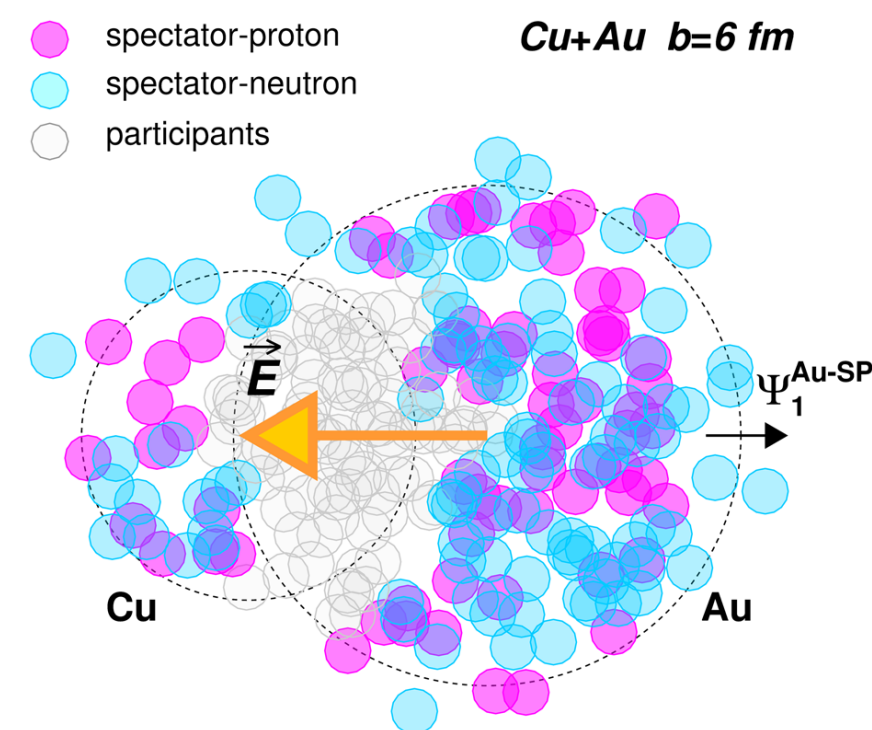
S. Voloshin, EPJ Web Conf.171, 07002 (2018)

ALICE, PRL125.022301 (2020)  
 Gursoy, Kharzeev, and Rajagopal, PRC89.054905 (2014)  
 Das et al., PLB768(2017)260

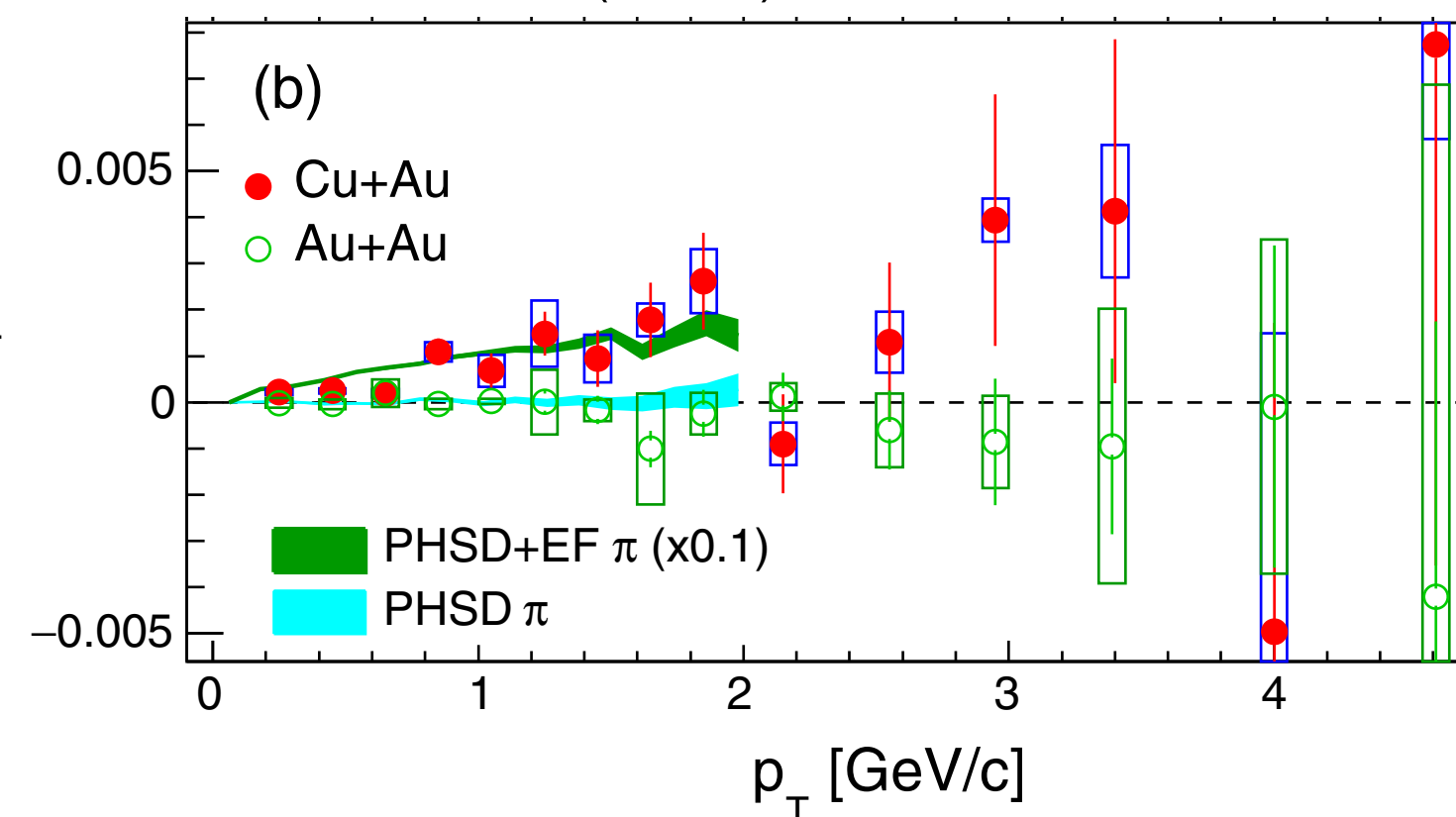


Cu+Au  $v_1$ : EM-field lifetime, quark density evolution, conductivity

Y. Hirono, M. Hongo, and T. Hirano,  
 PRC90.021903(R) (2014)  
 V. Voronyuk et al., PRC90.064903 (2014)



STAR, PRL118.012301 (2017)



# Outlook

## □ STAR

- High statistics data of BES-II 7.7-19.6 GeV and FXT 3-7.7 GeV
- Isobaric collision data (Ru+Ru, Zr+Zr), ~10% difference in B-field
- Global polarization of multi-strangeness ( $\Xi$  and  $\Omega$ )
- Forward upgrade in Run-2023

## □ ALICE/CMS/ATLAS

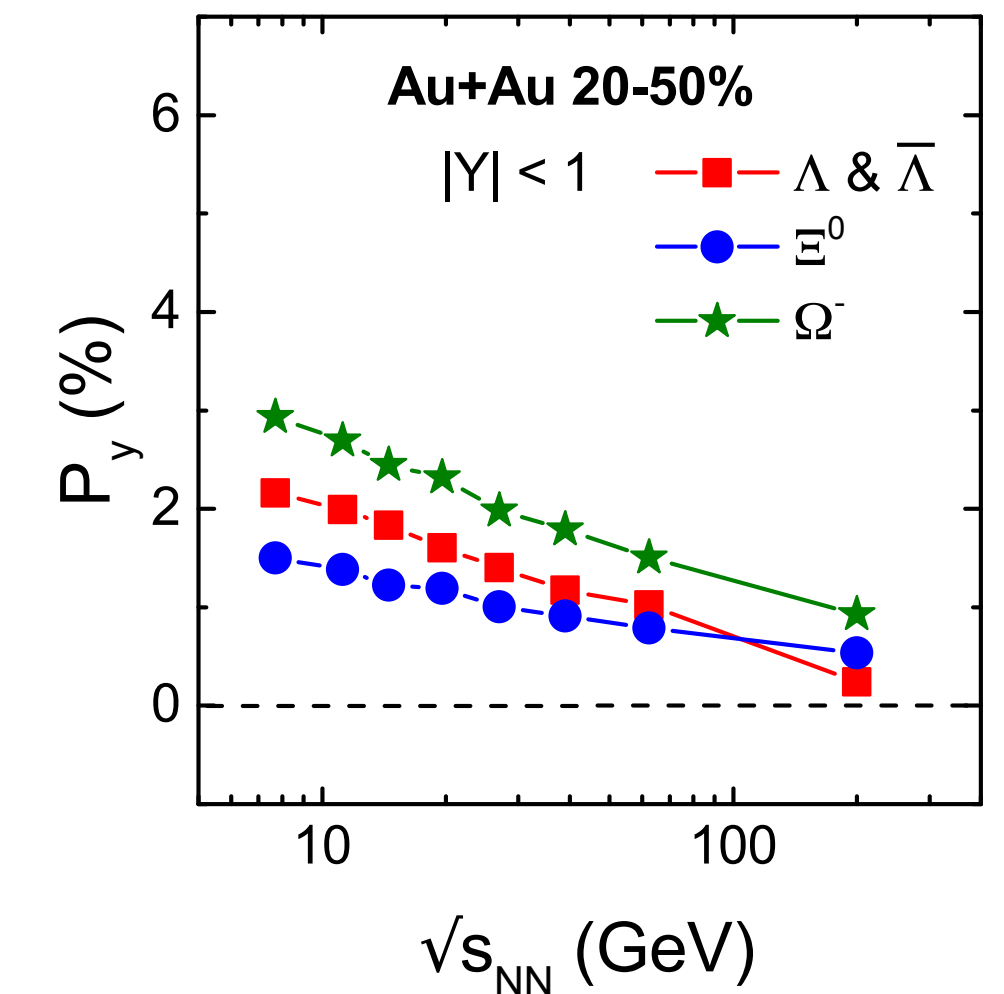
- Global/local polarizations at 5.02 TeV in LHC Run3

## □ HADES

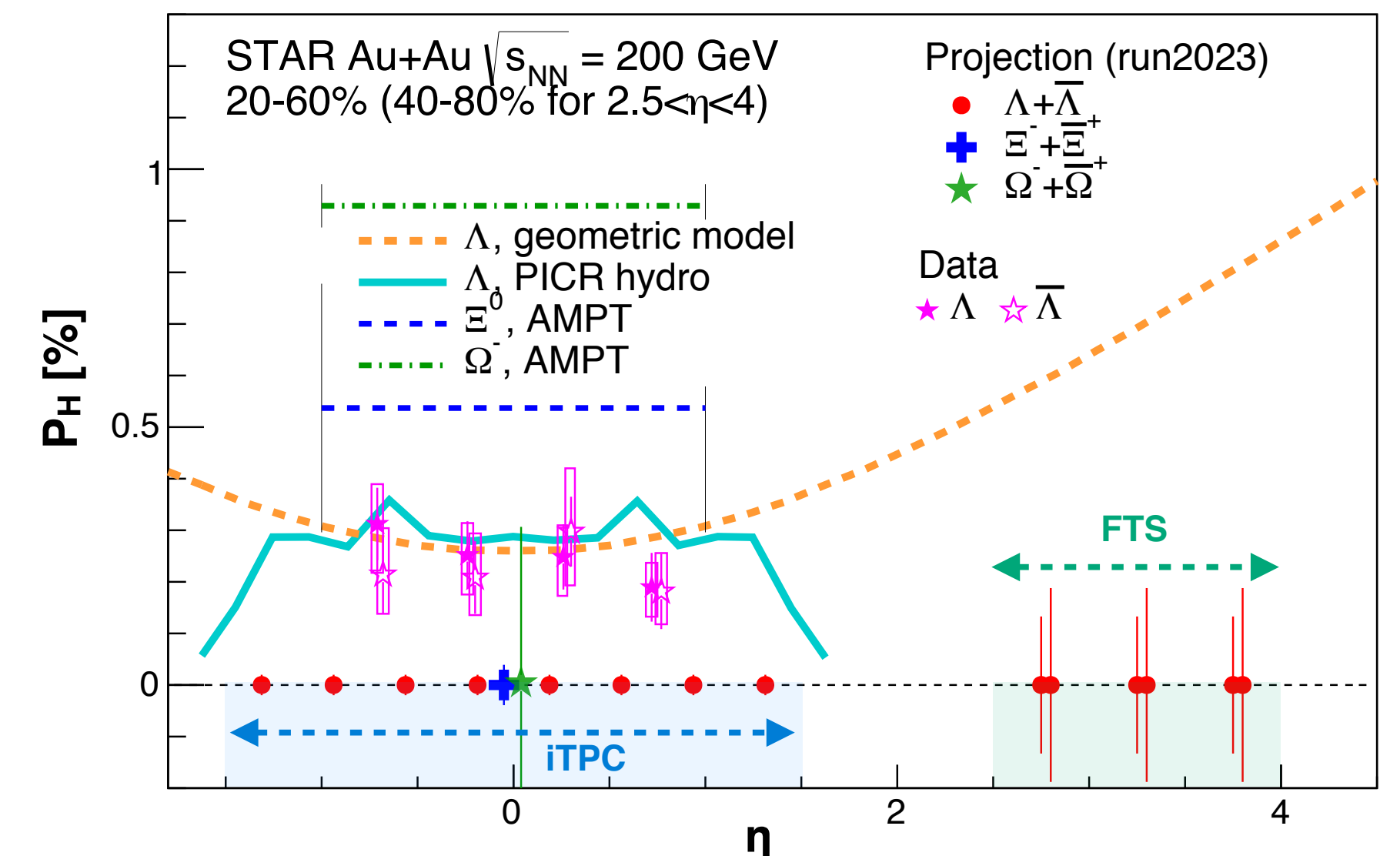
- Measurements at lowest energies (2-2.4 GeV)

## □ Future facilities/experiments

W.-T. Deng and X.-G. Huang, PRC93.064907 (2016)



STAR BUR2020





# Summary

---

- Global polarization of  $\Lambda$  has been observed at  $\sqrt{s_{NN}} = 7.7-200$  GeV
  - Most vortical fluid ( $\omega \sim 10^{21} \text{ s}^{-1}$ ) created in heavy-ion collisions
  - Energy dependence, increasing in lower  $\sqrt{s_{NN}}$ , is captured well by theoretical models
  - $\Lambda$ -anti $\Lambda$  splitting is not significant
  - Azimuthal angle dependence is not understood yet
- Global spin alignment shows larger deviation from  $1/3$ 
  - $\phi$  meson field may explain this large deviation?
  - Different trend between RHIC and LHC  $\phi$  or between  $\phi$  and  $K^*$  at RHIC
- Polarization along the beam direction has been observed at  $\sqrt{s_{NN}} = 200$  GeV
  - Qualitatively consistent with a picture of the elliptic flow but agreement/disagreement among the data and theoretical calculations in the sign

There are still many open questions and more precise data are needed.